Complementary material to "Role of Integral Experiment Covariance Data for Criticality Safety Validation: EG UACSA Benchmark Phase IV" (NEA/NSC/R(2021)1)

This document serves as complementary material to the main report the *Role of Integral Experiment Covariance Data for Criticality Safety Validation, EG UACSA Benchmark Phase IV*, NEA/NSC/R(2021)1, and compiles all individual contributions received within the framework of the Phase IV benchmark on the role of integral experiment covariance data for criticality safety validation, an activity led under the auspices of the Expert Group on Uncertainty Analysis for Criticality Safety Assessment (UACSA) under the Working Party on Nuclear Criticality Safety (WPNCS). The exercise comprised two complementary steps: 1) a simple analytic toy model; and 2) a more realistic case involving fuel lattice experiences from the LEU-COMP-THERM-007/039 (Poullot, 2015a, 2015b) series of the ICSBEP Handbook (NEA, 2015).

These contributions illustrate the wide interest within the criticality safety community on this topic and highlights a variety of approaches, simulation codes and nuclear data libraries used both to assess covariances between metrics of criticality safety benchmark experiments, and their impact on validation.

Table of contents

1. Participant A 6

1.1. The analytic toy model 6
1.2. PWR Fuel bundle – Realistic case 15

2. Participant B 21

2.1. Mathematical framework 21
2.2. Toy model 23
2.3. Realistic case: Experiments with water-reflected UO_2 fuel rod arrays 24

3. Participant C 28

4. Participant D 29

4.1. Introduction 29
4.2. Some definitions and clarifications 29
4.3. Background 30
4.4. The analytic toy model 30
4.5. Realistic case 42
4.6. Conclusions 62

5. Participant E 63

5.1. Toy model 63
5.2. UACSA BM Phase IV Results 70

6. Participant F 75

7. Participant G 77

7.1. CSAS/KENO 77
7.2. Sampler 77
7.3. Scenario A 77
7.4. Scenario E 77

8. Participant H 78

8.1. Methods 78
8.2. Results of the analysis 81

References 90

List of tables

Table 1.1 No $\boldsymbol{x1}$ correlation, covariance matrix 6
Table 1.2 No $\boldsymbol{x1}$correlation, standard deviations 7
Table 1.3 Shared $\boldsymbol{x1}$, covariance matrix 8
Table 1.4 Shared $\boldsymbol{x1}$, standard deviations 8
Table 1.5 No $\boldsymbol{x1}$correlation, no nuclear data uncertainties, covariance matrix 10
Table 1.6. No $\boldsymbol{x1}$correlation, no nuclear data uncertainties, standard deviations 10
Table 1.7 Shared $\boldsymbol{x1}$, no nuclear data uncertainties, covariance matrix 11
Table 1.8 Shared $\boldsymbol{x1}$, no nuclear data uncertainties, standard deviations 11
Table 1.9 Summary of results for analytic toy model 15
Table 1.10 Sensitivity coefficients for PWR fuel bundle – Scenario A 17
Table 1.11 Estimated bias for application case, based on differing numbers of experiments – unweighted average 19
Table 1.12 Summary of estimated uncertainty on bias 20
Table 2.1 Prior and posterior application k_{eff} values and their standard deviations σ 24
Table 2.2: Prior and posterior application case k_{eff} values and their standard deviation using the sensitivity approach. 27
Table 2.3 Prior and posterior application case k_{eff} values and their standard deviation using the Monte Carlo approach. 27
Table 4.1 Task 1 specifications 33
Table 4.2 Task 1(a) – No $\boldsymbol{x1}$ correlation – Direct approach – Correlation coefficients 33
Table 4.3 Task 1(b) – $\boldsymbol{x1}$ correlation - Direct approach – Correlation coefficients 34
Table 4.4 Task 1(a) – No $\boldsymbol{x1}$ correlation - Perturbation approach – Correlation coefficients 34
Table 4.5 Task 1(b) – $\boldsymbol{x1}$ correlation - Perturbation approach – Correlation coefficients 34
Table 4.6 Additional calculation Cases 1(cx) and 1(dx) 35
Table 4.7 Case 1(cx) - no data uncertainties – no $\boldsymbol{x1}$ corr. – correlation coefficients 35
Table 4.8 Case 1(dx) - no data uncertainties – $\boldsymbol{x1}$ correlation – correlation coefficients 35
Table 4.9 Additional calculation Case 1(ex) 36
Table 4.10 No system parameter uncertainties – correlation coefficients 36
Table 4.11 A fitted Task 2(a) combination that results in zero biases 38
Table 4.12 A fitted Task 2(b) combination that results in zero biases 39
Table 4.13 Correlations within each benchmark 43
Table 4.14 Correlations between benchmarks 43
Table 4.15 SCALE 6.2 Sampler correlation coefficients for Scenario A 48
Table 4.16 SCALE 6.2 Sampler correlation coefficients for Scenario E-II 49
Table 4.17 Scenario A correlation coefficients based on sensitivity calculations 54
Table 4.18 Rejected Scenario E-I model correlation coefficients based on sensitivity calculations 54
Table 4.19 Selected Scenario E-I model correlation coefficients based on sensitivity calculations 55
Table 4.20 Scenario E-II correlation coefficients based on sensitivity calculations 55
Table 4.21 Scenario E-III correlation coefficients based on sensitivity calculations 56
Table 4.22 k_{eff} and corresponding EALF results for the LCT-007 and -039 benchmarks 58
Table 4.23 Uncertainties based on benchmark selections and whether correlations apply or not 59
Table 4.24 k_{eff} and EALF results for the Application Case 1 (theoretical) 60
Table 4.25 k_{eff} and EALF results for Application Case 2 (LCT-079 cases 1 and 6) 61
Table 5.1 Case 1 - Resulting k_{eff} mean values and standard deviations 63
Table 5.2 Case 2 - Resulting k_{eff} mean values and standard deviations 64
Table 5.3 Case 3 - Resulting k_{eff} mean values and standard deviations 65
Table 5.4 Case 4 - Resulting k_{eff} mean values and standard deviations 67
Table 5.5 Posterior distributions 69
Table 5.6 Prior and posterior distribution characteristics ($k_{eff}\pm\boldsymbol{1\sigma}$) 74
Table 6.1 Sources of uncertainties investigated in this work 76
Table 8.1 Covariances (top) and correlations (bottom) due to system parameters (Task 1a) 81
Table 8.2 Covariances (top) and correlations (bottom) due to system parameters (Task 1b) 82
Table 8.3 Covariances (top) und correlations (bottom) due to nuclear data (Task 2) 82
Table 8.4 Summary of results for Task 2 83
Table 8.5 Results for Task 2a and Task 2b 83
Table 8.6 Sensitivity coefficients to individual parameter variations for each experimental configuration 84
Table 8.7 Impact of parameter uncertainties on total uncertainty of each experimental configuration 84

Table 8.8 Correlation coefficients (x1000) for Scenario A (stochastic dependence of fuel rod positions) 85
Table 8.9 Correlation coefficients (x1000) for Scenario B (stochastic dependence of fuel rod positions) 86
Table 8.10 Correlation coefficients (x1000) for Scenario C (stochastic dependence of fuel rod positions) 86
Table 8.11 Correlation coefficients (x1000) for Scenario D (stochastic dependence of fuel rod positions) 87
Table 8.12 Correlation coefficients (x1000) for Scenario E (stochastic dependence of fuel rod positions) 87
Table 8.13 Correlation coefficients (x1000) for Scenario A (stochastic independence of fuel rod positions) 88
Table 8.14 Correlation coefficients (x1000) for Scenario E (stochastic independence of fuel rod positions) 88
Table 8.15 Summary of results for Application Case 1 89

List of figures

Figure 1.1 No $\boldsymbol{x1}$correlation, correlation matrix 7
Figure 1.2 Shared $\boldsymbol{x1}$, correlation matrix 8
Figure 1.3 No $\boldsymbol{x1}$correlation, no nuclear data uncertainties, correlation matrix 11
Figure 1.4 Shared $\boldsymbol{x1}$, no nuclear data uncertainties, correlation matrix 12
Figure 1.5 PWR Fuel bundle configuration 16
Figure 1.6 Correlation matrix for PWR fuel bundle – Scenario A 17
Figure 1.7 Correlation matrix for PWR fuel bundle – Scenario E 18
Figure 4.1 Calculation results for the toy model benchmarks with trend line 37
Figure 4.2 Reactivities after Task 2(a) data and system parameter adjustments 39
Figure 4.3 Reactivities after Task 2(b) data and system parameter adjustments 39
Figure 4.4 Parameter correlation coefficient matrix for Scenarios A and E-I 52
Figure 4.5 Parameter correlation coefficient matrix for Scenario E-II and Scenario E-III 53
Figure 4.6 k_{eff} results sorted after EALF results for the LCT-007 and -039 benchmarks 57
Figure 5.1 Case 1 - Scatter plot of k_{eff} values between benchmark experiments 63
Figure 5.2 Correlation coefficients assuming Case 1 64
Figure 5.3 Case 2 - Scatter plot of k_{eff} values between benchmark experiments 64
Figure 5.4 Correlation coefficients assuming Case 2 65
Figure 5.5 Case 3 - Scatter plot of k_{eff} values between benchmark experiments 66
Figure 5.6 Correlation coefficients assuming Case 3 67
Figure 5.7 Case 4 - Scatter plot of k_{eff} values between benchmark experiments 68
Figure 5.8 Correlation coefficients assuming Case 4 68
Figure 5.9 Distribution functions for prior and posterior distributions assuming sampled alpha values 69
Figure 5.10 Distribution functions for prior and posterior distributions assuming nominal alpha values 69
Figure 5.11 Experimental k_{eff} for LCT-07 and 39 in comparison to different calculation methods 70
Figure 5.12 Correlation coefficients of k_{eff} due to system parameter uncertainties for a subset of experiments for all five scenarios 71
Figure 5.13 Correlation coefficients of k_{eff} for scenarios A (left) and E (right) due to system parameter uncertainties 71
Figure 5.14 Correlation coefficients between experiments and application cases due to nuclear data uncertainties calculated with TSUNAMI 72
Figure 5.15 Sensitivity of k_{eff} on varied parameters for scenarios A (left) and E (right) for all experiments 73
Figure 5.16 Prior and posterior distributions for the application cases App.1 (left) and LCT-79-01 (right) 74
Figure 8.1 Example for determination of sensitivity coefficients 79

1. Participant A

Participant: Paul Smith (Amec Foster Wheeler, United Kingdom)

1.1. The analytic toy model

The benchmark specification presents an analytic toy problem with sufficient complexity to be of interest, but amenable to analysis with only modest computing requirements. The toy problem takes the form:

$$k_c = \frac{\alpha_1 \alpha_4 x_1}{\alpha_1 x_1 + \alpha_2 x_2 + \alpha_3 x_3}$$

Here the alpha terms are considered to represent nuclear data and the x terms represent system parameters. Best-estimate data and uncertainties on these seven parameters are presented in the specification, together with results for nine notional benchmark experiments.

The first task for the exercise was to estimate covariance and correlation matrices with two sets of assumptions:

- assuming no stochastic dependence between the system parameters;
- assuming x_1 is identical for all nine benchmarks.

The following results were obtained for the covariance matrix under the assumption of no stochastic dependence for the system parameters. This was achieved by sampling for the nuclear data (the alpha terms) and sampling for the nine sets of system parameters (the x terms), thus sampling for 31 variables in total. The nine resulting values of k_c could then be determined. By repeating this process many times, a table where each row comprises the nine values of k_c can be generated, and from this table the covariance (and hence also correlation) matrices can be generated. The matrices that follow were generated using 1,000,000 rows.

Table 1.1. No x_1 correlation, covariance matrix

	1	2	3	4	5	6	7	8	9
1	9.94E-05	7.10E-05	6.95E-05	6.78E-05	6.60E-05	6.51E-05	6.01E-05	5.71E-05	5.41E-05
2	7.10E-05	9.78E-05	7.10E-05	7.07E-05	7.04E-05	7.09E-05	7.02E-05	7.02E-05	6.99E-05
3	6.95E-05	7.10E-05	9.93E-05	7.35E-05	7.46E-05	7.66E-05	8.00E-05	8.28E-05	8.52E-05
4	6.78E-05	7.07E-05	7.35E-05	1.04E-04	7.86E-05	8.21E-05	8.96E-05	9.53E-05	1.00E-04
5	6.60E-05	7.04E-05	7.46E-05	7.86E-05	1.10E-04	8.72E-05	9.85E-05	1.07E-04	1.14E-04
6	6.51E-05	7.09E-05	7.66E-05	8.21E-05	8.72E-05	1.20E-04	1.09E-04	1.20E-04	1.31E-04
7	6.01E-05	7.02E-05	8.00E-05	8.96E-05	9.85E-05	1.09E-04	1.65E-04	1.56E-04	1.74E-04
8	5.71E-05	7.02E-05	8.28E-05	9.53E-05	1.07E-04	1.20E-04	1.56E-04	2.09E-04	2.04E-04
9	5.41E-05	6.99E-05	8.52E-05	1.00E-04	1.14E-04	1.31E-04	1.74E-04	2.04E-04	2.61E-04

The square root of the diagonal terms provide estimates for the standard deviations of k_c for each of the nine notional benchmark experiments, which can be thought of as the uncertainty (at the one standard deviation level) in each k_c as a result of the combined uncertainty in nuclear data and system parameters. These sampled standard deviations are shown below.

Table 1.2. No x_1 correlation, standard deviations

	1	2	3	4	5	6	7	8	9
S. D.	9.97E-03	9.89E-03	9.96E-03	1.02E-02	1.05E-02	1.10E-02	1.28E-02	1.45E-02	1.62E-02

The correlation matrix can be generated from the covariance matrix by dividing the $(i,j)^{th}$ entry by the product of the i^{th} and j^{th} standard deviation, resulting in a symmetric matrix with a diagonal of unity and off diagonal terms bounded in absolute value by unity. The correlation matrix corresponding to the above covariance matrix is shown in graphical form below.

Figure 1.1. No x_1 correlation, correlation matrix

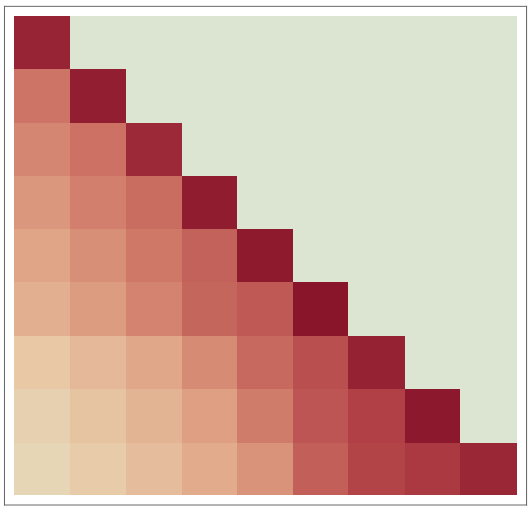

Source: NEA, 2020.

The off-diagonal terms give an indication of the correlation of the different experiments in the sense that for the more correlated experiments, an error in the calculated k_c in one experiment would likely be accompanied by an error in the other calculated k_c in the same direction. If there was no shared nuclear data then the off-diagonal terms would theoretically be zero, and any deviation from zero would be the result of the sampling process being used to estimate the entries in the matrix. This emphasises that there is a stochastic uncertainty associated with all the entries in the covariance matrix. We have not attempted here to quantify these uncertainties on the uncertainties.

The second scenario under consideration is to assume x_1 is identical for all nine benchmarks. This should result in a higher degree of correlation as it represents, say, the use of common equipment between experiments. The simulation differs in that when the nuclear data (alpha terms) and system parameters are sampled, only one value for x_1 is sampled, resulting in four values for the nuclear data, one value for x_1 and 18 values for the nine sets of x_2 and x_3. This results in 23 sampled variables (as opposed to 31 above) in order to calculate the nine values of k_c (one for each notional benchmark experiment).

The covariance matrix under the assumption that x_1 is shared (in addition to the nuclear data) is as follows:

Table 1.3. Shared x_1, covariance matrix

	1	2	3	4	5	6	7	8	9
1	9.96E-05	8.88E-05	8.73E-05	8.59E-05	8.45E-05	8.29E-05	7.88E-05	7.58E-05	7.31E-05
2	8.88E-05	9.80E-05	8.87E-05	8.87E-05	8.87E-05	8.86E-05	8.87E-05	8.86E-05	8.86E-05
3	8.73E-05	8.87E-05	9.93E-05	9.16E-05	9.30E-05	9.43E-05	9.85E-05	1.01E-04	1.04E-04
4	8.59E-05	8.87E-05	9.16E-05	1.04E-04	9.74E-05	1.00E-04	1.08E-04	1.14E-04	1.19E-04
5	8.45E-05	8.87E-05	9.30E-05	9.74E-05	1.10E-04	1.06E-04	1.18E-04	1.26E-04	1.34E-04
6	8.29E-05	8.86E-05	9.43E-05	1.00E-04	1.06E-04	1.21E-04	1.28E-04	1.39E-04	1.50E-04
7	7.88E-05	8.87E-05	9.85E-05	1.08E-04	1.18E-04	1.28E-04	1.65E-04	1.75E-04	1.94E-04
8	7.58E-05	8.86E-05	1.01E-04	1.14E-04	1.26E-04	1.39E-04	1.75E-04	2.09E-04	2.24E-04
9	7.31E-05	8.86E-05	1.04E-04	1.19E-04	1.34E-04	1.50E-04	1.94E-04	2.24E-04	2.61E-04

Again, the square root of the diagonal terms provides an estimate for the standard deviations of k_c for each of the nine notional benchmark experiments. Note that the sharing of x_1 should have no effect on the expected value of these standard deviation estimators, and so they should agree (within statistics) with the values for independent x_1. Without doing any sophisticated analysis, it can be seen that there seems to be good agreement.

Table 1.4. Shared x_1, standard deviations

	1	2	3	4	5	6	7	8	9
S. D.	9.98E-03	9.90E-03	9.97E-03	1.02E-02	1.05E-02	1.10E-02	1.28E-02	1.45E-02	1.62E-02

Again the covariance matrix can be generated.

Figure 1.2. Shared x_1, correlation matrix

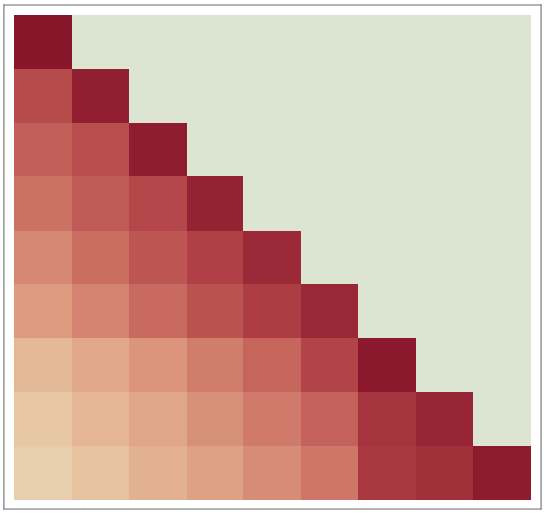

Source: NEA, 2020.

Armed with these data we now turn to how they may be used in order to do an uncertainty quantification analysis. The second task for the Toy problem is to estimate the bias-corrected k_{eff} and to quantify the uncertainty for an application case, using the same two sets of assumptions as before:

- assuming no stochastic dependence between the system parameters;
- assuming x_1 is identical for all nine benchmarks.

The specification allows us to assume the system parameters are known exactly for the application case, and that the computational bias is due to errors in the data – that is, we can assume the model is an exact representation of the physics.

In order to look at this we considered four possible approaches:

- ignore benchmark data and just use the uncertainty on the nuclear data to provide an overall uncertainty, with no explicit quantification of a bias;
- use a single, closest, benchmark to estimate the bias;
- use all nine benchmarks to estimate the bias;
- use the MOCABA (Hoefer et al., 2015) Bayesian approach (again using all nine of the benchmarks).

1.1.1. Quantifying bias

If we ignore the benchmark data, there is no need to estimate or quantify the bias. This is all wrapped up in the overall uncertainty.

If we use the closest benchmark, we would need to:

- estimate the bias;
- estimate the uncertainty in the bias;
- quantify the effect of extrapolation from benchmark to application system data;
- quantify the uncertainty on the extrapolation.

Similarly, if all nine benchmarks are used in a simple way, the same list of issues to quantify the uncertainties applies.

However, in the MOCABA Bayesian approach, the bias and uncertainty in the bias are generated as an integral part of the method. In a sense it picks out only the nuclear data that is consistent with the benchmarks; and uses this for the application with revised uncertainties on the nuclear data.

The expectation would be that any of the methods that use the benchmark data would give a tighter bound on k_{eff} than ignoring the benchmark data (and indeed this will always be the case with the MOCABA approach).

Approach 1 – Ignore the benchmark data

If the benchmark data is ignored then the uncertainty in k_{eff} can be generated by sampling the nuclear data (remembering that we are entitled, according to the specification to assume the system data is known exactly in the application case). The following results were obtained:

- k_{eff}, evaluated for the best estimate nuclear data, 0.9536;
- uncertainty based on sampled calculations, 0.0097, at the one standard deviation level;

- k_{eff} plus 3 standard deviations, 0.9824.

Approach 2 – Single, closest, benchmark

We now need to decide what closest might mean in this context. It could mean, closest in terms of system parameters, or closest in terms of some other similarity measure, for example based on sensitivity analysis. For the toy problem we chose just to use the closest system parameters. For the application case, the system parameter vector (x_1, x_2, x_3) is (1.5, -6, 10), and all the benchmark cases have x_1=2.0072, so whatever happens, this variable is extrapolated. Bearing this in mind, the closest benchmark experiment would seem to be benchmark 6, which has system variables (2.0072, -6.0613, 9.8448).

We need to recognise that the covariance data generated so far is not appropriate for use in the quantification of uncertainty using the closest benchmark data, as this already has the nuclear data uncertainty included. The point of using the experimental data is to account for the bias in the nuclear data, and so we do not want to include this twice. The covariance data therefore needs to be recalculated, with only the system data varying, again for each of the two sets of assumptions.

Table 1.5. No $x_1$correlation, no nuclear data uncertainties, covariance matrix

	1	2	3	4	5	6	7	8	9
1	2.7E-05	0	0	0	0	0	0	0	0
2	0	2.68E-05	0	0	0	0	0	0	0
3	0	0	2.7E-05	0	0	0	0	0	0
4	0	0	0	2.76E-05	0	0	0	0	0
5	0	0	0	0	2.79E-05	0	0	0	0
6	0	0	0	0	0	2.68E-05	0	0	0
7	0	0	0	0	0	0	2.82E-05	0	0
8	0	0	0	0	0	0	0	2.81E-05	0
9	0	0	0	0	0	0	0	0	2.84E-05

Table 1.6. No $x_1$correlation, no nuclear data uncertainties, standard deviations

	1	2	3	4	5	6	7	8	9
S. D.	5.19E-03	5.17E-03	5.19E-03	5.25E-03	5.29E-03	5.18E-03	5.31E-03	5.30E-03	5.33E-03

Figure 1.3. No x_1 correlation, no nuclear data uncertainties, correlation matrix

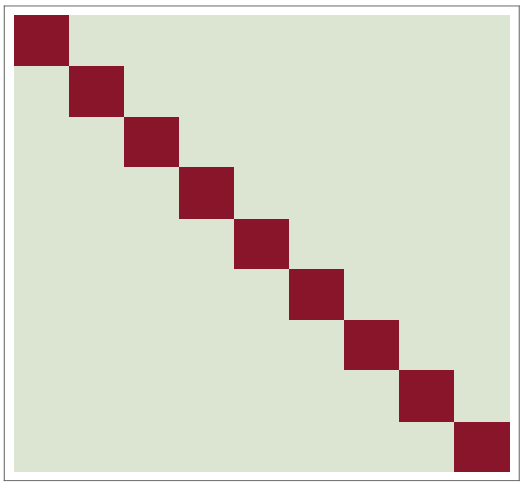

Source: NEA, 2020.

Table 1.7. Shared x_1, no nuclear data uncertainties, covariance matrix

	1	2	3	4	5	6	7	8	9
1	2.7E-05	1.76E-05	1.78E-05	1.82E-05	1.84E-05	1.77E-05	1.85E-05	1.85E-05	1.88E-05
2	1.76E-05	2.68E-05	1.76E-05	1.81E-05	1.82E-05	1.75E-05	1.84E-05	1.84E-05	1.86E-05
3	1.78E-05	1.76E-05	2.7E-05	1.82E-05	1.84E-05	1.77E-05	1.85E-05	1.85E-05	1.88E-05
4	1.82E-05	1.81E-05	1.82E-05	2.76E-05	1.88E-05	1.81E-05	1.9E-05	1.9E-05	1.92E-05
5	1.84E-05	1.82E-05	1.84E-05	1.88E-05	2.79E-05	1.82E-05	1.91E-05	1.91E-05	1.94E-05
6	1.77E-05	1.75E-05	1.77E-05	1.81E-05	1.82E-05	2.69E-05	1.85E-05	1.84E-05	1.87E-05
7	1.85E-05	1.84E-05	1.85E-05	1.9E-05	1.91E-05	1.85E-05	2.82E-05	1.93E-05	1.96E-05
8	1.85E-05	1.84E-05	1.85E-05	1.9E-05	1.91E-05	1.84E-05	1.93E-05	2.81E-05	1.96E-05
9	1.88E-05	1.86E-05	1.88E-05	1.92E-05	1.94E-05	1.87E-05	1.96E-05	1.96E-05	2.85E-05

Table 1.8. Shared x_1, no nuclear data uncertainties, standard deviations

	1	2	3	4	5	6	7	8	9
S. D.	5.19E-03	5.17E-03	5.19E-03	5.26E-03	5.28E-03	5.19E-03	5.31E-03	5.30E-03	5.34E-03

Figure 1.4. Shared x_1, no nuclear data uncertainties, correlation matrix

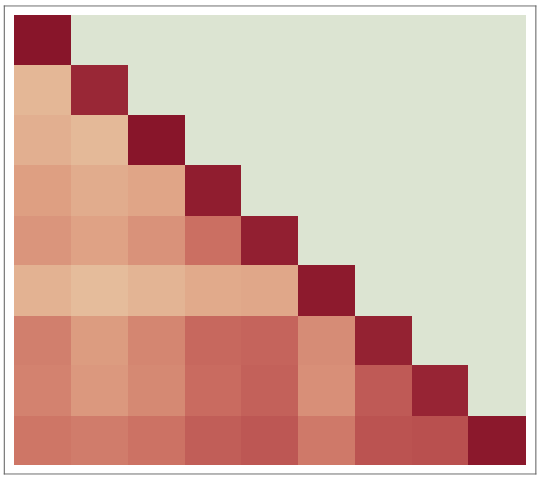

Source: NEA, 2020.

The bias for benchmark 6, $k_c - 1$ is 1.0185-1=0.0185, so based on this we would be entitled to subtract 0.0185 from our application calculated value – so long as we take account of the uncertainty on the bias and the uncertainty due to extrapolation. The uncertainty on the bias can be taken from the 6th diagonal entry from the covariance matrix given in Table , noting that this is the matrix generated without any uncertainty on the nuclear data. So the uncertainty on the bias at the one standard deviation level is 0.0052.

We still have the difficulty over extrapolating the bias to the application case. Assuming we can linearise liberally, an approximation to the bias is given by:

$$bias(x_1, x_2, x_3) = k_c(x_1, x_2, x_3, \hat{\alpha}) - k_c(x_1, x_2, x_3, \alpha) \cong \sum_i \frac{\partial k_c}{\partial \alpha_i} \delta\alpha_i$$

where $\hat{\alpha}$ is the assumed nuclear data vector, α is the true nuclear data, and $\delta\alpha_i = \hat{\alpha}_i - \alpha_i$. We are interested in how the bias varies with x_1 so it appears we need the second order partial derivatives to express:

$$\frac{\partial\ bias(x_1, x_2, x_3)}{\partial x_1} = \sum_i \frac{\partial^2 k_c}{\partial \alpha_i \partial x_1} \delta\alpha_i$$

For the toy problem the derivatives can be calculated explicitly, and evaluate to: -0.0078, -0.1121, 0.1868, 0.1137 as i varies from one to four. So an approximate bound on the uncertainty due to extrapolation can be found by summing in quadrature the coefficients multiplied by the standard deviations on the α_i terms, and multiplying the result by the movement in x_1. That is, uncertainty in the bias due to extrapolation equals:

$$|\Delta x_1| \sum_i \left(\frac{\partial^2 k_c}{\partial \alpha_i \partial x_1} \right)^2 \sigma_i^2$$

This evaluates to 0.5072*0.2459*0.01=0.00123.

No attempt has been made to justify the linearity assumption, and it may be that in practice it is not justifiable. In summary, we have the following results from using the closest benchmark:

- best estimate k_{eff} 0.9536;
- bias based on benchmark 6 (to be subtracted) 0.0185;
- uncertainty on bias for benchmark 6 0.00518;
- uncertainty due to extrapolation 0.00123;
- overall uncertainty 0.00532;
- bounded value of k_{eff} - 3 standard deviations 0.9511.

Approach 3 – Use all benchmark data

An alternative to using a single benchmark is to use them all and take a weighted average of the bias from each benchmark. The choice of weighting might include:

- just using a straight average;
- weighting the average according to the uncertainty in the benchmark;
- weighting the average in some way according to the similarity in the application case.

Here we look at the first and second of these approaches:

- we will look at the estimated bias and uncertainty on this estimate;
- we will use the same approach and values as for the single benchmark case in order to deal with extrapolation.

Suppose b_i is the observed bias for benchmark i. $b_i = (k_c(\hat{\alpha}) - 1)_i$. Then if we estimate the bias as $b = \sum_i a_i b_i$, where the a_i terms are constants, normalised to sum to unity, the variance on b can be expressed as $\sigma_b^2 = \sum_{i,j} a_i C_{i,j} a_j$, where $C_{i,j}$is the covariance of b_i and b_j.

Just taking the straight average of the benchmark biases, ie $a_i = 1/n$ where n is the number of benchmarks, then the variance in this case is just the sum of all the covariance matrix terms, divided by the square of the number of benchmarks.

An alternative is to attempt to minimise σ_b^2 with respect to the a_i coefficients, subject to the constraint $\sum a_i = 1$. This results in $\boldsymbol{a} = \frac{\boldsymbol{C}^{-1}\mathbf{1}}{\mathbf{1}^T\boldsymbol{C}^{-1}\mathbf{1}}$ and $\sigma_b^2 = \frac{1}{\mathbf{1}^T\boldsymbol{C}^{-1}\mathbf{1}}$, ie the variance on the bias for the application is the reciprical of the sum of all the terms in the inverse of the covariance matrix. If the covariance matrix is diagonal this corresponds to $a_i = \frac{1/\sigma_i^2}{\sum_j 1/\sigma_j^2}$.

using this approach the following results were obtained.

Unweighted average, stochastically independent x_1.

- best estimate k_{eff} 0.9536;
- bias (to be subtracted) 0.0120;
- uncertainty on bias 0.00175;
- uncertainty due to extrapolation 0.00123;

- overall uncertainty 0.00214;
- bounded value of k_{eff} - 3 standard deviations 0.9480.

Weighted average (to minimise variance), stochastically independent x_1.

- best estimate k_{eff} 0.9536;
- bias (to be subtracted) 0.0121;
- uncertainty on bias 0.00175;
- uncertainty due to extrapolation 0.00123;
- overall uncertainty 0.00214;
- bounded value of k_{eff} - 3 standard deviations 0.9479.

Unweighted average, shared x_1.

- best estimate k_{eff} 0.9536;
- bias (to be subtracted) 0.0120;
- uncertainty on bias 0.00442;
- uncertainty due to extrapolation 0.00123;
- overall uncertainty 0.00459;
- bounded value of k_{eff} - 3 standard deviations 0.9554.

Weighted average (to minimise variance), shared x_1.

- best estimate k_{eff} 0.9536;
- bias (to be subtracted) 0.0143;
- uncertainty on bias 0.00440;
- uncertainty due to extrapolation 0.00457;
- overall uncertainty 0.00214;
- bounded value of k_{eff} - 3 standard deviations 0.9530.

Approach 4 MOCABA method (Hoefer et al., 2015)

The MOCABA method is a Bayesian approach. In a sense it picks out the nuclear data that is consistent with the experimental results, but maintaining a probabilistic element. The method requires the covariance matrices including nuclear data uncertainties. Using the nomenclature from the paper, the estimated bias (to be added) is $\Sigma_{0AB}\Sigma_{0B}^{-1}(v_B - y_{0B})$, where this represents matrix multiplication of the covariances of the application case with the benchmarks, the inverse of the covariance matrix for the benchmarks, and the negative of the observed biases in the benchmarks. There is an associated reduction in variance given by $\Sigma_{0AB}\Sigma_{0B}^{-1}{\Sigma_{0AB}}^{T}$, where this represents matrix multiplication of the covariances of the application case with the benchmarks, the inverse of the covariance matrix for the benchmarks, and the transpose of the covariances of the application case with the benchmarks.

MOCABA methodology – system parameters stochastically independent:

- best estimate k_{eff} 0.9536;
- bias (to be subtracted) 0.0099;
- uncertainty 0.00173;
- bounded value of k_{eff} - 3 standard deviations 0.9489.

MOCABA methodology – shared x_1 in benchmarks:

- best estimate k_{eff} 0.9537;
- bias (to be subtracted) 0.00759;
- uncertainty 0.00378;
- bounded value of k_{eff} - 3 standard deviations 0.9574.

1.1.2. Summary table

Table 1.9. Summary of results for analytic toy model

Approach	Raw k_{eff}	Bias applied	Uncertainty (one s.d.)	Extrapolation uncertainty	Bounded k_{eff}
No Benchmarks	0.9536	0	0.0097	N/A	0.9824
Closest Benchmark	0.9536	-0.0185	0.0052	0.00123	0.9511
Average Bias – Stochastically independent	0.9536	-0.0120	0.00175	0.00123	0.9480
Weighted Average Bias – Stochastically independent	0.9536	-0.0121	0.00175	0.00123	0.9479
Average Bias – shared x1	0.9536	-0.0120	0.00442	0.00123	0.9554
Weighted Average Bias – shared x_1	0.9536	-0.0143	0.00440	0.00123	0.9531
MOCABA – Stochastically independent	0.9536	-0.00990	0.00173	N/A	0.9489
MOCABA – shared x_1	0.9536	-0.00759	0.00378	N/A	0.9574

1.2. PWR Fuel bundle – Realistic case

The benchmark also specifies more realistic configurations, incorporating real experimental data. One of these is a PWR fuel bundle. Details of the specification are provided in the benchmark report (NEA, 2022), but Figure 1.5. below shows the general configuration.

Figure 1.5. PWR Fuel bundle configuration

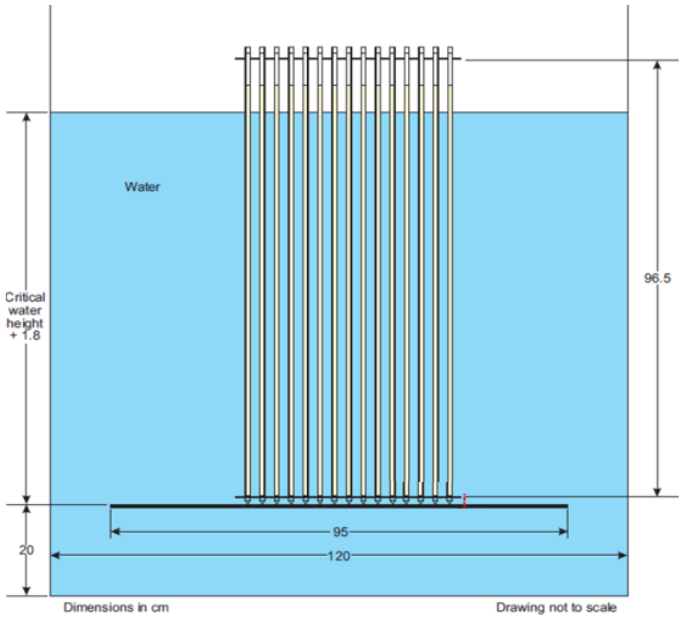

Source: Poullot and Hanlon, 2015a.

The fuel rods in the experiments are held in place in a square pitch configuration by grids, and although uncertainties are specified for geometric parameters relating to the positions and sizes of grid holes, how to treat these uncertainties may be open to interpretation. Therefore, five different sets of assumptions were given as part of the benchmark specification, labelled A - E. We chose to analyse Scenarios A and E. In scenario A, the assumption is that all rods are positioned at their nominal grid position, i.e. the positioning uncertainty is neglected. Additionally, it assumes that all other parameters are fully correlated over the grid, so whilst there is uncertainty on the fuel rod dimensions, the rod dimensions are fully correlated. This makes Scenario A amenable to a sensitivity analysis as there are only a few (12 in total) uncertain parameters. In scenario E the rods are all leaning on the walls of their grid holes, the grid holes are independently and randomly distributed, and the fuel radial dimensions and hole diameters are independent for all rods. There is therefore a very much increased set of uncertain parameters in scenario E compared to scenario A, making a Monte Carlo style analysis more appropriate.

1.2.1. Analysis of benchmarks

Scenario A

Table 1.10 below presents sensitivities for each of the 21 experiments for each of the 12 uncertain parameters, based on MONK calculations where each of the uncertain parameters was varied in turn – so 13 calculations for each experiment, including a base case. 5% perturbations were used where that made sense, but for some parameters a different perturbation was used.

Table 1.10. Sensitivity coefficients for PWR fuel bundle – Scenario A

	clad inner diameter	clad thickness	fuel diameter	hole diameter	fuel height	water height	density	B10 impurity	U234 frac	U235 frac	U236 frac	U238 frac
LCT07-001	-0.0265	-0.0034	0.00775	0.0001	0.0008	0.0012	0.001	-0.00003	-0.0002	0.007	-0.0001	-0.003
LCT07-002	-0.0111	-0.0015	0.0145	0.	0.	0.0033	0.0007	0.	-0.0001	0.0091	-0.0001	-0.002
LCT07-003	-0.0022	-0.0003	0.021	-0.0002	-0.0002	0.0028	0.0002	-0.00002	-0.0002	0.0119	-0.0001	0.
LCT07-004	0.002	0.0001	0.02725	0.0001	0.0002	0.003	0.0002	0.00002	0.0002	0.0141	0.	-0.002
LCT39-001	-0.0247	-0.0033	0.00875	-0.0001	0.0002	0.0027	0.0007	-0.00002	-0.0002	0.0068	-0.0002	-0.003
LCT39-002	-0.0237	-0.0029	0.009	0.0001	0.	0.0031	0.0008	-0.00001	-0.0001	0.0072	-0.0002	-0.004
LCT39-003	-0.022	-0.003	0.0095	-0.0001	0.	0.0036	0.0008	-0.00002	-0.0003	0.0073	-0.0001	-0.003
LCT39-004	-0.021	-0.0025	0.00975	0.0002	0.0005	0.0017	0.0011	0.00001	0.0001	0.0076	0.0001	-0.001
LCT39-005	-0.0157	-0.0021	0.01125	-0.0001	0.0002	0.0025	0.001	-0.00003	-0.0002	0.0083	-0.0001	-0.003
LCT39-006	-0.0161	-0.0022	0.01275	0.0001	0.0001	0.005	0.0009	0.	0.0001	0.0082	0.0001	-0.001
LCT39-007	-0.0237	-0.0032	0.00925	-0.0001	-0.0002	0.0036	0.0007	-0.00003	-0.0001	0.007	-0.0001	-0.005
LCT39-008	-0.0224	-0.0032	0.00975	0.	0.	0.004	0.0009	-0.00003	-0.0003	0.0073	0.	-0.003
LCT39-009	-0.022	-0.0032	0.0095	-0.0002	-0.0003	0.0041	0.0009	-0.00004	-0.0003	0.0072	-0.0004	-0.005
LCT39-010	-0.0191	-0.0024	0.01175	0.0003	0.	0.005	0.0008	-0.00001	-0.0001	0.0076	0.	-0.002
LCT39-011	-0.0247	-0.0031	0.009	0.0001	0.0002	0.0026	0.0011	-0.00001	0.	0.007	-0.0001	-0.004
LCT39-012	-0.0242	-0.0032	0.0095	-0.0001	0.	0.0031	0.0009	-0.00002	-0.0001	0.0072	-0.0001	-0.002
LCT39-013	-0.0236	-0.003	0.009	0.0001	0.0001	0.0036	0.0009	-0.00001	0.0001	0.0073	-0.0001	-0.004
LCT39-014	-0.0235	-0.0031	0.009	-0.0003	-0.0002	0.0033	0.0007	-0.00003	-0.0004	0.0068	-0.0002	-0.005
LCT39-015	-0.0231	-0.003	0.0095	-0.0001	0.	0.0037	0.001	0.00001	-0.0001	0.0073	-0.0001	-0.003
LCT39-016	-0.0232	-0.0029	0.00925	0.	-0.0001	0.0039	0.001	-0.00002	-0.0001	0.0073	-0.0002	-0.003
LCT39-017	-0.023	-0.003	0.01	0.	-0.0001	0.0038	0.0011	-0.00003	-0.0001	0.0072	-0.0002	-0.002

The following observations can be made:

- sensitivity to clad parameters appears to dominate for most experiments, and this turns out to be true for the uncertainties when the tolerances are included;
- sensitivity to clad parameters is much lower in LCT07-003 and LCT07-004 than the other experiments;
- LCT07-003 and LCT07-004 have greater pitch than all other experiments.

The sensitivity data can be used to generate covariance and correlation matrices. The correlation matrix is illustrated in Figure below.

Figure 1.6. Correlation matrix for PWR fuel bundle – Scenario A

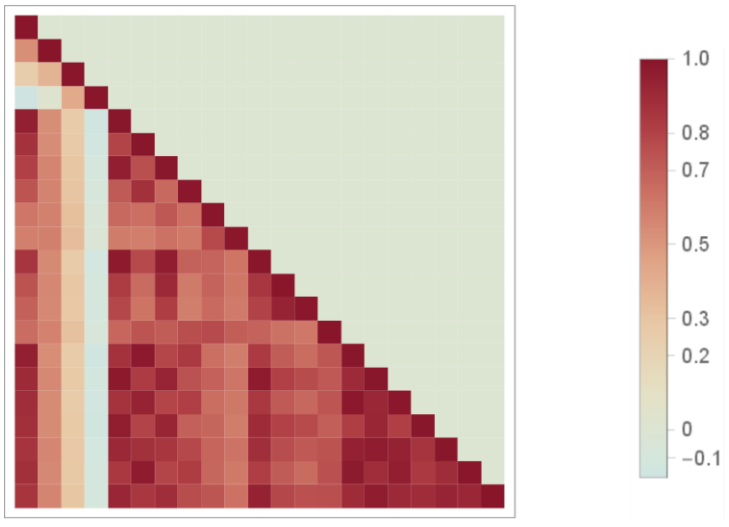

Source: NEA, 2020.

It may be observed the fourth experiment, i.e. LCT07-004 is very much an outlier in that it is relatively uncorrelated to the bulk of the experiments. The same is true to a lesser extent for LCT07-003. This is consistent with the observations from the sensitivity coefficient results.

Scenario E

Whilst for Scenario A a sensitivity analysis approach was used, with 13 MONK calculations run for each of the 21 experiments, a different approach was adopted for Scenario E, where the uncertain parameters were defined by a sampling process. The benchmark specification recognises the increased computational requirements for the analysis of Scenario E, and so a smaller subset of the experiments is specified: specifically the eight experiments LCT07-001 to LCT07-004, and LCT39, experiments 1, 6, 7 and 8.

To cover this scenario 100 MONK calculations were performed for each of the eight experiments. Latin Hypercube sampling was used, to try to make the process more efficient in terms of number of MONK runs required.

The correlation matrix for the eight experiments is shown in Figure 1.7 below.

Figure 1.7. Correlation matrix for PWR fuel bundle – Scenario E

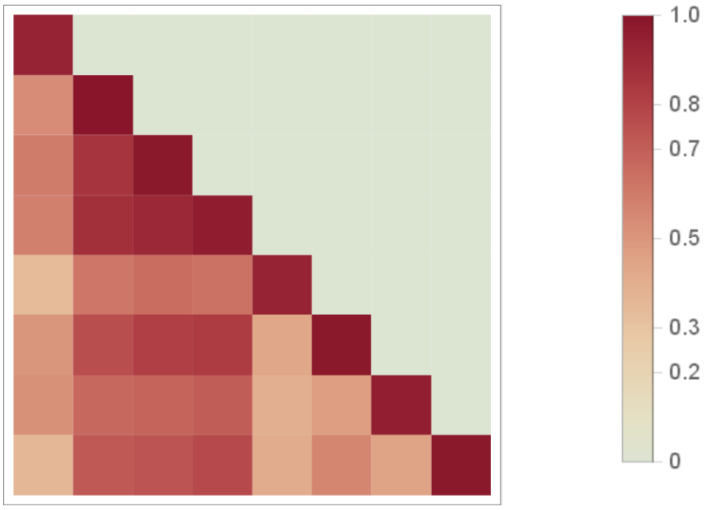

Source: NEA, 2020.

1.2.2. Application case

Now moving to the application case, the application case is a simplified 16x16 PWR fuel assembly, and six parameters are specified as uncertain – all are geometric. For the fuel rod these are: pellet diameter; cladding inner diameter; cladding outer diameter; active length. For the guide thimble these are: inner diameter; outer diameter. In the spirit of Scenario A, uncertainties (at the one standard deviation level) using MONK were calculated as follows:

Pellet diameter	-0.000205737
Cladding Inner Diameter	0.00128555
Cladding Outer Diameter	-0.00191305
ActiveLength	-9.51×10^{-6}
Thimble Inner Diameter	0.000206169
Thimble Outer Diameter	-0.000252769

This leads to an overall uncertainty of 0.00234, and this uncertainty is dominated by the uncertainty on cladding dimensions. Because in Scenario A, the cladding dimensions are fully correlated within each experiment, this accentuates the uncertainty due to these quantities. We may expect that these uncertainties will be significantly reduced in scenario E analysed below.

The overall uncertainty due to the specified geometry uncertainties, assuming independence, is therefore 0.00234 at the one standard deviation level, and this uncertainty does not take account of nuclear data uncertainty. By running a MONK covariance calculation, the nuclear data uncertainty could be incorporated to give an overall uncertainty (and this would then be closer to the idea of a prior uncertainty).

Estimation of bias

We now consider the experimental data and consider the bias correction arising from observing the difference between calculated and experimental values for k_{eff}. In this way the effect of possible nuclear data discrepancies is taken into account. We only consider reasonably simple treatments here where either a straight average, or a weighted average of the experimental database, or a subset of the experimental database, is taken. For our purposes here the experimental database is the 21 experiments under consideration for the benchmark exercise.

As noted in earlier discussions, experiments LCT07-003 & 004, with their greater pitch, can be considered outliers, and for example have a much lower sensitivity to the clad geometrical parameters than the other experiments. These considerations suggest they may be much less appropriate than the other experiments for use as benchmarks for the application. We therefore consider inclusion and exclusion of these experiments in the discussion below.

The combination of experiments we have considered are therefore: the full set of 21 experiments; the full set, but excluding LCT07-003 and LCT07-004; the set of 8 experiment used for scenario E; the set of 8, but excluding LCT07-003 and LCT07-004. The bias taken from calculations using an unweighted average is as follows (here bias is set as calculation minus experiment):

Table 1.11. Estimated bias for application case, based on differing numbers of experiments – unweighted average

	21 experiments	19 experiments	8 experiments	6 experiments
bias	-0.00341	-0.00342	-0.00317	-0.00273

Uncertainty on the bias

We already have a number of considerations/options for quantifying the uncertainty on the bias:

- choice of which experiments to choose as benchmarks;
- choice over whether to use an unweighted or weighted average of the benchmark results;
- choice over assumptions made regarding correlations of parameters within an experiment (Scenario A vs Scenario E);
- choice over assumptions made regarding correlations of parameters between experiments (fuel composition and dimensions).

Table 1.12. Summary of estimated uncertainty on bias

Scenario A, 21 experiments				
	uncorrelated	correlated		
unweighted	0.000915	0.003939		
weighted	0.000600	0.000289		
Scenario A, 19 experiments				
	uncorrelated	correlated		
unweighted	0.001008	0.004333		
weighted	0.000935	0.000511		
Scenario A, 8 experiments			Scenario E, 8 experiments	
	uncorrelated	correlated	uncorrelated	correlated
unweighted	0.001341	0.003206	0.000267	0.000657
weighted	0.000694	0.000509	0.0002151	0.000200
Scenario A, 6 experiments			Scenario E, 6 experiments	
	uncorrelated	correlated	uncorrelated	correlated
unweighted	0.001768	0.004195	0.0002313	0.000503
weighted	0.001500	0.000838	0.0002235	0.000363

These results appear reasonable, in that for the unweighted case the introduction of an assumption of correlations between the experiments leads to a much higher uncertainty. For example in the six experiment scenario A case there is approximately a factor of the square root of six between them, as might be expected. Also with the assumption of no correlation between experiments, using the weighted average gives a decrease in the estimated uncertainty – as intended. However, the cases where a weighted average is used with correlations assumed between experiments appear to give unbelievably low uncertainties – including correlations between experiments is actually reducing the estimated uncertainty. What is happening here is that the methodology is allowing large positive and negative coefficients to be applied in the weighted average, which seems counterintuitive. Possibly the methodology should modified in a way to prohibit negative coefficients.

2. Participant B

Participants: Oliver Buss, Axel Hoefer (Framatome GmbH, Germany)

2.1. Mathematical framework

For the evaluation of the Benchmark IV exercises, the Monte Carlo Bayes framework MOCABA is used (Hoefer et al., 2015).

MOCABA is a Bayesian learning procedure for improving predictions of integral observables (such as k_{eff}) by combining uncertainty information on basic input parameters (such as nuclear data) with information from integral measurements (e.g. criticality benchmark experiments). In contrast to the widely used Generalised Linear Least Squares (GLLS) methodology, MOCABA uses Monte Carlo sampling instead of first-order perturbation theory for uncertainty propagation. This allows one to apply Bayesian updating directly to the integral observables of interest without taking the detour via updating the input parameter distributions. As a result, MOCABA does not require the computation of any sensitivities of k_{eff} with respect to input parameter variations.

Applying the MOCABA framework to criticality safety validation, the application case and benchmark k_{eff} values, $\boldsymbol{k}_A$ and $\boldsymbol{k}_B$, are expressed as sub-vectors of a combined vector $\boldsymbol{k} = (\boldsymbol{k}_A, \boldsymbol{k}_B)^T$, which is viewed to be a function $\boldsymbol{k}(\boldsymbol{\alpha}, \boldsymbol{x})$ of a nuclear data vector $\boldsymbol{\alpha}$ and a system parameter vector $\boldsymbol{x} = (\boldsymbol{x}_A^T, \boldsymbol{x}_B^T)^T$ describing the application case and benchmark configurations (geometry, material composition, spatial arrangement, and physical state variables such as temperature).

Before taking into account the benchmark measurements, the uncertainty of $\boldsymbol{k}$ is defined by the uncertainty of the nuclear data vector $\boldsymbol{\alpha}$ and the uncertainty of the system parameter vector $\boldsymbol{x}$. The uncertainties of $\boldsymbol{\alpha}$ and $\boldsymbol{x}$ are expressed in terms of the multivariate probability density functions (pdfs) $p(\boldsymbol{\alpha})$ and $p(\boldsymbol{x})$, respectively.

Since $\boldsymbol{k}$ is a function of the random vectors $\boldsymbol{\alpha}$ and $\boldsymbol{x}$, $\boldsymbol{k}$ is itself a random vector, defined by a multivariate pdf $p(\boldsymbol{k})$. This prior pdf of $\boldsymbol{k}$ represents our knowledge about $\boldsymbol{k}$ before taking into account the benchmark measurements. Within the basic MOCABA framework considered in this paper, a multivariate normal distribution model is assumed for $p(\boldsymbol{k})$: [1]

$$p(\boldsymbol{k}) = N(\boldsymbol{k}_0, \boldsymbol{\Sigma}_0) \propto exp\left(-\frac{Q_0}{2}\right), \quad Q_0 = (\boldsymbol{k} - \boldsymbol{k}_0)^T \boldsymbol{\Sigma}_0^{-1} (\boldsymbol{k} - \boldsymbol{k}_0), \tag{2.1}$$

with:

$$\boldsymbol{k}_0 = (\boldsymbol{k}_{0A}^T, \boldsymbol{k}_{0B}^T)^T, \quad \boldsymbol{\Sigma}_0 = \begin{pmatrix} \boldsymbol{\Sigma}_{0A} & \boldsymbol{\Sigma}_{0AB} \\ \boldsymbol{\Sigma}_{0AB}^T & \boldsymbol{\Sigma}_{0B} \end{pmatrix}. \tag{2.2}$$

[1] It should be mentioned that the MOCABA method is not limited to normal distribution models. As mentioned in (Hoefer et al., 2015), it is straightforward to extend the model space to more general classes of multivariate distribution models by making use of invertible variable transformations. However, as has been verified by the authors, such model expansions hardly change the inferences for typical application cases in criticality safety analysis.

$\boldsymbol{k}_0$ is the vector of prior application case and benchmark k_{eff} values, and $\boldsymbol{\Sigma}_0$ is the corresponding prior covariance matrix due to nuclear data and system parameter uncertainties.

To calculate the prior model parameters, $\boldsymbol{k}_0$ and $\boldsymbol{\Sigma}_0$, random samples of the nuclear data vector $\boldsymbol{\alpha}$ and of the system parameter vector $\boldsymbol{x}$ are drawn from the nuclear data pdf $p(\boldsymbol{\alpha})$ and from the system parameter pdf $p(\boldsymbol{x})$, respectively. For each random draw $\left(\boldsymbol{\alpha}_j^{MC}, \boldsymbol{x}_j^{MC}\right)$, the corresponding k_{eff} values $\boldsymbol{k}_j^{MC} = \boldsymbol{k}\left(\boldsymbol{\alpha}_j^{MC}, \boldsymbol{x}_j^{MC}\right)$ are calculated. The prior mean vector and prior covariance matrix are then estimated by applying the corresponding unbiased estimators to the Monte Carlo data:

$$\boldsymbol{k}_0 = \frac{1}{m}\sum_{j=1}^{m} \boldsymbol{k}_j^{MC}, \quad \boldsymbol{\Sigma}_0 = \frac{1}{m-1}\sum_{j=1}^{m}\left(\boldsymbol{k}_j^{MC} - \boldsymbol{k}_0\right)\left(\boldsymbol{k}_j^{MC} - \boldsymbol{k}_0\right)^T. \tag{2.3}$$

In the above equation, m is the number of Monte Carlo draws. The measurements of benchmark k_{eff} values are expressed in terms of the measurement vector $\boldsymbol{v}_B$, whose uncertainty (limited knowledge of experimental configurations) is expressed in terms of the likelihood function $p(\boldsymbol{v}_B|\boldsymbol{k})$, which, for the basic MOCABA framework, is also expressed in terms of a normal distribution model:

$$p(\boldsymbol{v}_B|\boldsymbol{k}) \propto exp\left(-\frac{Q_V}{2}\right), \quad Q_V = (\boldsymbol{k}_B - \boldsymbol{v}_B)^T \boldsymbol{\Sigma}_{VB}^{-1}(\boldsymbol{k}_B - \boldsymbol{v}_B). \tag{2.4}$$

Here, $\boldsymbol{\Sigma}_{VB}$ is the covariance matrix of the experimental k_{eff} values due to uncertainties of the experimental system parameters. The diagonal elements of $\boldsymbol{\Sigma}_{VB}$ contain the variances of the experimental k_{eff} values due to uncertainties of the experimental setups (e.g. manufacturing tolerances) and measurements. The off-diagonal elements of $\boldsymbol{\Sigma}_{VB}$ are generally non-zero if different criticality benchmark experiments use the same experimental components, e.g. the same fuel rods. This leads to correlations between the experimental k_{eff} values of different experiments due to uncertainties of their shared components. Such correlations may have to be taken into account if different experiments from the same experimental series are included in the analysis.

The posterior distribution $p(\boldsymbol{k}|\boldsymbol{v}_B)$ represents the uncertainty of $\boldsymbol{k}$ when combining the prior knowledge about $\boldsymbol{k}$ and the information from the benchmark experiments. According to Bayes' theorem, the posterior distribution is given by the normalised product of the prior distribution and the likelihood function:

$$p(\boldsymbol{k}|\boldsymbol{v}_B) \propto p(\boldsymbol{v}_B|\boldsymbol{k})\, p(\boldsymbol{k}). \tag{2.5}$$

As shown in (Hoefer et al., 2015), the posterior distribution of k can be expressed as:

$$p(\boldsymbol{k}) = N(\boldsymbol{k}^*, \boldsymbol{\Sigma}^*) \propto exp\left(-\frac{Q^*}{2}\right), \quad Q^* = (\boldsymbol{k} - \boldsymbol{k}^*)^T \boldsymbol{\Sigma}^{*-1}(\boldsymbol{k} - \boldsymbol{k}^*), \tag{2.6}$$

with the posterior model parameters:

$$\boldsymbol{k}^* = (\boldsymbol{k}_A^{*T}, \boldsymbol{k}_B^{*T})^T, \quad \boldsymbol{\Sigma}^* = \begin{pmatrix} \boldsymbol{\Sigma}_A^* & \boldsymbol{\Sigma}_{AB}^* \\ \boldsymbol{\Sigma}_{AB}^{*T} & \boldsymbol{\Sigma}_B^* \end{pmatrix}, \tag{2.7}$$

$$\boldsymbol{k}_A^* = \boldsymbol{k}_{0A} + \boldsymbol{\Sigma}_{0AB}(\boldsymbol{\Sigma}_{0B} + \boldsymbol{\Sigma}_{VB})^{-1}(\boldsymbol{v}_B - \boldsymbol{k}_{0B}), \tag{2.8}$$

$$\boldsymbol{k}_B^* = \boldsymbol{k}_{0B} + \boldsymbol{\Sigma}_{0B}(\boldsymbol{\Sigma}_{0B} + \boldsymbol{\Sigma}_{VB})^{-1}(\boldsymbol{v}_B - \boldsymbol{k}_{0B}), \tag{2.9}$$

$$\boldsymbol{\Sigma}_A^* = \boldsymbol{\Sigma}_{0A} - \boldsymbol{\Sigma}_{0AB}(\boldsymbol{\Sigma}_{0B} + \boldsymbol{\Sigma}_{VB})^{-1}\boldsymbol{\Sigma}_{0AB}^T, \tag{2.10}$$

$$\boldsymbol{\Sigma}_B^* = \boldsymbol{\Sigma}_{0B} - \boldsymbol{\Sigma}_{0B}(\boldsymbol{\Sigma}_{0B} + \boldsymbol{\Sigma}_{VB})^{-1}\boldsymbol{\Sigma}_{0B}, \tag{2.11}$$

$$\boldsymbol{\Sigma}_{AB}^* = \boldsymbol{\Sigma}_{0AB} - \boldsymbol{\Sigma}_{0AB}(\boldsymbol{\Sigma}_{0B} + \boldsymbol{\Sigma}_{VB})^{-1}\boldsymbol{\Sigma}_{0B}. \tag{2.12}$$

Two alternative approaches are used to calculate the benchmark covariance matrix $\boldsymbol{\Sigma}_{VB}$, a sensitivity approach and a Monte Carlo approach.

For the sensitivity approach, $\boldsymbol{\Sigma}_{VB}$ is expressed as a linear transformation of the (diagonal) covariance matrix $\boldsymbol{\Sigma}_{XB}$ of independent input parameters (linear error propagation):

$$\boldsymbol{\Sigma}_{VB} = \boldsymbol{S}_B \boldsymbol{\Sigma}_{XB} \boldsymbol{S}_B^T. \tag{2.13}$$

Here $\boldsymbol{S}_B$ denotes the matrix of sensitivities (first derivatives) of the benchmark k_{eff} values with respect to the benchmark system parameters. The sensitivities (components of $\boldsymbol{S}_B$) are identified with the slopes of the first order fits of the benchmark k_{eff} values as functions of the system parameters.

For the Monte Carlo approach, the benchmark system parameters $\boldsymbol{x}_B$ are sampled from the specified uncertainty distribution $p(\boldsymbol{x}_B)$, and each random set of input parameters $\boldsymbol{x}_{B,j}^{MC}$ is used in a separate calculation of the vector $\boldsymbol{k}_B(\boldsymbol{x}_{B,j}^{MC})$ of benchmark k_{eff} values. The covariance matrix $\boldsymbol{\Sigma}_{VB}$ is then estimated according to:

$$\boldsymbol{\Sigma}_{VB} = \frac{1}{m-1}\sum_{i=1}^{m}\left(\boldsymbol{k}_B(\boldsymbol{x}_{B,j}^{MC}) - \bar{\boldsymbol{k}}_B\right)\left(\boldsymbol{k}_B(\boldsymbol{x}_{B,j}^{MC}) - \bar{\boldsymbol{k}}_B\right)^T, \quad \text{with} \quad \bar{\boldsymbol{k}}_B = \frac{1}{m}\sum_{i=1}^{m}\boldsymbol{k}_B(\boldsymbol{x}_{B,j}^{MC}). \tag{2.14}$$

2.2. Toy model

Used software: Microsoft Excel.

The covariance matrix $\boldsymbol{\Sigma}_{VB}$ of benchmark k_{eff} values due to benchmark system parameter uncertainties is obtained according to Equation (2.13), thus by a linear transformation of the
19-dimensional diagonal covariance matrix of independent system parameters $\boldsymbol{\Sigma}_{VB} = diag(0.0025, \ldots, 0.0025)$ using the matrix $\boldsymbol{S}_B$ of sensitivities $s_{ij} = \partial k_i / \partial p_j$ of benchmark k_{eff} values k_i to the system parameters p_j as a transformation matrix.

Under the assumption that the first system parameter x_1 is identical for all nine benchmark experiments, the resulting matrix $\boldsymbol{\Sigma}_{VB}$ is given by:

2.689E-05	1.755E-05	1.767E-05	1.813E-05	1.829E-05	1.761E-05	1.845E-05	1.844E-05	1.866E-05
1.755E-05	2.669E-05	1.753E-05	1.798E-05	1.815E-05	1.747E-05	1.831E-05	1.829E-05	1.852E-05
1.767E-05	1.753E-05	2.686E-05	1.810E-05	1.827E-05	1.759E-05	1.843E-05	1.841E-05	1.864E-05
1.813E-05	1.798E-05	1.810E-05	2.755E-05	1.875E-05	1.804E-05	1.891E-05	1.889E-05	1.912E-05
1.829E-05	1.815E-05	1.827E-05	1.875E-05	2.781E-05	1.821E-05	1.908E-05	1.907E-05	1.930E-05
1.761E-05	1.747E-05	1.759E-05	1.804E-05	1.821E-05	2.677E-05	1.837E-05	1.835E-05	1.858E-05
1.845E-05	1.831E-05	1.843E-05	1.891E-05	1.908E-05	1.837E-05	2.806E-05	1.923E-05	1.947E-05
1.844E-05	1.829E-05	1.841E-05	1.889E-05	1.907E-05	1.835E-05	1.923E-05	2.803E-05	1.945E-05
1.866E-05	1.852E-05	1.864E-05	1.912E-05	1.930E-05	1.858E-05	1.947E-05	1.945E-05	2.839E-05

Source: NEA, 2020.

The corresponding matrix of Pearson correlations is given by:

1.00	0.66	0.66	0.67	0.67	0.66	0.67	0.67	0.68
0.66	1.00	0.65	0.66	0.67	0.65	0.67	0.67	0.67
0.66	0.65	1.00	0.67	0.67	0.66	0.67	0.67	0.67
0.67	0.66	0.67	1.00	0.68	0.66	0.68	0.68	0.68
0.67	0.67	0.67	0.68	1.00	0.67	0.68	0.68	0.69
0.66	0.65	0.66	0.66	0.67	1.00	0.67	0.67	0.67
0.67	0.67	0.67	0.68	0.68	0.67	1.00	0.69	0.69
0.67	0.67	0.67	0.68	0.68	0.67	0.69	1.00	0.69
0.68	0.67	0.67	0.68	0.69	0.67	0.69	0.69	1.00

Source: NEA, 2020.

For the case that x_1 is independent for all nine benchmark experiments, the corresponding covariance and correlation matrix is obtained simply by setting all off-diagonal elements of the above two matrices to zero.

The prior model parameters, $\boldsymbol{k}_0$ and $\boldsymbol{\Sigma}_0$, are calculated according to Equation (2.3) based on $m = 10{,}000$ Monte Carlo samples of the nuclear data vector $\boldsymbol{\alpha}$.

The posterior application case k_{eff} value and the corresponding posterior covariance matrix are obtained by inserting the benchmark k_{eff} values (represented by the vector $\boldsymbol{v}_B$), $\boldsymbol{\Sigma}_{VB}$, $\boldsymbol{k}_0$, and $\boldsymbol{\Sigma}_0$ into Equations (2.8) and (2.10).

The obtained prior and posterior application k_{eff} values and their standard deviations σ are given in Table 2.1.

Table 2.1. Prior and posterior application k_{eff} values and their standard deviations $\boldsymbol{\sigma}$

	Prior k_{eff}	Prior σ	Posterior k_{eff}	Posterior σ
x_1 identical	9.53627E-01	9.71403E-03	9.46170E-01	3.85426E-03
x_1 independent	9.53627E-01	9.71403E-03	9.43733E-01	1.92914E-03

2.3. Realistic case: Experiments with water-reflected UO_2 fuel rod arrays

Used software: SCALE 6.0 / NITAWL (ORNL, 2009).

Nuclear Data Library: 238 group AMPX random libraries generated from ENDF/B-VII.1 data with NUDUNA (Buss, Hoefer and Neuber, 2011) for ^{235}U, ^{238}U, ^{1}H and ^{16}O.

As regards the modelling of fuel rod position uncertainties, only Scenario A is analysed.

Two alternative approaches are followed to calculate the covariance matrix $\boldsymbol{\Sigma}_{VB}$ of benchmark k_{eff} values due to benchmark system parameter uncertainties:

- Sensitivity approach according Equation (2.13) taking into account uncertainties of three system parameters: fuel rod cladding inner diameter, fuel rod cladding thickness, and fuel density.
- Monte Carlo approach according to Equation (2.14) based on 200 Monte Carlo samples of 30 benchmark parameters: fuel rod cladding inner diameter, fuel rod cladding thickness, fuel density, fuel pellet diameter, height of fissile column, B-10 impurity, ^{234}U in U, ^{235}U in U, ^{236}U in U, and the critical water heights of all 21-benchmark experiment.

For the sensitivity approach, the following covariance matrix $\boldsymbol{\Sigma}_{VB}$ is obtained:

2.36E-05	1.01E-05	2.77E-06	-1.70E-07	2.24E-05	2.06E-05	1.94E-05	1.82E-05	1.42E-05	1.50E-05	2.11E-05	2.09E-05	1.93E-05	1.83E-05	2.17E-05	2.13E-05	2.07E-05	1.98E-05	2.12E-05	2.09E-05	2.04E-05
1.01E-05	4.44E-06	1.51E-06	3.15E-07	9.60E-06	8.80E-06	8.36E-06	7.77E-06	6.17E-06	6.55E-06	9.03E-06	9.00E-06	8.39E-06	7.88E-06	9.29E-06	9.14E-06	8.87E-06	8.49E-06	9.06E-06	8.97E-06	8.76E-06
2.77E-06	1.51E-06	1.32E-06	1.21E-06	2.60E-06	2.36E-06	2.47E-06	2.07E-06	1.93E-06	2.13E-06	2.56E-06	2.63E-06	2.66E-06	2.30E-06	2.49E-06	2.51E-06	2.38E-06	2.36E-06	2.48E-06	2.53E-06	2.52E-06
-1.70E-07	3.15E-07	1.21E-06	1.59E-06	-2.21E-07	-2.38E-07	5.84E-08	-2.42E-07	2.30E-07	3.40E-07	2.55E-09	8.91E-08	3.55E-07	8.16E-08	-2.51E-07	-1.58E-07	-2.47E-07	-1.10E-07	-1.40E-07	-5.40E-08	-2.25E-08
2.24E-05	9.60E-06	2.60E-06	-2.21E-07	2.13E-05	1.95E-05	1.84E-05	1.73E-05	1.35E-05	1.42E-05	2.00E-05	1.98E-05	1.83E-05	1.74E-05	2.06E-05	2.02E-05	1.97E-05	1.88E-05	2.01E-05	1.98E-05	1.93E-05
2.06E-05	8.80E-06	2.36E-06	-2.38E-07	1.95E-05	1.79E-05	1.69E-05	1.58E-05	1.23E-05	1.30E-05	1.83E-05	1.82E-05	1.68E-05	1.59E-05	1.89E-05	1.86E-05	1.81E-05	1.72E-05	1.84E-05	1.82E-05	1.77E-05
1.94E-05	8.36E-06	2.47E-06	5.84E-08	1.84E-05	1.69E-05	1.59E-05	1.49E-05	1.17E-05	1.24E-05	1.72E-05	1.71E-05	1.59E-05	1.50E-05	1.78E-05	1.75E-05	1.70E-05	1.62E-05	1.73E-05	1.71E-05	1.67E-05
1.82E-05	7.77E-06	2.07E-06	-2.42E-07	1.73E-05	1.58E-05	1.49E-05	1.40E-05	1.09E-05	1.15E-05	1.62E-05	1.60E-05	1.48E-05	1.41E-05	1.67E-05	1.64E-05	1.60E-05	1.52E-05	1.63E-05	1.61E-05	1.57E-05
1.42E-05	6.17E-06	1.93E-06	2.30E-07	1.35E-05	1.23E-05	1.17E-05	1.09E-05	8.60E-06	9.11E-06	1.27E-05	1.26E-05	1.17E-05	1.10E-05	1.30E-05	1.28E-05	1.24E-05	1.19E-05	1.27E-05	1.26E-05	1.23E-05
1.50E-05	6.55E-06	2.13E-06	3.40E-07	1.42E-05	1.30E-05	1.24E-05	1.15E-05	9.11E-06	9.65E-06	1.34E-05	1.33E-05	1.24E-05	1.17E-05	1.38E-05	1.35E-05	1.31E-05	1.26E-05	1.34E-05	1.33E-05	1.30E-05
2.11E-05	9.03E-06	2.56E-06	2.55E-09	2.00E-05	1.83E-05	1.72E-05	1.62E-05	1.27E-05	1.34E-05	1.88E-05	1.86E-05	1.72E-05	1.63E-05	1.93E-05	1.90E-05	1.84E-05	1.76E-05	1.89E-05	1.86E-05	1.81E-05
2.09E-05	9.00E-06	2.63E-06	8.91E-08	1.98E-05	1.82E-05	1.71E-05	1.60E-05	1.26E-05	1.33E-05	1.86E-05	1.85E-05	1.71E-05	1.62E-05	1.92E-05	1.88E-05	1.83E-05	1.75E-05	1.87E-05	1.84E-05	1.80E-05
1.93E-05	8.39E-06	2.66E-06	3.55E-07	1.83E-05	1.68E-05	1.59E-05	1.48E-05	1.17E-05	1.24E-05	1.72E-05	1.71E-05	1.59E-05	1.50E-05	1.77E-05	1.74E-05	1.69E-05	1.62E-05	1.73E-05	1.71E-05	1.67E-05
1.83E-05	7.88E-06	2.30E-06	8.16E-08	1.74E-05	1.59E-05	1.50E-05	1.41E-05	1.10E-05	1.17E-05	1.63E-05	1.62E-05	1.50E-05	1.42E-05	1.68E-05	1.65E-05	1.60E-05	1.53E-05	1.64E-05	1.62E-05	1.58E-05
2.17E-05	9.29E-06	2.49E-06	-2.51E-07	2.06E-05	1.89E-05	1.78E-05	1.67E-05	1.30E-05	1.38E-05	1.93E-05	1.92E-05	1.77E-05	1.68E-05	2.00E-05	1.96E-05	1.91E-05	1.82E-05	1.94E-05	1.92E-05	1.87E-05
2.13E-05	9.14E-06	2.51E-06	-1.58E-07	2.02E-05	1.86E-05	1.75E-05	1.64E-05	1.28E-05	1.35E-05	1.90E-05	1.88E-05	1.74E-05	1.65E-05	1.96E-05	1.92E-05	1.87E-05	1.78E-05	1.91E-05	1.88E-05	1.84E-05
2.07E-05	8.87E-06	2.38E-06	-2.47E-07	1.97E-05	1.81E-05	1.70E-05	1.60E-05	1.24E-05	1.31E-05	1.84E-05	1.83E-05	1.69E-05	1.60E-05	1.91E-05	1.87E-05	1.82E-05	1.74E-05	1.86E-05	1.83E-05	1.79E-05
1.98E-05	8.49E-06	2.36E-06	-1.10E-07	1.88E-05	1.72E-05	1.62E-05	1.52E-05	1.19E-05	1.26E-05	1.76E-05	1.75E-05	1.62E-05	1.53E-05	1.82E-05	1.78E-05	1.74E-05	1.66E-05	1.77E-05	1.75E-05	1.70E-05
2.12E-05	9.06E-06	2.48E-06	-1.40E-07	2.01E-05	1.84E-05	1.73E-05	1.63E-05	1.27E-05	1.34E-05	1.89E-05	1.87E-05	1.73E-05	1.64E-05	1.94E-05	1.91E-05	1.86E-05	1.77E-05	1.90E-05	1.87E-05	1.82E-05
2.09E-05	8.97E-06	2.53E-06	-5.40E-08	1.98E-05	1.82E-05	1.71E-05	1.61E-05	1.26E-05	1.33E-05	1.86E-05	1.84E-05	1.71E-05	1.62E-05	1.92E-05	1.88E-05	1.83E-05	1.75E-05	1.87E-05	1.84E-05	1.80E-05
2.04E-05	8.76E-06	2.52E-06	-2.25E-08	1.93E-05	1.77E-05	1.67E-05	1.57E-05	1.23E-05	1.30E-05	1.81E-05	1.80E-05	1.67E-05	1.58E-05	1.87E-05	1.84E-05	1.79E-05	1.70E-05	1.82E-05	1.80E-05	1.76E-05

Source: NEA, 2020.

The corresponding correlation matrix is given by:

Correlation Coefficients X 1000																				
Option 2	LCT-07-01	LCT-07-02	LCT-07-03	LCT-07-04	LCT-39-01	LCT-39-02	LCT-39-03	LCT-39-04	LCT-39-05	LCT-39-06	LCT-39-07	LCT-39-08	LCT-39-09	LCT-39-10	LCT-39-11	LCT-39-12	LCT-39-13	LCT-39-14	LCT-39-15	LCT-39-16	LCT-39-17
LCT-07-01	1000	988	495	-28	1000	1000	998	999	996	992	999	999	995	999	1000	1000	999	1000	1000	1000	999
LCT-07-02	988	1000	624	118	987	986	994	985	997	999	989	993	998	992	986	988	986	989	987	991	992
LCT-07-03	495	624	1000	834	490	484	538	480	572	597	512	532	580	529	484	498	485	504	494	513	522
LCT-07-04	-28	118	834	1000	-38	-45	12	-51	62	87	0	16	71	17	-44	-28	-46	-21	-25	-10	-4
LCT-39-01	1000	987	490	-38	1000	1000	998	1000	995	992	998	998	994	998	1000	1000	1000	1000	999	1000	999
LCT-39-02	1000	986	484	-45	1000	1000	998	1000	994	991	998	998	993	997	1000	1000	1000	1000	999	999	999
LCT-39-03	998	994	538	12	998	998	1000	998	998	997	996	998	998	997	998	999	998	999	997	999	1000
LCT-39-04	999	985	480	-51	1000	1000	998	1000	993	990	997	997	993	997	1000	1000	1000	1000	999	999	999
LCT-39-05	996	997	572	62	995	994	998	993	1000	999	997	999	1000	998	994	996	994	996	996	997	997
LCT-39-06	992	999	597	87	992	991	997	990	999	1000	993	996	1000	995	991	993	991	994	992	995	996
LCT-39-07	999	989	512	0	998	998	996	997	997	993	1000	999	996	1000	998	998	997	998	999	999	997
LCT-39-08	999	993	532	16	998	998	998	997	999	996	999	1000	998	1000	998	999	998	999	999	1000	999
LCT-39-09	995	998	580	71	994	993	998	993	1000	1000	996	998	1000	998	993	995	993	996	995	997	997
LCT-39-10	999	992	529	17	998	997	997	997	998	995	1000	1000	998	1000	997	998	997	998	999	999	998
LCT-39-11	1000	986	484	-44	1000	1000	998	1000	994	991	998	998	993	997	1000	1000	1000	1000	999	999	999
LCT-39-12	1000	988	498	-28	1000	1000	999	1000	996	993	998	999	995	998	1000	1000	1000	1000	999	1000	999
LCT-39-13	999	986	485	-46	1000	1000	998	1000	994	991	997	998	993	997	1000	1000	1000	1000	999	999	999
LCT-39-14	1000	989	504	-21	1000	1000	999	1000	996	994	998	999	996	998	1000	1000	1000	1000	999	1000	1000
LCT-39-15	1000	987	494	-25	999	999	997	999	996	992	999	999	995	999	999	999	999	999	1000	999	998
LCT-39-16	1000	991	513	-10	1000	999	999	999	997	995	999	1000	997	999	999	1000	999	1000	999	1000	1000
LCT-39-17	999	992	522	-4	999	999	1000	999	997	996	997	999	997	998	999	999	999	1000	998	1000	1000

Source: NEA, 2020.

For the Monte Carlo approach, the following covariance matrix $\boldsymbol{\Sigma}_{VB}$ is obtained:

2.23E-05	9.36E-06	2.46E-06	-5.40E-07	2.04E-05	1.98E-05	1.81E-05	1.77E-05	1.32E-05	1.37E-05	1.96E-05	1.86E-05	1.81E-05	1.59E-05	2.05E-05	2.02E-05	1.96E-05	1.93E-05	1.91E-05	1.91E-05	1.90E-05
9.36E-06	4.40E-06	1.50E-06	3.48E-07	8.69E-06	8.43E-06	7.74E-06	7.58E-06	5.77E-06	6.00E-06	8.36E-06	7.96E-06	7.80E-06	6.87E-06	8.73E-06	8.62E-06	8.37E-06	8.25E-06	8.16E-06	8.16E-06	8.12E-06
2.46E-06	1.50E-06	1.39E-06	1.14E-06	2.34E-06	2.34E-06	2.18E-06	2.15E-06	1.79E-06	1.92E-06	2.31E-06	2.22E-06	2.23E-06	2.01E-06	2.39E-06	2.39E-06	2.29E-06	2.29E-06	2.27E-06	2.30E-06	2.28E-06
-5.40E-07	3.48E-07	1.14E-06	1.76E-06	-4.06E-07	-3.26E-07	-2.22E-07	-1.90E-07	8.39E-08	1.56E-07	-2.93E-07	-2.72E-07	-1.90E-07	-7.44E-08	-3.74E-07	-3.57E-07	-3.77E-07	-2.96E-07	-2.93E-07	-2.53E-07	-2.34E-07
2.04E-05	8.69E-06	2.34E-06	-4.06E-07	1.91E-05	1.83E-05	1.67E-05	1.63E-05	1.22E-05	1.27E-05	1.81E-05	1.72E-05	1.68E-05	1.47E-05	1.89E-05	1.87E-05	1.81E-05	1.79E-05	1.76E-05	1.76E-05	1.75E-05
1.98E-05	8.43E-06	2.34E-06	-3.26E-07	1.83E-05	1.79E-05	1.62E-05	1.58E-05	1.19E-05	1.23E-05	1.75E-05	1.67E-05	1.62E-05	1.42E-05	1.83E-05	1.81E-05	1.75E-05	1.73E-05	1.71E-05	1.71E-05	1.70E-05
1.81E-05	7.74E-06	2.18E-06	-2.22E-07	1.67E-05	1.62E-05	1.50E-05	1.45E-05	1.09E-05	1.13E-05	1.60E-05	1.52E-05	1.49E-05	1.30E-05	1.68E-05	1.65E-05	1.61E-05	1.58E-05	1.57E-05	1.56E-05	1.55E-05
1.77E-05	7.58E-06	2.15E-06	-1.90E-07	1.63E-05	1.58E-05	1.45E-05	1.44E-05	1.06E-05	1.10E-05	1.57E-05	1.49E-05	1.46E-05	1.28E-05	1.64E-05	1.62E-05	1.57E-05	1.55E-05	1.53E-05	1.53E-05	1.52E-05
1.32E-05	5.77E-06	1.79E-06	8.39E-08	1.22E-05	1.19E-05	1.09E-05	1.06E-05	8.24E-06	8.36E-06	1.18E-05	1.12E-05	1.09E-05	9.61E-06	1.23E-05	1.22E-05	1.18E-05	1.16E-05	1.15E-05	1.15E-05	1.14E-05
1.37E-05	6.00E-06	1.92E-06	1.56E-07	1.27E-05	1.23E-05	1.13E-05	1.10E-05	8.36E-06	8.89E-06	1.22E-05	1.16E-05	1.14E-05	9.95E-06	1.28E-05	1.26E-05	1.22E-05	1.21E-05	1.19E-05	1.19E-05	1.18E-05
1.96E-05	8.36E-06	2.31E-06	-2.93E-07	1.81E-05	1.75E-05	1.60E-05	1.57E-05	1.18E-05	1.22E-05	1.75E-05	1.65E-05	1.61E-05	1.41E-05	1.82E-05	1.79E-05	1.74E-05	1.71E-05	1.69E-05	1.69E-05	1.68E-05
1.86E-05	7.96E-06	2.22E-06	-2.72E-07	1.72E-05	1.67E-05	1.52E-05	1.49E-05	1.12E-05	1.16E-05	1.65E-05	1.59E-05	1.53E-05	1.34E-05	1.73E-05	1.71E-05	1.65E-05	1.63E-05	1.61E-05	1.61E-05	1.60E-05
1.81E-05	7.80E-06	2.23E-06	-1.90E-07	1.68E-05	1.62E-05	1.49E-05	1.46E-05	1.09E-05	1.14E-05	1.61E-05	1.53E-05	1.51E-05	1.31E-05	1.68E-05	1.66E-05	1.61E-05	1.59E-05	1.57E-05	1.57E-05	1.56E-05
1.59E-05	6.87E-06	2.01E-06	-7.44E-08	1.47E-05	1.42E-05	1.30E-05	1.28E-05	9.61E-06	9.95E-06	1.41E-05	1.34E-05	1.31E-05	1.17E-05	1.48E-05	1.46E-05	1.41E-05	1.39E-05	1.38E-05	1.37E-05	1.37E-05
2.05E-05	8.73E-06	2.39E-06	-3.74E-07	1.89E-05	1.83E-05	1.68E-05	1.64E-05	1.23E-05	1.28E-05	1.82E-05	1.73E-05	1.68E-05	1.48E-05	1.92E-05	1.88E-05	1.82E-05	1.79E-05	1.77E-05	1.77E-05	1.76E-05
2.02E-05	8.62E-06	2.39E-06	-3.57E-07	1.87E-05	1.81E-05	1.65E-05	1.62E-05	1.22E-05	1.26E-05	1.79E-05	1.71E-05	1.66E-05	1.46E-05	1.88E-05	1.87E-05	1.80E-05	1.77E-05	1.75E-05	1.75E-05	1.73E-05
1.96E-05	8.37E-06	2.29E-06	-3.77E-07	1.81E-05	1.75E-05	1.61E-05	1.57E-05	1.18E-05	1.22E-05	1.74E-05	1.65E-05	1.61E-05	1.41E-05	1.82E-05	1.80E-05	1.76E-05	1.72E-05	1.69E-05	1.69E-05	1.68E-05
1.93E-05	8.25E-06	2.29E-06	-2.96E-07	1.79E-05	1.73E-05	1.58E-05	1.55E-05	1.16E-05	1.21E-05	1.71E-05	1.63E-05	1.59E-05	1.39E-05	1.79E-05	1.77E-05	1.72E-05	1.71E-05	1.67E-05	1.67E-05	1.66E-05
1.91E-05	8.16E-06	2.27E-06	-2.93E-07	1.76E-05	1.71E-05	1.57E-05	1.53E-05	1.15E-05	1.19E-05	1.69E-05	1.61E-05	1.57E-05	1.38E-05	1.77E-05	1.75E-05	1.69E-05	1.67E-05	1.67E-05	1.65E-05	1.64E-05
1.91E-05	8.16E-06	2.30E-06	-2.53E-07	1.76E-05	1.71E-05	1.56E-05	1.53E-05	1.15E-05	1.19E-05	1.69E-05	1.61E-05	1.57E-05	1.37E-05	1.77E-05	1.75E-05	1.69E-05	1.67E-05	1.65E-05	1.67E-05	1.64E-05
1.90E-05	8.12E-06	2.28E-06	-2.34E-07	1.75E-05	1.70E-05	1.55E-05	1.52E-05	1.14E-05	1.18E-05	1.68E-05	1.60E-05	1.56E-05	1.37E-05	1.76E-05	1.73E-05	1.68E-05	1.66E-05	1.64E-05	1.64E-05	1.64E-05

Source: NEA, 2020.

The corresponding correlation matrix is given by:

Correlation Coefficients X 1000

Option 2	LCT-07-01	LCT-07-02	LCT-07-03	LCT-07-04	LCT-39-01	LCT-39-02	LCT-39-03	LCT-39-04	LCT-39-05	LCT-39-06	LCT-39-07	LCT-39-08	LCT-39-09	LCT-39-10	LCT-39-11	LCT-39-12	LCT-39-13	LCT-39-14	LCT-39-15	LCT-39-16	LCT-39-17
LCT-07-01	1000	946	443	-86	991	991	989	987	976	976	990	990	988	985	992	990	991	991	990	989	990
LCT-07-02	946	1000	608	125	948	951	953	953	959	960	952	952	956	957	951	950	952	951	951	952	955
LCT-07-03	443	608	1000	730	454	469	479	482	530	547	469	473	487	498	462	470	464	471	470	477	477
LCT-07-04	-86	125	730	1000	-70	-58	-43	-38	22	39	-53	-51	-37	-16	-64	-62	-68	-54	-54	-47	-43
LCT-39-01	991	948	454	-70	1000	990	988	987	977	977	989	989	986	984	989	990	989	989	987	987	989
LCT-39-02	991	951	469	-58	990	1000	988	988	978	977	989	989	988	985	989	990	989	989	988	989	990
LCT-39-03	989	953	479	-43	988	988	1000	987	978	978	988	987	986	984	988	988	989	988	988	986	989
LCT-39-04	987	953	482	-38	987	988	987	1000	979	978	987	987	988	984	988	987	987	987	986	986	987
LCT-39-05	976	959	530	22	977	978	978	979	1000	977	980	978	979	979	977	980	978	979	979	977	980
LCT-39-06	976	960	547	39	977	977	978	978	977	1000	978	977	979	975	977	977	977	977	978	977	978
LCT-39-07	990	952	469	-53	989	989	988	987	980	978	1000	989	989	986	991	990	989	990	988	988	990
LCT-39-08	990	952	473	-51	989	989	987	987	978	977	989	1000	987	984	989	989	988	989	988	987	989
LCT-39-09	988	956	487	-37	986	988	986	988	979	979	989	987	1000	985	987	987	987	987	987	986	987
LCT-39-10	985	957	498	-16	984	985	984	984	979	975	986	984	985	1000	986	984	985	984	983	983	986
LCT-39-11	992	951	462	-64	989	989	988	988	977	977	991	989	987	986	1000	989	991	990	988	989	990
LCT-39-12	990	950	470	-62	990	990	988	987	980	977	990	989	987	984	989	1000	990	990	989	988	989
LCT-39-13	991	952	464	-68	989	989	989	987	978	977	989	988	987	985	991	990	1000	990	987	988	990
LCT-39-14	991	951	471	-54	989	989	988	987	979	978	990	989	987	984	990	990	990	1000	988	987	989
LCT-39-15	990	951	470	-54	987	988	988	986	979	977	988	988	987	983	988	989	987	988	1000	987	988
LCT-39-16	989	952	477	-47	987	989	986	986	977	977	988	987	986	983	989	988	988	987	987	1000	989
LCT-39-17	990	955	477	-43	989	990	989	987	980	978	990	989	987	986	990	989	990	989	988	989	1000

Source: NEA, 2020.

The prior model parameters, $\boldsymbol{k}_0$ and $\boldsymbol{\Sigma}_0$, are calculated according to Equation (3) based on $m = 400$ Monte Carlo samples of the nuclear data vector $\boldsymbol{\alpha}$ (random nuclear data libraries obtained with NUDUNA).

The posterior application case k_{eff} values and the corresponding posterior covariance matrices are obtained by inserting the benchmark k_{eff} values (represented by the vector $\boldsymbol{v}_B$), $\boldsymbol{\Sigma}_{VB}$, $\boldsymbol{k}_0$, and $\boldsymbol{\Sigma}_0$ into Equations (2.8) and (2.10).

Using the sensitivity approach, the obtained prior and posterior application case k_{eff} values and their standard deviations σ are given in Table 2.2.

Table 2.1. Prior and posterior application case k_{eff} values and their standard deviation using the sensitivity approach

Application Case	Prior k_{eff}	Prior σ	Posterior k_{eff} (benchmark correlations taken into account)	Posterior σ (benchmark correlations taken into account)	Posterior k_{eff} (benchmark correlations neglected)	Posterior σ (benchmark correlations neglected)
LCT-079 Case 1	9.97852E-01	6.05446E-03	1.00160E+00	1.83840E-03	1.00210E+00	1.62620E-03
LCT-079 Case 1	9.97600E-01	5.12314E-03	1.00042E+00	1.06877E-03	1.00135E+00	9.68741E-04
16x16 FA	9.69213E-01	5.80334E-03	9.72428E-01	2.07158E-03	9.73219E-01	2.10594E-03

Using the Monte Carlo approach, the obtained prior and posterior application case k_{eff} values and their standard deviations σ are given in Table 2.2.

Table 2.2 Prior and posterior application case k_{eff} values and their standard deviation using the Monte Carlo approach

Application Case	Prior k_{eff}	Prior σ	Posterior k_{eff} (benchmark correlations taken into account)	Posterior σ (benchmark correlations taken into account)	Posterior k_{eff} (benchmark correlations neglected)	Posterior σ (benchmark correlations neglected)
LCT-079 Case 1	9.97852E-01	6.05446E-03	1.00141E+00	2.14961E-03	1.00210E+00	1.60982E-03
LCT-079 Case 1	9.97600E-01	5.12314E-03	1.00054E+00	1.34324E-03	1.00134E+00	9.67028E-04
16x16 FA	9.69213E-01	5.80334E-03	9.72326E-01	2.29061E-03	9.73215E-01	2.09709E-03

3. Participant C

The contribution of Participant C is currently not available.

4. Participant D

Participant: D. Mennerdahl (EMS, Sweden)

4.1. Introduction

The primary interest is to study correlations between benchmarks, based on evaluated integral experiments (or other measurements, including during normal operations of a reactor) and related to fission chain-reactions, e.g. as quantified by the effective neutron multiplication factor k_{eff} (or by changes to k_{eff} as expressed by various reactivity parameters). In addition to correlations between experiment parameters and procedures, benchmark correlations also include correlations between simplifications made to develop the benchmark specifications (including results).

Correlations applicable within the same benchmark need to be separated from correlations between different benchmarks. Those within the same benchmark have become more and more properly accounted for in ICSBEP evaluations (NEA, 2015). Correlations between different benchmarks (within the same evaluation or in different evaluations) have not been accounted for adequately, neither in ICSBEP evaluations or in nuclear criticality safety validation.

An important task is to determine how various benchmark correlations affect k_{eff} values of applications of the methods that are validated using the benchmarks. Another important task is to support development of procedures to determine and document the essential correlations.

4.2. Some definitions and clarifications

It is essential to define some of the terms used in this text. Most of the sources are quoted from Wikipedia. That is not always a reliable or complete source but is here found to be consistent with other sources, not focused on statistics only, and adequate.

Causality is the relationship between causes and effects.

Covariance is a measure of how much two variables change together. There is no requirement for linearity or causality.

Correlation is a measure of relationship between two mathematical variables or measured data values.

Correlation coefficient is a numerical measure of some type of correlation (not necessarily only statistical, preferably not). A Pearson correlation coefficient does not require linearity but determines a linear relationship from whatever there is (an exactly known, full-cycle, sinus wave correlation would become a straight line with a zero Pearson correlation coefficient).

Bias is a deviation from the best-estimate value. It may be an error or intentional (e.g. simplification or value rounding-off). It is accounted for, by correction, if significant.

Uncertainty is a measure of the remaining deviation after the bias has been accounted for. Since the deviation is currently not known, it is usually represented by some probability distribution function. An uncertainty is often subjective; it may even be a bias to someone else (the analytic toy model had examples, before the true values were released). An

uncertainty can often be reduced by obtaining more information and may even be completely converted to a bias (e.g. a rounding-off uncertainty).

$\mathbf{C_k}$ is a correlation coefficient (Pearson), expressing the degree of uncertainty similarity between two k_{eff} calculation results due to common nuclear data covariances.

Biases are sometimes treated as uncertainties in the ICSBEP Handbook. Causality, covariance and correlation apply to biases as well as to uncertainties.

The term correlation is thus applied in a general way. Uncertainty distributions for different parameters can be correlated (if they change together) even if the uncertainties of specific samples are stochastically distributed within the distribution. A common calibration method is an example (systematic effect if there is calibration before a set of multiple samples, random effect if calibrated before each sample).

4.3. Background

Correlations lead to common biases and uncertainties between parameters within one benchmark (a single specification) and between parameters in different benchmarks (whether within the same series of benchmarks or not).

Correlations may be expressed as normalized covariances (useful when linearity applies) or, preferably, as direct equations when such information is available and more accurate.

It is essential to distinguish between correlations between benchmark parameters and between benchmark results or effects (k_{eff} or reactivity effects):

- Specifications of benchmarks (e.g. the ICSBEP and IRPhEP Handbooks) should focus on parameter correlations, both within the same benchmark and between different benchmarks. Such information is often available in existing ICSBEP and IRPhEP evaluations.
- Correlations between benchmark k_{eff} or reactivity values can be determined from the parameter correlations if adequate sensitivities are available or can be made easily available. It is already an essential part of an ICSBEP or IRPhEP evaluation to determine sensitivities of k_{eff} or a reactivity effect to significant parameters.

Correlations of k_{eff} or reactivity effects are useful information. Changes of k_{eff} or reactivity effects within a single benchmark are never independent (the same fission chain reaction) and linearity should not be postulated. This also means that any correlation between different benchmarks affects all k_{eff} values or reactivity effects in all associated benchmarks. Most of those effects, perhaps all, will typically be insignificant.

A simple example of correlation is the average grid plate hole separation in a grid plate used to position fuel rods in water. A potential error (bias and uncertainty) in the specification would affect moderation and thus the neutron energy spectrum. That would change the k_{eff} or reactivity effect values related to all other parameter changes in the benchmark. If the same grid plate has been used in more than one benchmark, the neutron spectra in all those benchmarks would change.

4.4. The analytic toy model

4.4.1. Analytic equation

The neutron multiplication factor (k_{eff}) is specified as a function of three system parameters x_1, x_2 and x_3 and four data parameters $\hat{\alpha}_1$, $\hat{\alpha}_2$, $\hat{\alpha}_3$ and $\hat{\alpha}_4$. The data parameters are considered as nuclear data. This function is given in Equation (4.1). The parameters are

defined as being independent. Their normal distribution variations in a set of nine benchmarks are specified using standard deviations or variances. System and nuclear data are considered as input data with associated biases (unspecified) and uncertainties.

$$k_C(\mathbf{x}, \hat{\boldsymbol{\alpha}}) = \frac{\hat{\alpha}_1 \hat{\alpha}_4 x_1}{\hat{\alpha}_1 x_1 + \hat{\alpha}_2 x_2 + \hat{\alpha}_3 x_3} \quad (4.1)$$

Equation (4.1) is assumed to be "correct" in that it would provide exact results if the data parameters ($\hat{\boldsymbol{\alpha}}$) and the system parameters (**x**) were exact. This may be compared with an accurate neutron transport method.

The calculated values and the benchmark values thus need to be consistent with the provided uncertainties, including information on parameter correlations. This is not always the case with evaluated experiments and benchmarks based on such evaluations. The human factor explains the inconsistencies.

As suggested in the specifications, Microsoft Excel has been applied to study the toy model. This is not recommended for "production" evaluations since the potential influence of the human factor is highly significant.

For convenience, Equation (4.1) is re-structured into Equation (4.2) to provide the eigenvalue λ_C (inverse k_{eff}):

$$\lambda_C = \frac{1}{k_C} = \frac{1}{\hat{\alpha}_4}\left(1 + \frac{(\hat{\alpha}_2 x_2 + \hat{\alpha}_3 x_3)}{\hat{\alpha}_1 x_1}\right) \quad (4.2)$$

Each parameter is now separated, and a sensitivity propagation is straightforward using first order perturbation, see Equations (4.3) to (4.9).

$$S_{\lambda\hat{\alpha}1} = -\frac{1}{\hat{\alpha}_1^2}\frac{(\hat{\alpha}_2 x_2 + \hat{\alpha}_3 x_3)}{\hat{\alpha}_4 x_1} \quad (4.3)$$

$$S_{\lambda\hat{\alpha}2} = \frac{x_2}{\hat{\alpha}_4 \hat{\alpha}_1 x_1} \quad (4.4)$$

$$S_{\lambda\hat{\alpha}3} = \frac{x_3}{\hat{\alpha}_4 \hat{\alpha}_1 x_1} \quad (4.5)$$

$$S_{\lambda\hat{\alpha}4} = -\frac{1}{\hat{\alpha}_4^2}\left(1 + \frac{(\hat{\alpha}_2 x_2 + \hat{\alpha}_3 x_3)}{\hat{\alpha}_1 x_1}\right) \quad (4.6)$$

$$S_{\lambda x1} = -\frac{1}{x_1^2}\frac{(\hat{\alpha}_2 x_2 + \hat{\alpha}_3 x_3)}{\hat{\alpha}_4 \hat{\alpha}_1} \quad (4.7)$$

$$S_{\lambda x2} = \frac{\hat{\alpha}_2}{\hat{\alpha}_4 \hat{\alpha}_1 x_1} \quad (4.8)$$

$$S_{\lambda x3} = \frac{\hat{\alpha}_3}{\hat{\alpha}_4 \hat{\alpha}_1 x_1} \quad (4.9)$$

The uncertainty relationship between k_c and λ_c is shown in Equation (4.10).

$$\sigma_{k_C} = k_c^2 \cdot \sigma_{\lambda C} \quad (4.10)$$

Again, the uncertainties of the seven different input parameters in Equation (4.2) are defined as not correlated to each other. Each of the four data parameter uncertainties is correlated (identical) between combinations of benchmarks and between benchmarks and the application case. The system parameter x_1 has identical values in all benchmarks but its uncertainty is either fully correlated or uncorrelated between benchmarks (two different alternatives). The uncertainties of the other two system parameters x_2 and x_3 are defined as not correlated with the corresponding uncertainties in other benchmarks. There are no system parameter correlations between the benchmarks and the application.

It is recognised here that at least some input parameter values for the benchmarks are correlated in the sense that k_{eff} is a constant (unity, determined by "the system"). It is also quite evident that the system values x_2 and x_3 are correlated (their sums appear to be constant).

4.4.2. Direct and perturbation calculation methods

The covariances and correlation coefficients were determined in two different ways, both using sensitivities:

- **Direct approach:** Equation (4.2) was applied to calculate λ_C directly, where one parameter per benchmark case was modified by some variation. The variation was selected as a single standard deviation. The parameter variances, covariances (between benchmarks) and Pearson correlation coefficients could be obtained directly from the direct eigenvalue sensitivities. The k_{eff} covariances were obtained from Equation (4.10) while the k_{eff} correlation coefficients are identical to the λ_C correlation coefficients.
- **Perturbation**: Equation (4.2) was applied to derive Equations (4.3) to (4.9) for individual parameter sensitivities related to the eigenvalue λ_C. Such sensitivities were determined for each parameter in each benchmark. The λ_C covariances and Pearson correlation coefficients could then be determined from the sensitivities. The k_{eff} covariances were obtained from Equation (4.10).

The direct approach is more accurate since it does not rely on linearity in the same way as the perturbation approach. Equation (4.1) is clearly not linear.

4.4.3. Task 1

Covariances and correlation coefficients are requested for two different Task 1 specifications, as shown in Table 3.1. The specifications include (nuclear) data parameter uncertainties, together with associated information. Each nuclear data parameter value was fixed for all benchmarks and for the application. The parameters were sampled once for all benchmarks and for the application. The "true values" have been made available to the participants after the results have been submitted. This information confirms the sampling procedure and that the nuclear data parameters have common true values.

Table 4.1. Task 1 specifications

Task	Data parameters $\hat{\alpha}$ (independent)	System parameters (independent)
1(a)	Fully correlated between benchmarks (identical) and with uncertainties	Stochastically varied between benchmarks
1(b)	Fully correlated (identical) between benchmarks and with uncertainties	x_1 fully correlated (identical), x_2 and x_3 are stochastically varied

Task 1(a) may be considered as an uncertainty similarity check (like C_k), accounting for nuclear data covariances but not for benchmark covariances. Task 1(b) shows how this similarity check is affected by an additional uncertainty source from benchmarks.

A 9×9 covariance matrix $\boldsymbol{\Sigma}_k$ and the corresponding 9×9 correlation coefficient matrix of the calculated benchmark k_{eff} values were determined for Task 1(a) and for Task 1(b). The calculations account for all uncertainties, see Table 4.1. Uncertainties for each data parameter were fully correlated in both subtasks. Uncertainties for the system parameter x_1 were stochastically varied for Task 1(a) and fully correlated (identical) for Task 1(b). Uncertainties for system parameters x_2 and x_3 were stochastically varied.

There is no ambiguity in the final report Task 1 definitions about presence of nuclear data uncertainties and their correlations between benchmarks. Also: "For Task 2, it may be assumed that the computational bias of k_{eff} is predominantly due to errors in the nuclear data". The basis for those correlated uncertainties is obtained from Task 1(a) and Task 1(b).

4.4.4. Direct approach results for Task 1(a) and Task 1(b)

The direct approach results of correlation coefficients are provided in Table 4.2 to Table 4.3.

Table 4.2. Task 1(a) – No x_1 correlation – Direct approach – Correlation coefficients

Phase IV – Toy Model Task 1(a) – No x_1 correlation – Direct – Correlation coefficients									
BM	1	2	3	4	5	6	7	8	9
1	1	0.72	0.70	0.67	0.63	0.60	0.47	0.39	0.33
2	0.72	1	0.72	0.70	0.68	0.66	0.55	0.49	0.44
3	0.70	0.72	1	0.73	0.72	0.70	0.63	0.58	0.53
4	0.67	0.70	0.73	1	0.74	0.74	0.69	0.65	0.61
5	0.63	0.68	0.72	0.74	1	0.76	0.74	0.71	0.68
6	0.60	0.66	0.70	0.74	0.76	1	0.78	0.76	0.74
7	0.47	0.55	0.63	0.69	0.74	0.78	1	0.84	0.84
8	0.39	0.49	0.58	0.65	0.71	0.76	0.84	1	0.88
9	0.33	0.44	0.53	0.61	0.68	0.74	0.84	0.88	1

Table 4.3. Task 1(b) – x_1 correlation - Direct approach – Correlation coefficients

Phase IV – Toy Model Task 1(b) – x_1 correlation - Direct – Correlation coefficients									
BM	1	2	3	4	5	6	7	8	9
1	1	0.90	0.88	0.84	0.80	0.75	0.61	0.52	0.45
2	0.90	1	0.90	0.88	0.85	0.81	0.69	0.61	0.55
3	0.88	0.90	1	0.90	0.89	0.86	0.77	0.70	0.64
4	0.84	0.88	0.90	1	0.91	0.89	0.83	0.77	0.72
5	0.80	0.85	0.89	0.91	1	0.91	0.87	0.83	0.79
6	0.75	0.81	0.86	0.89	0.91	1	0.91	0.87	0.84
7	0.61	0.69	0.77	0.83	0.87	0.91	1	0.94	0.93
8	0.52	0.61	0.70	0.77	0.83	0.87	0.94	1	0.96
9	0.45	0.55	0.64	0.72	0.79	0.84	0.93	0.96	1

4.4.5. Perturbation approach results for Task 1(a) and Task 1(b)

The perturbation results for correlation coefficients are provided in Table 4.4. to Table 4.5.

Table 4.4. Task 1(a) – No x_1 correlation - Perturbation approach – Correlation coefficients

Phase IV – Toy Model Task 1(a) – No x_1 correlation - Perturbation – Correlation coefficients									
BM	1	2	3	4	5	6	7	8	9
1	1	0.72	0.70	0.67	0.63	0.60	0.47	0.40	0.34
2	0.72	1	0.72	0.70	0.68	0.65	0.55	0.49	0.44
3	0.70	0.72	1	0.72	0.71	0.70	0.63	0.58	0.53
4	0.67	0.70	0.72	1	0.74	0.73	0.69	0.65	0.61
5	0.63	0.68	0.71	0.74	1	0.76	0.73	0.70	0.68
6	0.60	0.65	0.70	0.73	0.76	1	0.78	0.76	0.74
7	0.47	0.55	0.63	0.69	0.73	0.78	1	0.84	0.84
8	0.40	0.49	0.58	0.65	0.70	0.76	0.84	1	0.87
9	0.34	0.44	0.53	0.61	0.68	0.74	0.84	0.87	1

Table 4.5. Task 1(b) – x_1 correlation - Perturbation approach – Correlation coefficients

Phase IV – Toy Model Task 1(b) – x_1 correlation - Perturbation – Correlation coefficients									
BM	1	2	3	4	5	6	7	8	9
1	1	0.90	0.88	0.85	0.81	0.76	0.61	0.52	0.45
2	0.90	1	0.90	0.88	0.85	0.82	0.70	0.62	0.55
3	0.88	0.90	1	0.90	0.89	0.86	0.77	0.70	0.65
4	0.85	0.88	0.90	1	0.91	0.90	0.83	0.78	0.73
5	0.81	0.85	0.89	0.91	1	0.92	0.87	0.83	0.79
6	0.76	0.82	0.86	0.90	0.92	1	0.91	0.88	0.84
7	0.61	0.70	0.77	0.83	0.87	0.91	1	0.94	0.93
8	0.52	0.62	0.70	0.78	0.83	0.88	0.94	1	0.96
9	0.45	0.55	0.65	0.73	0.79	0.84	0.93	0.96	1

There are some small deviations between the corresponding correlation coefficients from the two methods. The linearity assumption for the perturbation approach holds.

4.4.6. Additional cases - Case 1(cx) and Case 1(dx)

Some participants appear to have made calculations assuming no nuclear data uncertainties. This may have some interest and are here referred to as additional Cases 1(cx) and 1(dx), see Table 4.6. Since they are not included in the Phase IV specifications they are referred to as Cases rather than Tasks.

Table 4.6. Additional calculation Cases 1(cx) and 1(dx)

Case	Nuclear Data Parameters	System Parameters
1(cx)	Fully correlated between benchmarks (identical) with no uncertainties	Stochastically varied between the benchmarks
1(dx)	Fully correlated (identical) between benchmarks with no uncertainties	x_1 fully correlated (identical) between benchmarks, x_2 and x_3 stochastically varied

Case 1(cx) calculation results are assumed to have no correlations. Case 1(cx) still has some value in checking Monte Carlo sampling methods that will generate covariances and correlations when there are none.

Case 1(dx) may be seen as a benchmark correlation check, ignoring influences of nuclear data covariances. This is of direct relevance to the Phase IV agenda. If it is calculated separately for each parameter, as in case 1(dx), it will clearly be informative. If there are simultaneous variations of multiple parameters, the usefulness is more limited.

Only the direct approach was applied to these additional cases.

4.4.7. Direct approach results for Case 1(cx) and Case 1(dx)

The Excel spreadsheets were modified slightly for these cases. The system parameter uncertainties were studied separately by setting all nuclear data uncertainties to zero in Task 1 (a) and (b). The results are presented in Table 4.7 to Table 4.8. Only the direct approach results are included, since the perturbation results are very similar.

Table 4.7. Case 1(cx) - no data uncertainties – no x_1 corr. – correlation coefficients

Case 1(cx) – No data uncertainties – No X1 correlation – Correlation coefficients									
BM	1	2	3	4	5	6	7	8	9
1	1	0	0	0	0	0	0	0	0
2	0	1	0	0	0	0	0	0	0
3	0	0	1	0	0	0	0	0	0
4	0	0	0	1	0	0	0	0	0
5	0	0	0	0	1	0	0	0	0
6	0	0	0	0	0	1	0	0	0
7	0	0	0	0	0	0	1	0	0
8	0	0	0	0	0	0	0	1	0
9	0	0	0	0	0	0	0	0	1

Table 4.8. Case 1(dx) - no data uncertainties – x_1 correlation – correlation coefficients

Case 1(dx) – No data uncertainties – x_1 correlation – Correlation coefficients									
BM	1	2	3	4	5	6	7	8	9
1	1	0.64	0.65	0.65	0.66	0.65	0.66	0.66	0.66
2	0.64	1	0.64	0.65	0.66	0.64	0.66	0.66	0.66
3	0.65	0.64	1	0.65	0.66	0.64	0.66	0.66	0.66
4	0.65	0.65	0.65	1	0.67	0.65	0.67	0.67	0.67
5	0.66	0.66	0.66	0.67	1	0.66	0.67	0.67	0.68
6	0.65	0.64	0.64	0.65	0.66	1	0.66	0.66	0.66
7	0.66	0.66	0.66	0.67	0.67	0.66	1	0.67	0.68
8	0.66	0.66	0.66	0.67	0.67	0.66	0.67	1	0.68
9	0.66	0.66	0.66	0.67	0.68	0.66	0.68	0.68	1

4.4.8. Additional case - Case 1(ex)

Cases 1(cx) and 1(dx) were added to study the correlation effect of a single system parameter. The basis is an assumption of no data uncertainties. A similar study of each single data correlation at a time may be useful. This would mean that all system parameter uncertainties are set to zero while one data uncertainty correlation is assumed. This may have some interest but has not been calculated. Only one case 1(ex) has been added, with each of the four data uncertainties being correlated between benchmarks and with no system parameter uncertainties, see Table 4.9.

Table 4.9. Additional calculation Case 1(ex)

Case	Nuclear data parameters	System parameters
1(ex)	Fully correlated between benchmarks (identical)	No system parameter uncertainties

Case 1(ex) calculation results are different from Task 1(a) since the stochastically determined system parameter uncertainties in Task 1(a) are removed from Case 1(ex).

Only the direct approach was applied to the additional Case 1(ex). The results are presented in Table 4.10.

Table 4.10. No system parameter uncertainties – correlation coefficients

Case 1(ex) – No system parameter uncertainties – Correlation coefficients									
BM	1	2	3	4	5	6	7	8	9
1	1	0.99	0.96	0.91	0.85	0.79	0.60	0.49	0.41
2	0.99	1	0.99	0.96	0.92	0.87	0.71	0.62	0.54
3	0.96	0.99	1	0.99	0.97	0.93	0.80	0.72	0.65
4	0.91	0.96	0.99	1	0.99	0.97	0.88	0.81	0.75
5	0.85	0.92	0.97	0.99	1	0.99	0.93	0.88	0.83
6	0.79	0.87	0.93	0.97	0.99	1	0.97	0.93	0.89
7	0.60	0.71	0.80	0.88	0.93	0.97	1	0.99	0.98
8	0.49	0.62	0.72	0.81	0.88	0.93	0.99	1	1
9	0.41	0.54	0.65	0.75	0.83	0.89	0.98	1	1

4.4.9. Task 2 – Approach to using a Generalised Linear Least Square Method (GLLSM)

In Task 2, an application is specified, based on Equation (4.1). The results of Task 1 are used to establish bias-corrections to improve the accuracy and to reduce the uncertainty. Tasks 2(a) and 2(b) refer to the assumptions of no x_1 correlation and full x_1 correlation, respectively

The biases observed from the toy model specifications appear to follow a trend line (almost linear) with increasing benchmark ID number, or rather the system parameter x_3, see Figure 4.1. This may be a coincidence, or not. More complicated trends can also be imagined.

Figure 4.1. Calculation results for the toy model benchmarks with trend line

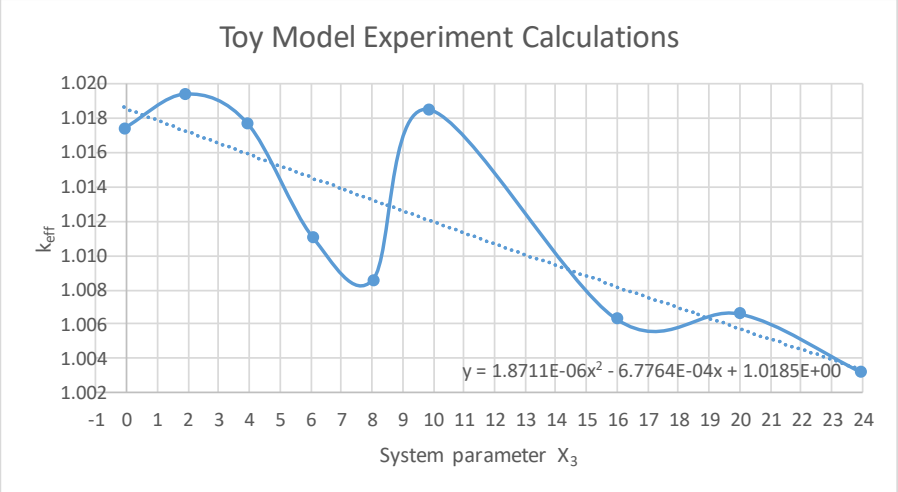

Source: NEA, 2020.

Equation (4.2) shows how parameters influence a trend-curve.

- The $\hat{\boldsymbol{\alpha}}_4$ parameter is proportional to k_{eff}. Maybe it could be considered as k_{inf}. It has a large uncertainty contribution to the total uncertainty.
- The $\hat{\boldsymbol{\alpha}}_1$ parameter is coupled with the system parameter x_1.
- The $\hat{\boldsymbol{\alpha}}_2$ and $\hat{\boldsymbol{\alpha}}_3$ parameters are coupled with the system parameters x_2 and x_3, respectively, in the sum of the products $\hat{a}_2 \cdot x_2$ and $\hat{a}_3 \cdot x_3$. With increasing values of x_2 and x_3, they cause larger uncertainties than the $\hat{\boldsymbol{\alpha}}_1$ parameter.

Increases of the associated covariance and correlation coefficient values can be observed with increasing benchmark ID number.

In Task 2(b) of fully correlated x_1 values between all benchmarks, the only variable is the sum of the products $\hat{a}_2 \cdot x_2$ and $\hat{a}_3 \cdot x_3$. The products have different signs, leading to a total sum of about four for each benchmark, even for very large x_2 and x_3 values.

- The x_1 system parameter has a much larger relative uncertainty than the $\hat{\boldsymbol{\alpha}}_1$ data parameter that it is coupled with. For Task 2(a), with uncorrelated x_1 uncertainties, they could explain some of the variation in Figure 4.1. The x_1 uncertainty is significant even though its effect is smaller than for $\hat{\boldsymbol{\alpha}}_4$.
- The x_2 and x_3 parameters are discussed above with the $\hat{\boldsymbol{\alpha}}_2$ and $\hat{\boldsymbol{\alpha}}_3$ parameters. The relative uncertainties of the x_2 and x_3 parameters become smaller with increasing values of x_2 and x_3. However, the effect of an x_2 or x_3 uncertainty does not change significantly with the absolute values of x_2 or x_3 (cancelling effects). These uncertainties contribute to the random-effect variations.

4.4.10. Results – Modification of parameters to obtain zero biases (GLLSM)

Since the characteristics of the system parameters are not specified, there is no basis for using expert-judgement to recognise trends or similarity between the application and a specific benchmark (one parameter may have a very strong k_{eff} sensitivity). A Generalised Linear Least Square Method (GLLSM) appears to be most appropriate.

GLLSM approach: All input parameters (system and data) are adjusted within two standard deviations to approach zero biases for all benchmarks.

A simple play with such an approach is meaningful. It has been done in a trial-and-error way.

The study of Equation (4.2), together with sensitivity and covariance calculations, shows that the over-prediction of k_{eff} could be reduced significantly, even completely, by fitting $\hat{\boldsymbol{\alpha}}_4$ (and x_1 uncertainties when fully correlated). This simplistic fitting could involve up to two standard deviations.

Benchmark VI appears to have a result that is too far away from the trend-curve to be fixed by the above suggestions. A random-effect uncertainty is needed to explain the large deviation. If the x_1 uncertainties are uncorrelated, that could alone explain the benchmark VI deviation. For both the correlated and uncorrelated x_1 uncertainty alternatives, system parameter x_2 random-effect uncertainties could cover the deviation of benchmark VI.

During the trial-and-error fits, also some other individual benchmarks could be difficult to fit within one standard deviation (the initial target). The results are provided below.

A direct perturbation of Equation (4.2) was applied for each parameter. Task 2(a) has four parameters ($\hat{\boldsymbol{\alpha}}_1, \hat{\boldsymbol{\alpha}}_2, \hat{\boldsymbol{\alpha}}_3$ and $\hat{\boldsymbol{\alpha}}_4$) that are fully correlated between benchmarks while Task 1(b) has five such parameters (adding x_1).

Perturbations that result in biases smaller than 1 pcm for all benchmarks are provided in Tables 4.11 and 4.12. There are other parameter combinations that would also lead to such low biases. This will be used to obtain some estimate of the adjusted k_{eff} uncertainty.

Table 4.11. A fitted Task 2(a) combination that results in zero biases

Task 2(a). Fitted parameter values. Original uncertainties specified in headings							
Exp. ID	$\hat{\boldsymbol{\alpha}}_1$ (0.01)	$\hat{\boldsymbol{\alpha}}_2$ (0.01)	$\hat{\boldsymbol{\alpha}}_3$ (0.01)	$\hat{\boldsymbol{\alpha}}_4$ (0.01)	x_1 (0.05)	x_2 (0.05)	x_3 (0.05)
1	-0.01	0.01	0.00822	-0.01409	-0.0243	0.02	0.02
2	r=1(1)	r=1	r=1	r=1	-0.0394	0.03	0.03
3	r=1	r=1	r=1	r=1	-0.03	0.0233	0.02
4	r=1	r=1	r=1	r=1	0.01	-0.012	-0.0149
5	r=1	r=1	r=1	r=1	0.0501	0.05	-0.05
6	r=1	r=1	r=1	r=1	-0.03735	0.03	0.03
7	r=1	r=1	r=1	r=1	0.0403	-0.03	-0.03
8	r=1	r=1	r=1	r=1	0.03385	-0.03	-0.03
9	r=1	r=1	r=1	r=1	0.0501	-0.05	-0.05

Note: "r=1" signifies full correlation between the benchmarks for this parameter.

Table 4.12. A fitted Task 2(b) combination that results in zero biases

Task 2(b). Fitted parameter values. Original uncertainties specified in headings							
Exp. ID	$\hat{\alpha}_1$ (0.01)	$\hat{\alpha}_2$ (0.01)	$\hat{\alpha}_3$ (0.01)	$\hat{\alpha}_4$ (0.01)	x_1 (0.05)	x_2 (0.05)	x_3 (0.05)
1	-0.01	0.01	0.002	-0.01138	-0.05	0.02	0.02
2	r=1[(1)]	r=1	r=1	r=1	r=1	0.0525	0.05
3	r=1	r=1	r=1	r=1	r=1	0.029	0.05
4	r=1	r=1	r=1	r=1	r=1	-0.039	-0.02
5	r=1	r=1	r=1	r=1	r=1	-0.05128	-0.05
6	r=1	r=1	r=1	r=1	r=1	0.0766	0.07
7	r=1	r=1	r=1	r=1	r=1	-0.0425	-0.05
8	r=1	r=1	r=1	r=1	r=1	-0.045	-0.0102
9	r=1	r=1	r=1	r=1	r=1	-0.0538	-0.05

Note: "r=1" signifies full correlation between benchmarks.

The adjusted data values result in the remaining reactivities of Figures 4.2 and 4.3

Figure 4.2. Reactivities after Task 2(a) data and system parameter adjustments

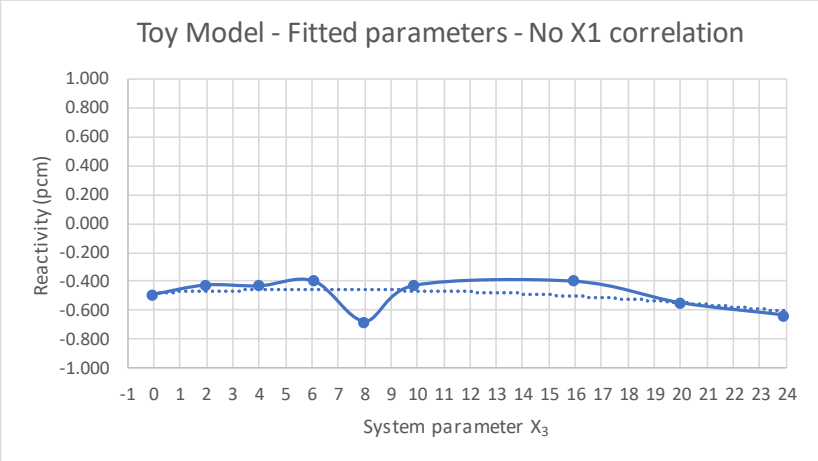

Source: NEA, 2020.

Figure 4.3. Reactivities after Task 2(b) data and system parameter adjustments

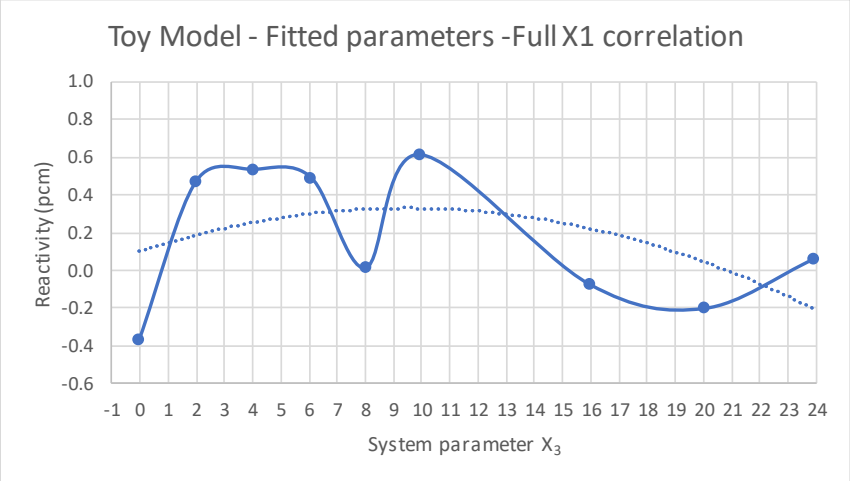

Source: NEA, 2020.

For both applications, the target to have all modifications at most one standard deviation did not quite succeed. The $\hat{\alpha}_4$ value modification is larger in both subtasks. The x_1 value is larger in Task 2(b).

A reliable solution should also lead to a normal distribution of the modifications, consistent with the uncertainty distribution. In the current evaluation results, shown in Tables 4.11 and 4.12, there are clear trends that indicate deviation from a normal distribution for all three random-effect parameters. This was intentional to reduce the adjustment of the $\hat{\alpha}_4$ values. A best-estimate approach should statistically optimise the deviation of the $\hat{\alpha}_4$ values and reduce the deviation of the random-effect parameter uncertainties from normal distributions.

4.4.11. Task 2 results for the application case

The provided Equation (4.2) results in a k_{eff} value of 0.9536 for the application case.

The fitted-parameter results appear successful since the maximum variation of a parameter was about one and a half standard deviation for both Task 2(a) and 2(b). The biases were less than 1 pcm using the adjusted parameter values for all benchmarks.

The adjusted data values of α_1, α_2, α_3 and α_4 were then applied to the application case.

For correlations according to Task 2(a), the adjusted values in Table 4.18 result in a k_{eff} of 0.9413.

For correlations according to Task 2(b), the adjusted values in Table 4.19 result in a k_{eff} of 0.9465.

4.4.12. Task 2 result uncertainties for the application case

There are uncertainties in these k_{eff} estimations but no direct way to estimate them has been found. The method chosen here for estimation of the k_{eff} uncertainties is to use other adjusted parameter value combinations that lead to adjusted deviations lower than 1 pcm.

The only parameter uncertainties that, each on its own, could credibly result in such small deviations relate to α_4 and x_1. Two alternatives have been chosen based on this observation, while a third was added to limit the too large x_1 adjustment:

- The values of x_1 and the associated σ_1 are not adjusted at all. The α_4 value is adjusted further to compensate for this. The other parameter adjustments remain as in Table 4.19. Using an α_4 adjustment of -0.01678, the adjusted k_{eff} values of the nine benchmarks have deviations less than 1 pcm. The α_4 adjustment is less than two standard deviations (0.01) from its nominal value. The adjusted application k_{eff} is 0.9425.
- The α_4 value is not adjusted at all adjustment of x_1 compensates for this while the associated σ_1 and the other parameter adjustments remain as in Table 4.19. Using an x_1 adjustment of -0.1513, the adjusted k_{eff} values of the nine benchmarks have deviations less than 1 pcm. This x_1 adjustment is more than three standard deviations (0.05) from its nominal value. This is possible but considered too much to base an uncertainty estimation on.
- Adjustment of x_1 is made with -0.10 (two standard deviations). The α_4 value is then adjusted to obtain the requested low adjusted reactivities (less than 1 pcm) in the calculated benchmarks. The other parameter adjustments remain as in Table 4.19.

Using an x_1 adjustment of -0.10 and an α_4 adjustment of -0.00613, the adjusted k_{eff} values of the nine benchmarks get deviations less than 1 pcm. The adjusted application k_{eff} is 0.9508. This is clearly a representative possibility.

Based on options 1 and 3, the nominal Task 2(b) application value 0.9465 is estimated to have a standard deviation of 0.0040 (400 pcm).

In Task 2(a), neglection of the parameter x_1 correlations lead to a bias of -0.0052 (-520 pcm). The assumed uncertainty of the Task 2(a) application value 0.9413 is also 0.0040 (400 pcm).

4.4.13. Analytic toy problem - Summary and conclusions

The results for the application Task 2 are:

- Task 2(a) $k_{eff} = 0.9413$ $\sigma = 0.0040$;
- Task 2(b) $k_{eff} = 0.9465$ $\sigma = 0.0040$.

The α_4 and x_1 uncertainties are the most important uncertainties for Tasks 1(b) and 2(b).

Learning about the "true values" of the parameters in July 2018, it is interesting to note that the sampled value (1.2198) of the most important parameter, α_4, has a deviation of almost two standard deviations (2×0.01) from its correct value (1.20). The method applied seems successful in adjusting for most of this bias. Another parameter, α_3 (sampled value 1.0225) is more than two standard deviations (2×0.01) from its true value (1.0000).

An early assumption was that the system parameters x_2 and x_3 were correlated by having their sum exactly 4. This has been confirmed in the final release of "true values", in July 2018.

The specifications for Task 1 and for Task 2 appear to be clear. Each of the nuclear data parameters have been sampled once and applied to all nine benchmarks. That means total correlations for both Task 1(a) and Task 1(b).

Direct sensitivity calculations and first-order perturbation calculations have been applied to determine correlation coefficients. The very small differences may be attributed to the non-linearity of the k_{eff} equation.

Early reports from other participants with very different results have caused some concern. The most likely reason for the differences appears to be that the uncertainties of the nuclear data parameters have been set to zero (thus making the issue of their correlations irrelevant). Such calculations may be of some interest and have been added as separate Cases 1(cx) and 1(dx). The results are close to those of other participants.

If the nuclear data uncertainties had been sampled stochastically, and not set to zero as in Cases 1(cx) and 1(dx), they would reduce the correlation coefficients substantially. The primary reason is that the α_4 uncertainty is so significant.

An approximation of a GLLSM has been applied to minimise the estimated biases in the results for the nine k_{eff} benchmarks. The target was to limit the adjustments to one standard deviation but that was not possible. Slightly larger adjustments were made. Typical for GLLSMs, there are several combinations of adjustments that will lead to the desired results. This has been used to estimate the uncertainties of the preferred solution.

4.5. Realistic case

4.5.1. Introduction

In Phase IV-a, benchmarks from the ICSBEP Handbook were selected for a comparison of calculations of Pearson correlation coefficients between the benchmarks. After some initial complications, a final specification was released in the second half of 2015. This contained two "mandatory" scenarios (A and E), together with three options (B, C and D).

Phase IV-b contains two Cases with altogether three Applications. The first Application is a simplified theoretical model with an unknown k_{eff} value. The other two Applications are benchmarks, based on critical experiments, with best estimates of benchmark k_{eff} values available. Validation of Case 1 and evaluation of Case 2 are based on results of Phase IV-a. Results with and without accounting for correlations between Phase IV-a benchmark specifications are requested.

Bias and uncertainty correlations can be found between sources (e.g. geometry) and between effects (e.g. reactivity worth). Correlations between effects may not necessarily involve correlations between the sources. A change in any parameter (source) will change the fission chain-reaction and thus all associated effects (e.g. reactivity parameters) will be correlated.

Correlated effects that are caused by uncorrelated sources are easily found in Phase IV. The fuel rod inner clad diameter and the clad thickness were specified as uncorrelated. Both parameters have very strong effects on the fission chain-reaction, primarily due to neutron energy spectrum effects. There are also other parameters that influence this spectrum. Again, each spectrum change affects all reactivity parameters and sensitivities.

During the Phase IV progress, it became evident that evaluation of benchmark critical experiments is complicated. Identification and estimation of source uncertainties need to be carried out adequately, accounting for correlations between the sources within each experiment as well as between sources in different experiments. Incomplete information and specifications lead to different interpretations and eventually to different results.

4.5.2. Phase IV-a - Specifications

The specifications of Phase IV-a are not necessarily consistent with the ICSBEP Handbook. However, it is important that they are clear before any comparison of results is made. If there are different interpretations, they should be clarified to interpret the results and to obtain valuable information from Phase IV.

Unfortunately, Scenario E was not initially interpreted in the same way by all participants. The specifications are probably clear enough, but the focus on correlations within each benchmark rather than on correlations between benchmarks resulted in some confusion. Three interpretations are informative, they are referred to as Scenario E-I, Scenario E-II and Scenario E-III.

Table 4.13 shows correlations within each benchmark. The only change from the formal specification's Table 1 is that the grid plate hole diameter is pointed out as irrelevant for Case A. It does not affect the results. Table 4.14 shows correlations between benchmarks, based on the formal specification text. The formal specifications appear to have a combined table.

Table 4.13. Correlations within each benchmark

Correlations within each benchmark					
Scenario	Displacement of grid plate hole position	Radial displacement of rod center from the hole center	Grid plate hole diameters ($2\times r_{hole}$)	Fuel rod clad inner diameters	Fuel rod clad thicknesses
A	None	R=0	Irrelevant	Correlated	Correlated
B	Uncorrelated	$R = r_{hole} - r_{gap} - t_{clad}$	Correlated	Correlated	Correlated
C	Uncorrelated	$R = r_{hole} - r_{gap} - t_{clad}$	Uncorrelated	Correlated	Correlated
D	Uncorrelated	$R = r_{hole} - r_{gap} - t_{clad}$	Uncorrelated	Uncorrelated	Correlated
E-I	Uncorrelated	$R = r_{hole} - r_{gap} - t_{clad}$	Uncorrelated	Uncorrelated	Uncorrelated
E-II	Uncorrelated	$R = r_{hole} - r_{gap} - t_{clad}$	Uncorrelated	Correlated	Correlated
E-III	Uncorrelated	$R = r_{hole} - r_{gap} - t_{clad}$	Uncorrelated	Uncorrelated	Uncorrelated

Table 4.14. Correlations between benchmarks

Correlations between benchmark					
Scenario	Displacement of grid plate hole position	Radial displacement of rod center from the hole center	Grid plate hole diameters ($2\times r_{hole}$)	Fuel rod clad inner diameters	Fuel rod clad thicknesses
A	None	R=0	Irrelevant	Correlated	Correlated
B	Correlated for identical grid plates	Correlated for clads (r_{gap} and t_{clad}) and for identical grid plates (r_{hole})	Correlated for identical grid plates	Correlated	Correlated
C	=	=	=	Correlated	Correlated
D	=	=	=	Correlated	Correlated
E-I	=	=	=	Correlated	Correlated
E-II	=	=	=	Uncorrelated	Uncorrelated
E-III	=	=	=	Uncorrelated	Uncorrelated

The focus here is on the mandatory Scenarios A and E. Scenario E is split into Scenario E-I, Scenario E-II and Scenario E-III. Correlations within and between benchmarks are discussed below, with some issues that were unclear when the calculations were being made.

4.5.3. Correlations between all specifications in all benchmarks for Scenarios A and E

Fuel pellet	radius:	identical for all fuel rods in all benchmarks;
	density:	identical for all fuel rods in all benchmarks;
	U isotopes:	identical fractions for all fuel rods in all benchmarks;
	impurities:	identical for all fuel rods in all benchmarks;
	column heights:	identical for all fuel rods in all benchmarks.

4.5.4. Correlations between all specifications in each benchmark for Scenarios A and E

Critical water heights:	identical within each benchmark.

4.5.5. Correlations between all specifications in all benchmarks for Scenario A only

Fuel clad inner radius:	identical for all fuel rods in all benchmarks;
Fuel clad thickness:	identical for all fuel rods in all benchmarks;
Fuel rod position in grid plate:	nominal for all fuel rods in all benchmarks (grid plate hole position irrelevant)

4.5.6. Full correlations within each benchmark for Scenario E-II

Fuel clad inner radius:	identical for all fuel rods in all benchmarks;
Fuel clad thickness:	identical for all fuel rods in all benchmarks.

4.5.7. No correlations within each benchmark for Scenario E-I and Scenario E-III

Fuel clad inner radius:	stochastic distribution;
Fuel clad thickness:	stochastic distribution.

4.5.8. No correlations within each benchmark for Scenario E (E-I, E-II and E-III)

Fuel rod position in grid plate:	Stochastic distribution involving grid plate hole position, grid plate hole dimension, angular fuel rod position and clad outer dimension (the last parameter is inconsistent for Scenario E-II).

4.5.9. Issue 1 for Scenario E – Full clad dimension correlation between benchmarks

The number of rods available (fuel rod bank) is larger than the number of rods in each benchmark. However, it is likely that many benchmarks contain the same fuel rods, perhaps in the same positions. The number of fuel rods vary between some benchmarks, making the issue more complicated.

Scenario E-I and Scenario E-III mean that all fuel rod clad dimensions are different within each benchmark. In different benchmarks the case is not clear. The actual conditions during the experiments probably varied significantly. Different grid plates and different number of fuel rods require differences in the fuel rod specifications between benchmarks. In benchmarks where the same grid plate was applied, with the same number of fuel rods, the correlations are probably strong.

Scenario E-II means that all fuel rod clad dimensions are identical within each benchmark. This is the same as for Scenario A. It may be credible if the same fabrication batch could include so many clads. In each benchmark, a different set of fuel rods is assumed for Scenario E-II. This is rarely likely, but it is the way that the ICSBEP evaluations have been documented (no correlation specifications). If there are many more fuel rods in the fuel bank than needed in an experiment, it could not be excluded that all rods are different. This Scenario E-II would also apply to the case of re-cladding of fuel rods. Such re-cladding was actually carried out with these fuel rods (not within the selected benchmarks though).

4.5.10. Issue 2 for Scenario E – No fuel rod position correlation between benchmarks

If the same grid plate is used for multiple benchmarks, each hole position and each hole radius are correlated. Each fuel rod in each benchmark is specified to lean on a grid plate hole wall. If the fuel rods were retained in the same positions between experiments, the fuel rod position may be unchanged between benchmarks. This may be likely for experiments where the same grid plates are used and where only a few fuel rods are shifted (e.g. to create empty positions in different lattice locations). It is not likely when different grid plates were used.

The specifications state that the fuel rod positions are uncorrelated. This appears to apply to positions within each benchmark, not between benchmarks.

Fortunately, the fuel rod position uncertainty does not appear to have a significant effect.

4.5.11. EMS methods applied in Phase IV-a

Two EMS approaches were initially applied to obtain Pearson correlation coefficients in Phase IV-a.

The first approach was to use quite sophisticated Monte Carlo sampling, using a beta version of the SCALE 6.2 Sampler procedure. The accuracy is reduced due to poor statistics in the Monte Carlo calculations. The method is considered very powerful and flexible. It is particularly useful when there are complex correlations and non-linear sensitivities. It was primarily used to support the validity of a simplified approach.

The second, simplified, approach was to assume linear behaviour of k_{eff} to all parameter changes. Equally important, the fission chain-reaction change from a parameter change is assumed to be negligible for effects of other parameter changes. This is not quite correct as has been pointed out earlier. Reliable actual measurements or Monte Carlo sampling simulations would demonstrate any significant correlation between different effects.

4.5.12. EMS interpretations of the Phase IV specifications – Clad outer dimension

The most important uncertainties for most benchmarks relate to moderation. Benchmarks LCT-007-03 and -04 are well-moderated or over-moderated while all other benchmarks are under-moderated.

The most important parameter is the clad outer dimension. It is obtained from a combination of inner clad dimension (same as gap outer dimension) and clad thickness.

The clad outer dimension options are mainly the following:

- All clad outer dimensions for all fuel rods in all experiments are identical. This means full correlation within each benchmark and between all benchmarks. This is the interpretation for Scenario A of Phase IV-a.
- All clad outer dimensions for all fuel rods in each experiment are stochastically distributed but those distributions are preserved between all benchmarks. This means no correlation within each benchmark but full correlation (or rather, as much correlation as possible, accounting for the different number of rods) between all benchmarks. This is the interpretation for Scenario E-I of Phase IV-a.
- All clad outer dimensions for all fuel rods in each experiment are identical but completely different in other benchmarks. This means full correlation within each benchmark but not between any benchmarks. This corresponds to many ICSBEP evaluations, where correlations within one experiment are accounted for but not correlations between experiments. It is typical for independent reproduction of experiments. This interpretation is referred to as Scenario E-II of Phase IV-a.
- All clad outer dimensions for all fuel rods in all experiments are stochastically distributed. This means no correlation within any benchmark or between any benchmarks. This interpretation is referred to as Scenario E-III of Phase IV-a.

4.5.13. Interpretations of specifications – Grid plate hole positions and separations

Another moderation parameter is the positions of the grid plate holes and of their separations. The distance between the centres of two grid plate holes is not referred to as a pitch, to avoid confusion with fuel rod pitch. The grid plate holes are fixed, once fabricated.

All grid plate holes were made independently of other grid plate holes. The intended position is referred to as the "nominal" grid plate hole position. A realistic distribution of grid plate hole positions is determined stochastically from a common reference point, with identical uncertainties for each position. This means that the distances between all pairs of grid plate hole centres have the same uncertainty. This includes the distance from the first to the last grid plate hole in a row or column. The average distance between two holes thus has a small uncertainty.

Neighbouring grid plate hole separations (distances) are correlated since the combined uncertainty over multiple grid plate hole separations is the same as each individual uncertainty.

Since the same grid plates are used in multiple benchmarks, there are full correlations between such benchmarks.

Some variations can be postulated:

- All grid plate holes have their nominal positions, leading to identical separations within each benchmark and in all benchmarks with identical grid plates. This applies to Scenario A of Phase IV-a.
- All individual grid plate holes are stochastically distributed from a fixed reference point. Neighbouring grid plate hole separations (distances) are correlated. Different grid plates are not correlated. These are the interpretations for Scenario E of Phase IV-a. However, the calculation models are simplified by assuming full correlations

between grid plate hole positions, even when different grid plates were used. This assumes that the effects of the grid plate hole position uncertainties are very small.

- The position of each grid plate hole is determined stochastically from the position of the neighbouring grid plate hole, with identical uncertainties for each separation. The total uncertainty of the distance from the first to the last grid plate hole position in each row or column becomes very large. This does not apply here and has not been calculated.

4.5.14. Interpretations of the Phase IV specifications – Fuel rod pitches

The fuel rod pitches vary, also within the same benchmark, by leaving some holes empty and by the position of each fuel rod in its current grid plate hole.

In benchmarks LCT-007-01 and -04, which use the same grid plates, the specified grid plate hole separation uncertainties between neighbouring fuel rods are the same, even though the fuel rod pitches are different due to every second position being empty.

In addition to the grid plate hole positions, the moderation is determined by each grid plate hole diameter, the fuel rod clad outer dimension and the fuel rod location inside its grid plate hole.

The grid plate hole diameters are correlated between benchmarks that use identical grid plates. Whether the fuel rods remain in the same position or has been shifted is not known. The fuel rod bank was larger than the number of rods in each benchmark.

The following alternatives are considered:

- The fuel rods are positioned with their centres in the nominal grid plate hole centres. All fuel rod dimensions are nominal (the grid plate hole diameter is irrelevant). The fuel rods are assumed to be inserted in the same order in different benchmarks. This is the interpretation for Scenario A of Phase IV-a.
- The grid plate hole dimension and the clad outer dimension are stochastically distributed for each position in each benchmark. Each fuel rod is leaning on the wall of its grid plate hole with stochastic angular distribution. The degree of correlation between benchmarks is not obvious.

4.5.15. Specific modelling of Phase IV-a fuel rod positions and pitches

The uncertainties related to the fuel rod positions and pitches were determined for a model of a lattice pattern of 2x2 cells (most with fuel rods and some empty). This approximates sampling of all fuel rod positions but is estimated to be accurate since neighbouring "super-cells" will be "anti-correlated". The total dimensions of the fuel rod arrays are preserved within the small total pitch uncertainty.

4.5.16. SCALE 6.2 Sampler calculations

Scenario A and Scenario E-II were calculated using a beta version 4 of SCALE 6.2, CSAS5 and Sampler. The ENDF/B-VII.1 continuous energy library was used. In the Sampler calculations, KENO-V.a was used with 50 samples (replicas), 1000 neutrons per generation and a total of 1300 generations of which the first 300 generations were skipped. One million neutron histories are not enough to get accurate correlation coefficients.

4.5.17. SCALE 6.2 Sampler results

The preliminary sampler results are presented in Table 4.15 for Scenario A and in Table 4.16 for Scenario E-II. The colour codes are different than in the Phase IV final report. The results are promising and would probably be accurate if many more histories were run, including more samples (replicas).

Table 4.15. SCALE 6.2 Sampler correlation coefficients for Scenario A

Scenario A	L07-01	L07-02	L07-03	L07-04	L39-01	L39-02	L39-03	L39-04	L39-05	L39-06	L39-07	L39-08	L39-09	L39-10	L39-11	L39-12	L39-13	L39-14	L39-15	L39-16	L39-17
L07-01	1.000	0.874	0.470	-0.086	0.948	0.969	0.962	0.971	0.937	0.933	0.965	0.960	0.963	0.945	0.978	0.953	0.964	0.965	0.965	0.958	0.965
L07-02	0.874	1.000	0.561	0.097	0.882	0.877	0.864	0.878	0.859	0.850	0.883	0.898	0.869	0.840	0.881	0.891	0.890	0.880	0.890	0.873	0.879
L07-03	0.470	0.561	1.000	0.465	0.461	0.489	0.494	0.498	0.520	0.560	0.502	0.512	0.532	0.459	0.487	0.467	0.525	0.500	0.521	0.479	0.500
L07-04	-0.086	0.097	0.465	1.000	-0.029	-0.031	0.002	-0.001	-0.018	0.108	0.006	-0.035	0.012	-0.062	-0.039	0.044	0.069	-0.027	-0.009	-0.013	-0.052
L39-01	0.948	0.882	0.461	-0.029	1.000	0.938	0.938	0.947	0.948	0.912	0.963	0.938	0.914	0.922	0.934	0.947	0.941	0.949	0.939	0.937	0.952
L39-02	0.969	0.877	0.489	-0.031	0.938	1.000	0.955	0.972	0.930	0.942	0.969	0.961	0.956	0.956	0.969	0.961	0.972	0.956	0.970	0.963	0.976
L39-03	0.962	0.864	0.494	0.002	0.938	0.955	1.000	0.974	0.923	0.946	0.964	0.969	0.960	0.934	0.966	0.959	0.964	0.961	0.967	0.961	0.963
L39-04	0.971	0.878	0.498	-0.001	0.947	0.972	0.974	1.000	0.940	0.951	0.979	0.958	0.960	0.949	0.977	0.970	0.972	0.967	0.970	0.968	0.976
L39-05	0.937	0.859	0.520	-0.018	0.948	0.930	0.923	0.940	1.000	0.901	0.959	0.926	0.925	0.913	0.926	0.928	0.943	0.952	0.942	0.918	0.946
L39-06	0.933	0.850	0.560	0.108	0.912	0.942	0.946	0.951	0.901	1.000	0.952	0.923	0.941	0.903	0.951	0.937	0.944	0.937	0.942	0.936	0.945
L39-07	0.965	0.883	0.502	0.006	0.963	0.969	0.964	0.979	0.959	0.952	1.000	0.958	0.957	0.942	0.966	0.965	0.973	0.967	0.963	0.965	0.974
L39-08	0.960	0.898	0.512	-0.035	0.938	0.961	0.969	0.958	0.926	0.923	0.958	1.000	0.954	0.937	0.962	0.954	0.956	0.962	0.969	0.961	0.969
L39-09	0.963	0.869	0.532	0.012	0.914	0.956	0.960	0.960	0.925	0.941	0.957	0.954	1.000	0.939	0.969	0.943	0.957	0.953	0.958	0.951	0.951
L39-10	0.945	0.840	0.459	-0.062	0.922	0.956	0.934	0.949	0.913	0.903	0.942	0.937	0.939	1.000	0.943	0.946	0.949	0.940	0.944	0.943	0.945
L39-11	0.978	0.881	0.487	-0.039	0.934	0.969	0.966	0.977	0.926	0.951	0.966	0.962	0.969	0.943	1.000	0.960	0.966	0.974	0.974	0.979	0.972
L39-12	0.953	0.891	0.467	0.044	0.947	0.961	0.959	0.970	0.928	0.937	0.965	0.954	0.943	0.946	0.960	1.000	0.971	0.966	0.965	0.955	0.965
L39-13	0.964	0.890	0.525	0.069	0.941	0.972	0.964	0.972	0.943	0.944	0.973	0.956	0.957	0.949	0.966	0.971	1.000	0.964	0.968	0.962	0.962
L39-14	0.965	0.880	0.500	-0.027	0.949	0.956	0.961	0.967	0.952	0.937	0.967	0.962	0.953	0.940	0.974	0.966	0.964	1.000	0.971	0.969	0.975
L39-15	0.965	0.890	0.521	-0.009	0.939	0.970	0.967	0.970	0.942	0.942	0.963	0.969	0.958	0.944	0.974	0.965	0.968	0.971	1.000	0.971	0.977
L39-16	0.958	0.873	0.479	-0.013	0.937	0.963	0.961	0.968	0.918	0.936	0.965	0.961	0.951	0.943	0.979	0.955	0.962	0.969	0.971	1.000	0.965
L39-17	0.965	0.879	0.500	-0.052	0.952	0.976	0.963	0.976	0.946	0.945	0.974	0.969	0.951	0.945	0.972	0.965	0.962	0.975	0.977	0.965	1.000

Table 4.16. SCALE 6.2 Sampler correlation coefficients for Scenario E-II

Scenario E-II	L07-01	L07-02	L07-03	L07-04	L39-01	L39-02	L39-03	L39-04	L39-05	L39-06	L39-07	L39-08	L39-09	L39-10	L39-11	L39-12	L39-13	L39-14	L39-15	L39-16	L39-17
L07-01	1.000	0.143	0.210	0.056	0.279	0.226	0.177	0.296	0.094	0.182	0.169	0.358	0.013	0.229	0.580	-0.039	0.236	0.166	0.132	0.229	0.256
L07-02	0.143	1.000	0.508	0.595	0.179	0.355	0.436	0.508	0.356	0.534	0.284	0.187	0.130	0.568	0.329	0.220	0.487	0.319	0.328	0.192	0.406
L07-03	0.210	0.508	1.000	0.693	0.288	0.480	0.517	0.229	0.356	0.308	0.402	0.361	0.308	0.478	0.452	0.256	0.432	0.361	0.371	0.242	0.378
L07-04	0.056	0.595	0.693	1.000	0.350	0.405	0.386	0.353	0.407	0.414	0.470	0.267	0.304	0.454	0.351	0.289	0.511	0.287	0.425	0.248	0.418
L39-01	0.279	0.179	0.288	0.350	1.000	0.354	0.021	0.381	0.124	0.173	0.309	0.115	0.135	0.347	0.231	0.136	-0.008	0.097	0.250	0.167	0.263
L39-02	0.226	0.355	0.480	0.405	0.354	1.000	0.116	0.232	0.102	0.284	0.277	0.089	0.109	0.418	0.438	0.368	0.108	0.336	0.423	0.314	0.295
L39-03	0.177	0.436	0.517	0.386	0.021	0.116	1.000	0.176	0.115	0.288	0.255	0.136	0.219	0.315	0.318	0.228	0.429	0.163	0.204	-0.006	0.171
L39-04	0.296	0.508	0.229	0.353	0.381	0.232	0.176	1.000	0.503	0.278	0.217	0.248	-0.078	0.352	0.224	-0.098	0.166	0.084	0.304	0.291	0.392
L39-05	0.094	0.356	0.356	0.407	0.124	0.102	0.115	0.503	1.000	0.295	0.104	0.183	0.021	0.130	0.184	-0.122	0.375	0.069	0.490	0.270	0.225
L39-06	0.182	0.534	0.308	0.414	0.173	0.284	0.288	0.278	0.295	1.000	0.168	0.174	0.139	0.337	0.289	0.329	0.394	0.059	0.114	0.148	0.237
L39-07	0.169	0.284	0.402	0.470	0.309	0.277	0.255	0.217	0.104	0.168	1.000	0.096	0.422	0.451	0.503	0.238	0.269	0.036	0.106	0.000	0.165
L39-08	0.358	0.187	0.361	0.267	0.115	0.089	0.136	0.248	0.183	0.174	0.096	1.000	-0.166	0.248	0.264	0.051	0.222	0.219	0.102	0.171	0.336
L39-09	0.013	0.130	0.308	0.304	0.135	0.109	0.219	-0.078	0.021	0.139	0.422	-0.166	1.000	0.232	0.252	0.209	0.069	0.082	0.036	0.025	-0.078
L39-10	0.229	0.568	0.478	0.454	0.347	0.418	0.315	0.352	0.130	0.337	0.451	0.248	0.232	1.000	0.449	0.345	0.181	0.196	0.344	0.337	0.252
L39-11	0.580	0.329	0.452	0.351	0.231	0.438	0.318	0.224	0.184	0.289	0.503	0.264	0.252	0.449	1.000	0.303	0.279	0.249	0.329	0.344	0.362
L39-12	-0.039	0.220	0.256	0.289	0.136	0.368	0.228	-0.098	-0.122	0.329	0.238	0.051	0.209	0.345	0.303	1.000	0.111	0.072	0.092	0.056	0.142
L39-13	0.236	0.487	0.432	0.511	-0.008	0.108	0.429	0.166	0.375	0.394	0.269	0.222	0.069	0.181	0.279	0.111	1.000	0.071	0.233	0.081	0.123
L39-14	0.166	0.319	0.361	0.287	0.097	0.336	0.163	0.084	0.069	0.059	0.036	0.219	0.082	0.196	0.249	0.072	0.071	1.000	0.199	0.469	0.303
L39-15	0.132	0.328	0.371	0.425	0.250	0.423	0.204	0.304	0.490	0.114	0.106	0.102	0.036	0.344	0.329	0.092	0.233	0.199	1.000	0.343	0.272
L39-16	0.229	0.192	0.242	0.248	0.167	0.314	-0.006	0.291	0.270	0.148	0.000	0.171	0.025	0.337	0.344	0.056	0.081	0.469	0.343	1.000	0.195
L39-17	0.256	0.406	0.378	0.418	0.263	0.295	0.171	0.392	0.225	0.237	0.165	0.336	-0.078	0.252	0.362	0.142	0.123	0.303	0.272	0.195	1.000

4.5.18. Phase IV-a approach 2: Direct sensitivity calculations

Sensitivities were calculated for all specified uncertainties, for at least one benchmark. Those results are not reported here. For the remaining benchmarks, five uncertainties were selected since they appeared to cover all significant uncertainties. In different correlations, different parameters may dominate. Whether those five uncertainties are needed, or enough, has not been evaluated separately. The parameters were often not varied sufficiently to avoid "contamination" with the Monte Carlo uncertainties, and the accuracy is not high for low sensitivities.

Further, the most important uncertainty in most cases, the outer clad diameter, was assumed to have a normal distribution obtained by combining the inner clad diameter uncertainty with the clad thickness uncertainty. This will not necessarily result in accurate correlation coefficients. However, this approach is fast and could be sufficiently informative for whatever purpose the correlation coefficients will be applied.

The uncertainties related to the pitch were combined into one single uncertainty covering the position of fuel rods within a lattice pattern of 2x2 rods (super-cells). This repeating geometry model was also previously used in the Monte Carlo sampling covered in the first approach. Every second neighbouring fuel rod pitch will be anti-correlated (large separation between two fuel rods in the supercell will be balanced by small separation to the nearest fuel rod in the next super-cell). The sensitivity thus accounts for correlations within the benchmark and is not dependent on the number of fuel rods or super-cells.

Scenario E-I and Scenario E-III reduce the reactivity impacts of the outer clad diameter uncertainty by the square root of the number N of fuel rods in each benchmark. An increase

in the number of benchmarks will not reduce the uncertainty for Scenario E-I (fully correlated) but will do that for Scenario E-III (uncorrelated).

Scenario E-II reduces the reactivity impacts of the outer clad diameter uncertainty by the square root of the number of benchmarks (uncorrelated) but not by the number N of fuel rods in each benchmark (correlated uncertainties).

4.5.19. SCALE 6.2.1 CSAS5 calculations of Phase IV-a – Direct sensitivity calculations

In all Phase IV-a calculations of sensitivities, the Monte Carlo code KENO-V.a in the SCALE 6.2.1 sequence CSAS5 was used, together with the ENDF/B-VII.1 continuous energy library. The final 2017 Monte Carlo statistics were based on one hundred million active neutron histories, leading to standard deviations of 0.00008 or 0.00009.

Microsoft Excel was used to evaluate the sensitivities obtained from SCALE 6.2.1 CSAS5. The procedure was similar to what has been reported for the analytic toy model. There are many calculations and links that invite influences of the human factor. Safety applications would require a more robust environment.

For each Scenario A, E-I, E-II and E-III, a 105x105 correlation matrix related to experiment uncertainties was prepared using Microsoft Excel, see Figure 4.4 and Figure 4.5. Each matrix covers the five original (source) uncertainties for each of the 21 benchmarks. Most matrix cell values are zero (white cells) while remaining cell (red) values are one.

In the Scenario A matrix shown in Figure 4.4, the parameter uncertainties of each type are fully correlated between the benchmarks but not between different parameter types.

In the Scenario E-I there are no changes between the benchmarks in the parameter correlation coefficients. The sensitivities for the outer clad dimension are reduced significantly (stochastic variation within each benchmark).

In Scenario E-II (large outer clad dimension sensitivity retained from Scenario A), the matrix shown in Figure 4.5 is changed in the repeating pattern of the 1st and of the 3rd position in every group of five rows and five columns which have only the main diagonal (variances but no covariances) filled. Those parameters are thus not correlated between benchmarks.

In the Scenario E-III there are stochastic (uncorrelated) changes between the benchmarks in the parameter correlation coefficients. The sensitivities for the outer clad dimension are reduced significantly (stochastic variation within each benchmark).

The positions that were made uncorrelated between benchmarks, going from Scenario A to Scenario E-III, correspond to uncertainty types 1 and 3 in the following list.

The five selected uncertainties are:

- clad outer diameter;
- fuel pellet diameter;
- fuel rod position (related to average pitch);
- UO_2 density;
- ^{235}U enrichment.

4.5.20. Reducing the rod position sensitivity to zero for Scenario E-I – Direct sensitivity

It is reasonable to assume that the influence of the rod position uncertainties, whether fixed (correlated) or stochastically distributed, have very small effect on the overall k_{eff} correlation coefficients. The average fuel rod pitch has essentially no uncertainty. Varying the rod positions within each grid plate hole will change the self-shielding of cross-section resonances a little but the results show that this effect is small.

The precision of the Monte Carlo calculations was not high enough, even with 100 million neutron histories per calculation for the chosen perturbations used to determine the sensitivities. The effect is expected to be non-linear and increasing the perturbation is not an obvious choice.

Further, changing the perturbation in the opposite direction should result in similar (same sign) sensitivities. This is due to the full correlation effect between neighbouring fuel rod pitches. Increasing the rod separation inside the 2×2 supercell (the chosen model) is essentially equivalent to reducing the rod separation within each 2×2 supercell. The only difference is for a fuel rod lattice row or column with an even number of fuel rods. For those, the first and last fuel rod will be moving away from each other or move closer together. This will change the average pitch very little.

To obtain the best solution for Scenario E-I and for Scenario E-III, using existing Monte Carlo calculation results, the fuel rod position sensitivities were set to zero. Results for the rejected solution is also of some interest.

Having calculated sensitivities for all the uncertainties, the determination of covariances and correlation coefficients using Microsoft Excel is quite straightforward. It requires significant data handling and is not recommended for production applications.

4.5.21. Phase IV-a – Correlation coefficients from sensitivity approach using SCALE 6.2.1

The results are presented in Table 4.17 for Scenario A, in Table 4.18 for the rejected Scenario E-I model, in Table 4.19 for the selected Scenario E-I model, in Table 4.20 for Scenario E-II and in Table 4.21 for Scenario E-III. The colour codes vary between the tables and are different to those in the Phase IV final report. The results for Scenario E-I. Scenario E-II and E-III are all included for discussion. There is nothing strange about the very large differences, they are expected and can easily be understood.

It is of interest to understand the large variations for the rejected Scenario E-I model. The low uncertainties related to fuel clad outer dimensions for each benchmark means that other parameter uncertainties will become important, in particular the fuel pellet radius uncertainties. This will dominate the correlation coefficients of the rejected Scenario E-I model, but the sensitivities are small and sometimes have different signs.

Even more accurate sensitivity calculations are expected to lead to higher correlation coefficients, close to 1, for Scenario E-I. The fuel pellet radius is expected to completely dominate the correlations. The selected Scenario E-I model is closer to this solution.

Figure 4.4. Parameter correlation coefficient matrix for Scenarios A and E-I

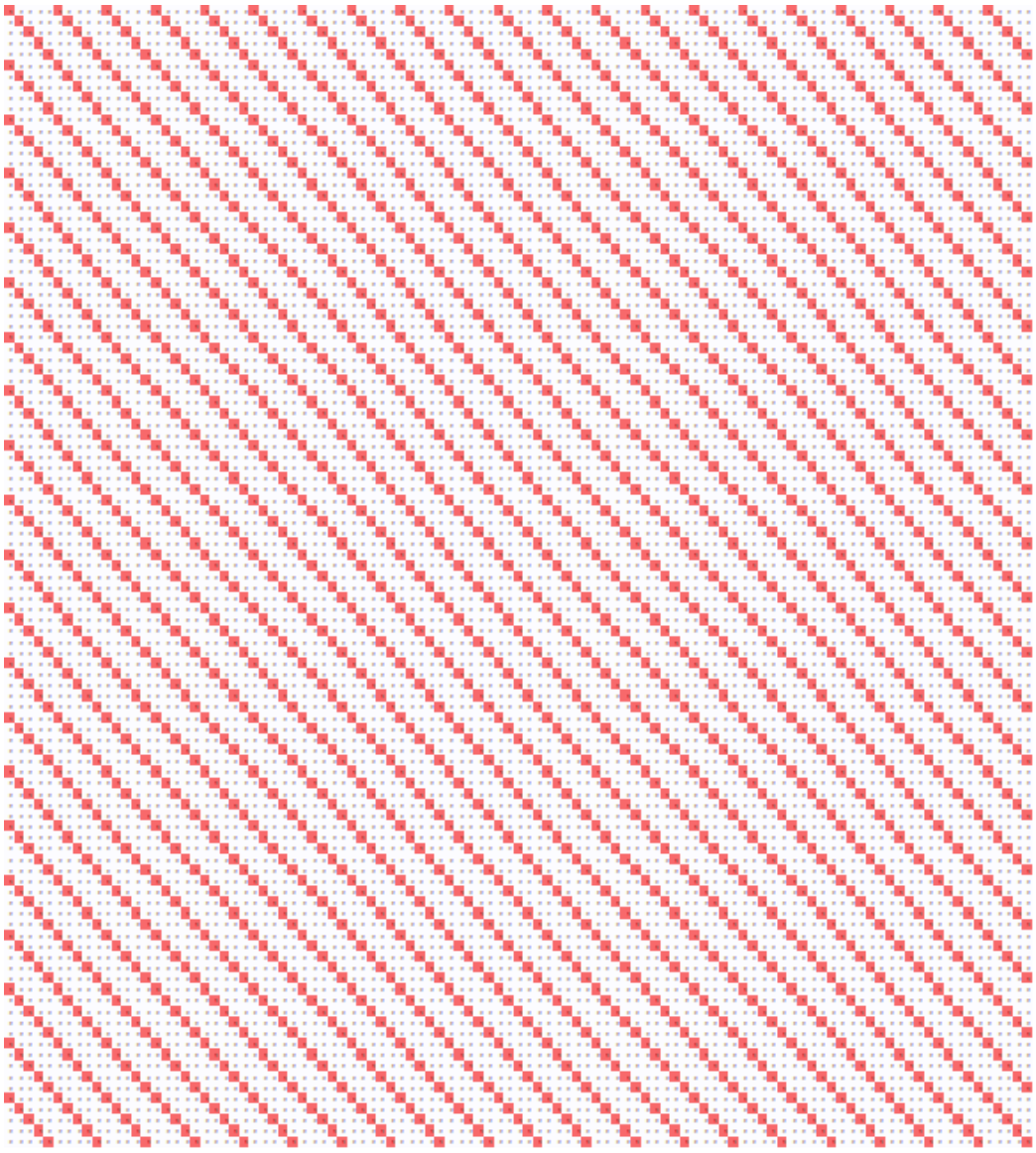

Source: NEA, 2020.

Figure 4.5. Parameter correlation coefficient matrix for Scenario E-II and Scenario E-III

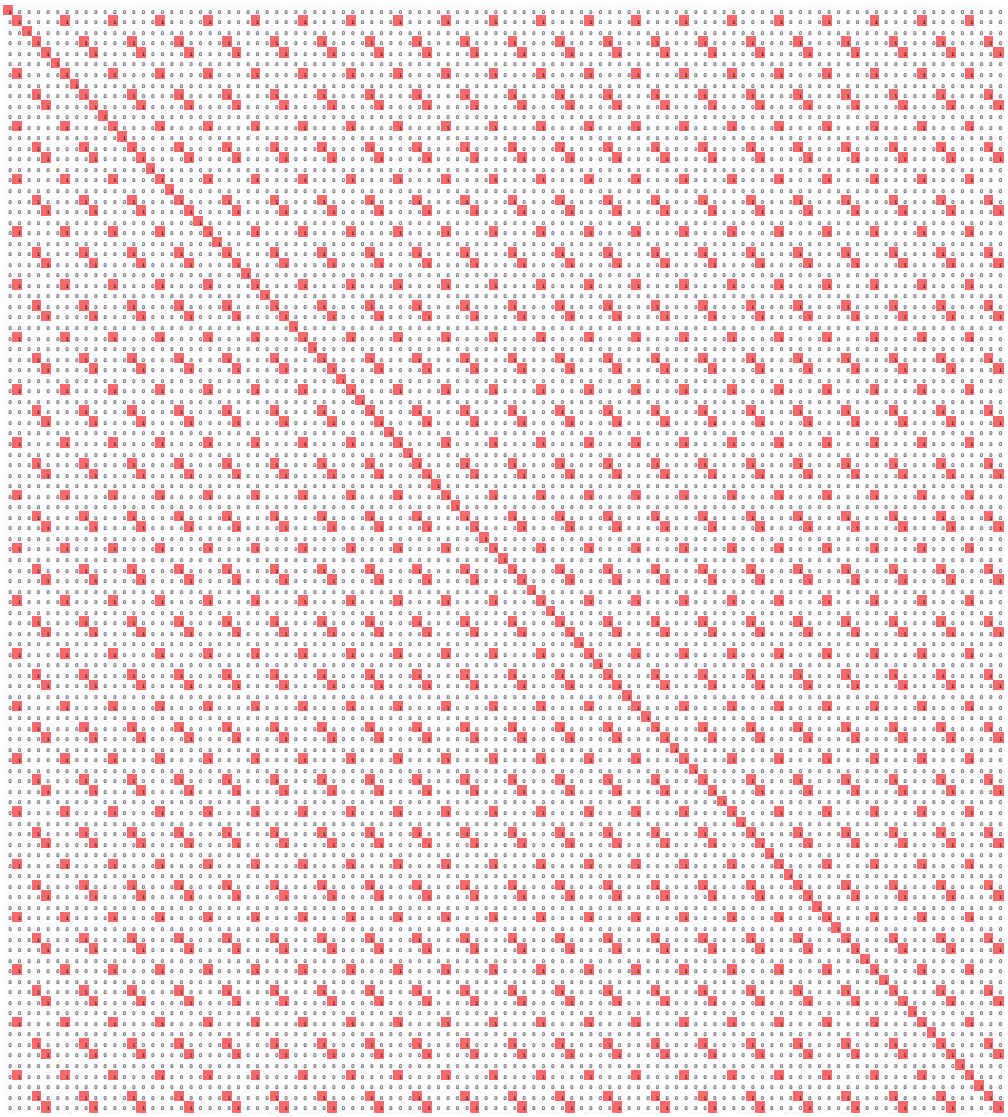

Source: NEA, 2020.

Table 4.17. Scenario A correlation coefficients based on sensitivity calculations

Scenario A	L07-01	L07-02	L07-03	L07-04	L39-01	L39-02	L39-03	L39-04	L39-05	L39-06	L39-07	L39-08	L39-09	L39-10	L39-11	L39-12	L39-13	L39-14	L39-15	L39-16	L39-17
L07-01	1.000	0.974	0.519	-0.137	0.998	0.999	0.998	0.998	0.992	0.992	0.999	0.998	0.996	0.996	0.999	0.998	0.999	0.997	0.998	0.997	0.998
L07-02	0.974	1.000	0.688	0.083	0.978	0.978	0.982	0.983	0.993	0.993	0.981	0.981	0.984	0.989	0.979	0.980	0.980	0.980	0.981	0.981	0.983
L07-03	0.519	0.688	1.000	0.748	0.532	0.533	0.547	0.553	0.609	0.611	0.542	0.545	0.561	0.581	0.534	0.541	0.539	0.546	0.545	0.547	0.554
L07-04	-0.137	0.083	0.748	1.000	-0.122	-0.121	-0.103	-0.097	-0.024	-0.022	-0.110	-0.107	-0.085	-0.061	-0.119	-0.111	-0.114	-0.104	-0.107	-0.103	-0.095
L39-01	0.998	0.978	0.532	-0.122	1.000	0.999	0.999	0.999	0.994	0.994	0.999	0.999	0.998	0.998	0.999	0.999	0.999	0.998	0.999	0.998	0.999
L39-02	0.999	0.978	0.533	-0.121	0.999	1.000	1.000	1.000	0.995	0.995	1.000	1.000	0.998	0.998	1.000	1.000	1.000	0.999	1.000	0.999	0.999
L39-03	0.998	0.982	0.547	-0.103	0.999	1.000	1.000	1.000	0.996	0.996	1.000	1.000	0.998	0.999	1.000	1.000	1.000	0.999	1.000	0.999	0.999
L39-04	0.998	0.983	0.553	-0.097	0.999	1.000	1.000	1.000	0.997	0.997	1.000	1.000	0.999	0.999	1.000	1.000	1.000	0.999	1.000	0.999	0.999
L39-05	0.992	0.993	0.609	-0.024	0.994	0.995	0.996	0.997	1.000	0.999	0.996	0.996	0.996	0.998	0.995	0.995	0.995	0.995	0.996	0.995	0.996
L39-06	0.992	0.993	0.611	-0.022	0.994	0.995	0.996	0.997	0.999	1.000	0.996	0.996	0.996	0.999	0.995	0.995	0.995	0.995	0.996	0.995	0.996
L39-07	0.999	0.981	0.542	-0.110	0.999	1.000	1.000	1.000	0.996	0.996	1.000	1.000	0.998	0.999	1.000	1.000	1.000	0.999	1.000	0.999	0.999
L39-08	0.998	0.981	0.545	-0.107	0.999	1.000	1.000	1.000	0.996	0.996	1.000	1.000	0.998	0.999	1.000	0.999	1.000	0.998	0.999	0.999	0.999
L39-09	0.996	0.984	0.561	-0.085	0.998	0.998	0.998	0.999	0.996	0.996	0.998	0.998	1.000	0.998	0.998	0.998	0.998	0.997	0.998	0.997	0.998
L39-10	0.996	0.989	0.581	-0.061	0.998	0.998	0.999	0.999	0.998	0.999	0.999	0.999	0.998	1.000	0.998	0.998	0.998	0.998	0.999	0.998	0.999
L39-11	0.999	0.979	0.534	-0.119	0.999	1.000	1.000	1.000	0.995	0.995	1.000	1.000	0.998	0.998	1.000	1.000	1.000	0.999	1.000	0.999	0.999
L39-12	0.998	0.980	0.541	-0.111	0.999	1.000	1.000	1.000	0.995	0.995	1.000	0.999	0.998	0.998	1.000	1.000	1.000	0.998	0.999	0.999	0.999
L39-13	0.999	0.980	0.539	-0.114	0.999	1.000	1.000	1.000	0.995	0.995	1.000	1.000	0.998	0.998	1.000	1.000	1.000	0.999	1.000	0.999	0.999
L39-14	0.997	0.980	0.546	-0.104	0.998	0.999	0.999	0.999	0.995	0.995	0.999	0.998	0.997	0.998	0.999	0.998	0.999	1.000	0.999	0.998	0.998
L39-15	0.998	0.981	0.545	-0.107	0.999	1.000	1.000	1.000	0.996	0.996	1.000	0.999	0.998	0.999	1.000	0.999	1.000	0.999	1.000	0.999	0.999
L39-16	0.997	0.981	0.547	-0.103	0.998	0.999	0.999	0.999	0.995	0.995	0.999	0.999	0.997	0.998	0.999	0.999	0.999	0.998	0.999	1.000	0.998
L39-17	0.998	0.983	0.554	-0.095	0.999	0.999	0.999	0.999	0.996	0.996	0.999	0.999	0.998	0.999	0.999	0.999	0.999	0.998	0.999	0.998	1.000

Table 4.18. Rejected Scenario E-I model correlation coefficients based on sensitivity calculations

Rejected Scenario E-I	L07-01	L07-02	L07-03	L07-04	L39-01	L39-02	L39-03	L39-04	L39-05	L39-06	L39-07	L39-08	L39-09	L39-10	L39-11	L39-12	L39-13	L39-14	L39-15	L39-16	L39-17
L07-01	1.000	0.884	0.647	0.754	0.712	0.863	0.844	0.898	0.932	0.918	0.930	0.955	0.978	0.826	0.925	0.962	0.946	0.990	0.951	0.655	0.961
L07-02	0.884	1.000	0.922	0.970	0.870	0.946	0.957	0.972	0.992	0.995	0.972	0.969	0.960	0.969	0.965	0.966	0.969	0.939	0.974	0.860	0.972
L07-03	0.647	0.922	1.000	0.971	0.906	0.889	0.916	0.893	0.877	0.895	0.864	0.835	0.782	0.950	0.858	0.822	0.843	0.739	0.844	0.931	0.828
L07-04	0.754	0.970	0.971	1.000	0.843	0.883	0.908	0.911	0.937	0.948	0.899	0.888	0.874	0.944	0.886	0.880	0.887	0.838	0.895	0.855	0.893
L39-01	0.712	0.870	0.906	0.843	1.000	0.966	0.967	0.940	0.863	0.873	0.913	0.877	0.787	0.963	0.921	0.868	0.894	0.760	0.880	0.994	0.853
L39-02	0.863	0.946	0.889	0.883	0.966	1.000	0.997	0.994	0.954	0.956	0.984	0.965	0.914	0.985	0.989	0.963	0.977	0.898	0.969	0.946	0.953
L39-03	0.844	0.957	0.916	0.908	0.967	0.997	1.000	0.992	0.956	0.961	0.980	0.959	0.907	0.991	0.984	0.955	0.971	0.888	0.965	0.954	0.945
L39-04	0.898	0.972	0.893	0.911	0.940	0.994	0.992	1.000	0.980	0.982	0.997	0.986	0.950	0.988	0.997	0.984	0.992	0.935	0.988	0.917	0.978
L39-05	0.932	0.992	0.877	0.937	0.863	0.954	0.956	0.980	1.000	0.998	0.987	0.989	0.985	0.961	0.980	0.989	0.988	0.971	0.991	0.840	0.993
L39-06	0.918	0.995	0.895	0.948	0.873	0.956	0.961	0.982	0.998	1.000	0.986	0.987	0.977	0.969	0.979	0.985	0.985	0.962	0.989	0.854	0.988
L39-07	0.930	0.972	0.864	0.899	0.913	0.984	0.980	0.997	0.987	0.986	1.000	0.996	0.970	0.974	0.999	0.995	0.999	0.959	0.997	0.884	0.990
L39-08	0.955	0.969	0.835	0.888	0.877	0.965	0.959	0.986	0.989	0.987	0.996	1.000	0.985	0.956	0.992	0.999	0.998	0.978	0.999	0.841	0.997
L39-09	0.978	0.960	0.782	0.874	0.787	0.914	0.907	0.950	0.985	0.977	0.970	0.985	1.000	0.906	0.962	0.988	0.978	0.998	0.984	0.749	0.993
L39-10	0.826	0.969	0.950	0.944	0.963	0.985	0.991	0.988	0.961	0.969	0.974	0.956	0.906	1.000	0.972	0.948	0.962	0.881	0.959	0.954	0.945
L39-11	0.925	0.965	0.858	0.886	0.921	0.989	0.984	0.997	0.980	0.979	0.999	0.992	0.962	0.972	1.000	0.991	0.997	0.952	0.994	0.891	0.984
L39-12	0.962	0.966	0.822	0.880	0.868	0.963	0.955	0.984	0.989	0.985	0.995	0.999	0.988	0.948	0.991	1.000	0.998	0.983	0.998	0.831	0.998
L39-13	0.946	0.969	0.843	0.887	0.894	0.977	0.971	0.992	0.988	0.985	0.999	0.998	0.978	0.962	0.997	0.998	1.000	0.970	0.998	0.862	0.994
L39-14	0.990	0.939	0.739	0.838	0.760	0.898	0.888	0.935	0.971	0.962	0.959	0.978	0.998	0.881	0.952	0.983	0.970	1.000	0.976	0.716	0.986
L39-15	0.951	0.974	0.844	0.895	0.880	0.969	0.965	0.988	0.991	0.989	0.997	0.999	0.984	0.959	0.994	0.998	0.998	0.976	1.000	0.848	0.995
L39-16	0.655	0.860	0.931	0.855	0.994	0.946	0.954	0.917	0.840	0.854	0.884	0.841	0.749	0.954	0.891	0.831	0.862	0.716	0.848	1.000	0.818
L39-17	0.961	0.972	0.828	0.893	0.853	0.953	0.945	0.978	0.993	0.988	0.990	0.997	0.993	0.945	0.984	0.998	0.994	0.986	0.995	0.818	1.000

Table 4.19. Selected Scenario E-I model correlation coefficients based on sensitivity calculations

Selected Scenario E-I	L07-01	L07-02	L07-03	L07-04	L39-01	L39-02	L39-03	L39-04	L39-05	L39-06	L39-07	L39-08	L39-09	L39-10	L39-11	L39-12	L39-13	L39-14	L39-15	L39-16	L39-17
L07-01	1.000	0.938	0.873	0.850	0.998	0.996	0.988	0.991	0.967	0.962	0.993	0.993	0.983	0.974	0.996	0.994	0.994	0.991	0.991	0.989	0.987
L07-02	0.938	1.000	0.987	0.978	0.957	0.961	0.976	0.975	0.995	0.996	0.971	0.970	0.985	0.991	0.964	0.969	0.969	0.976	0.975	0.978	0.977
L07-03	0.873	0.987	1.000	0.999	0.901	0.904	0.928	0.929	0.967	0.973	0.923	0.924	0.947	0.960	0.910	0.920	0.918	0.930	0.929	0.933	0.936
L07-04	0.850	0.978	0.999	1.000	0.881	0.884	0.910	0.912	0.955	0.961	0.905	0.906	0.932	0.947	0.890	0.902	0.899	0.913	0.911	0.916	0.921
L39-01	0.998	0.957	0.901	0.881	1.000	0.998	0.993	0.997	0.981	0.977	0.998	0.997	0.993	0.986	0.998	0.999	0.999	0.997	0.996	0.996	0.995
L39-02	0.996	0.961	0.904	0.884	0.998	1.000	0.997	0.997	0.983	0.977	0.998	0.995	0.992	0.985	0.999	0.998	0.999	0.997	0.996	0.997	0.993
L39-03	0.988	0.976	0.928	0.910	0.993	0.997	1.000	0.998	0.990	0.987	0.997	0.994	0.995	0.991	0.998	0.996	0.997	0.997	0.998	0.999	0.993
L39-04	0.991	0.975	0.929	0.912	0.997	0.997	0.998	1.000	0.992	0.989	1.000	0.999	0.998	0.995	0.998	1.000	1.000	1.000	0.999	1.000	0.998
L39-05	0.967	0.995	0.967	0.955	0.981	0.983	0.990	0.992	1.000	0.999	0.990	0.988	0.997	0.998	0.985	0.989	0.988	0.992	0.990	0.993	0.994
L39-06	0.962	0.996	0.973	0.961	0.977	0.977	0.987	0.989	0.999	1.000	0.987	0.987	0.995	0.999	0.981	0.986	0.985	0.990	0.989	0.990	0.991
L39-07	0.993	0.971	0.923	0.905	0.998	0.998	0.997	1.000	0.990	0.987	1.000	0.999	0.998	0.994	0.999	1.000	1.000	1.000	0.999	0.999	0.998
L39-08	0.993	0.970	0.924	0.906	0.997	0.995	0.994	0.999	0.988	0.987	0.999	1.000	0.997	0.994	0.997	0.999	0.998	0.999	0.999	0.997	0.998
L39-09	0.983	0.985	0.947	0.932	0.993	0.992	0.995	0.998	0.997	0.995	0.998	0.997	1.000	0.999	0.994	0.997	0.996	0.999	0.997	0.998	0.999
L39-10	0.974	0.991	0.960	0.947	0.986	0.985	0.991	0.995	0.998	0.999	0.994	0.994	0.999	1.000	0.988	0.993	0.991	0.995	0.995	0.995	0.996
L39-11	0.996	0.964	0.910	0.890	0.998	0.999	0.998	0.998	0.985	0.981	0.999	0.997	0.994	0.988	1.000	0.999	0.999	0.998	0.998	0.998	0.994
L39-12	0.994	0.969	0.920	0.902	0.999	0.998	0.996	1.000	0.989	0.986	1.000	0.999	0.997	0.993	0.999	1.000	1.000	1.000	0.999	0.999	0.998
L39-13	0.994	0.969	0.918	0.899	0.999	0.999	0.997	1.000	0.988	0.985	1.000	0.998	0.996	0.991	0.999	1.000	1.000	0.999	0.999	0.999	0.997
L39-14	0.991	0.976	0.930	0.913	0.997	0.997	0.997	1.000	0.992	0.990	1.000	0.999	0.999	0.995	0.998	1.000	0.999	1.000	0.999	0.999	0.999
L39-15	0.991	0.975	0.929	0.911	0.996	0.996	0.998	0.999	0.990	0.989	0.999	0.999	0.997	0.995	0.998	0.999	0.999	0.999	1.000	0.999	0.996
L39-16	0.989	0.978	0.933	0.916	0.996	0.997	0.999	1.000	0.993	0.990	0.999	0.997	0.998	0.995	0.998	0.999	0.999	0.999	0.999	1.000	0.998
L39-17	0.987	0.977	0.936	0.921	0.995	0.993	0.993	0.998	0.994	0.991	0.998	0.998	0.999	0.996	0.994	0.998	0.997	0.999	0.996	0.998	1.000

Table 4.20. Scenario E-II correlation coefficients based on sensitivity calculations

Scenario E-II	L07-01	L07-02	L07-03	L07-04	L39-01	L39-02	L39-03	L39-04	L39-05	L39-06	L39-07	L39-08	L39-09	L39-10	L39-11	L39-12	L39-13	L39-14	L39-15	L39-16	L39-17
L07-01	1.000	0.022	0.066	0.075	0.007	0.007	0.008	0.009	0.014	0.015	0.008	0.008	0.010	0.012	0.007	0.008	0.008	0.008	0.008	0.008	0.009
L07-02	0.022	1.000	0.253	0.286	0.027	0.027	0.032	0.034	0.055	0.056	0.030	0.031	0.037	0.044	0.028	0.030	0.029	0.032	0.031	0.032	0.035
L07-03	0.066	0.253	1.000	0.845	0.079	0.080	0.095	0.101	0.163	0.165	0.090	0.092	0.111	0.131	0.081	0.088	0.086	0.094	0.092	0.095	0.102
L07-04	0.075	0.286	0.845	1.000	0.089	0.090	0.108	0.114	0.184	0.186	0.101	0.104	0.125	0.148	0.092	0.100	0.097	0.106	0.104	0.108	0.115
L39-01	0.007	0.027	0.079	0.089	1.000	0.008	0.010	0.011	0.017	0.017	0.010	0.010	0.012	0.014	0.009	0.009	0.009	0.010	0.010	0.010	0.011
L39-02	0.007	0.027	0.080	0.090	0.008	1.000	0.010	0.011	0.018	0.018	0.010	0.010	0.012	0.014	0.009	0.010	0.009	0.010	0.010	0.010	0.011
L39-03	0.008	0.032	0.095	0.108	0.010	0.010	1.000	0.013	0.021	0.021	0.011	0.012	0.014	0.017	0.010	0.011	0.011	0.012	0.012	0.012	0.013
L39-04	0.009	0.034	0.101	0.114	0.011	0.011	0.013	1.000	0.022	0.022	0.012	0.013	0.015	0.018	0.011	0.012	0.012	0.013	0.013	0.013	0.014
L39-05	0.014	0.055	0.163	0.184	0.017	0.018	0.021	0.022	1.000	0.036	0.020	0.020	0.024	0.029	0.018	0.019	0.019	0.021	0.020	0.021	0.022
L39-06	0.015	0.056	0.165	0.186	0.017	0.018	0.021	0.022	0.036	1.000	0.020	0.020	0.024	0.029	0.018	0.020	0.019	0.021	0.020	0.021	0.023
L39-07	0.008	0.030	0.090	0.101	0.010	0.010	0.011	0.012	0.020	0.020	1.000	0.011	0.013	0.016	0.010	0.011	0.010	0.011	0.011	0.011	0.012
L39-08	0.008	0.031	0.092	0.104	0.010	0.010	0.012	0.013	0.020	0.020	0.011	1.000	0.014	0.016	0.010	0.011	0.011	0.012	0.011	0.012	0.013
L39-09	0.010	0.037	0.111	0.125	0.012	0.012	0.014	0.015	0.024	0.024	0.013	0.014	1.000	0.020	0.012	0.013	0.013	0.014	0.014	0.014	0.015
L39-10	0.012	0.044	0.131	0.148	0.014	0.014	0.017	0.018	0.029	0.029	0.016	0.016	0.020	1.000	0.014	0.016	0.015	0.017	0.016	0.017	0.018
L39-11	0.007	0.028	0.081	0.092	0.009	0.009	0.010	0.011	0.018	0.018	0.010	0.010	0.012	0.014	1.000	0.010	0.009	0.010	0.010	0.010	0.011
L39-12	0.008	0.030	0.088	0.100	0.009	0.010	0.011	0.012	0.019	0.020	0.011	0.011	0.013	0.016	0.010	1.000	0.010	0.011	0.011	0.011	0.012
L39-13	0.008	0.029	0.086	0.097	0.009	0.009	0.011	0.012	0.019	0.019	0.010	0.011	0.013	0.015	0.009	0.010	1.000	0.011	0.011	0.011	0.012
L39-14	0.008	0.032	0.094	0.106	0.010	0.010	0.012	0.013	0.021	0.021	0.011	0.012	0.014	0.017	0.010	0.011	0.011	1.000	0.012	0.012	0.013
L39-15	0.008	0.031	0.092	0.104	0.010	0.010	0.012	0.013	0.020	0.020	0.011	0.011	0.014	0.016	0.010	0.011	0.011	0.012	1.000	0.012	0.013
L39-16	0.008	0.032	0.095	0.108	0.010	0.010	0.012	0.013	0.021	0.021	0.011	0.012	0.014	0.017	0.010	0.011	0.011	0.012	0.012	1.000	0.013
L39-17	0.009	0.035	0.102	0.115	0.011	0.011	0.013	0.014	0.022	0.023	0.012	0.013	0.015	0.018	0.011	0.012	0.012	0.013	0.013	0.013	1.000

Table 4.21. Scenario E-III correlation coefficients based on sensitivity calculations

Scenario E-III	L07-01	L07-02	L07-03	L07-04	L39-01	L39-02	L39-03	L39-04	L39-05	L39-06	L39-07	L39-08	L39-09	L39-10	L39-11	L39-12	L39-13	L39-14	L39-15	L39-16	L39-17
L07-01	1.000	0.839	0.855	0.857	0.769	0.768	0.773	0.801	0.835	0.830	0.787	0.790	0.811	0.815	0.772	0.784	0.781	0.777	0.789	0.791	0.802
L07-02	0.839	1.000	0.980	0.981	0.869	0.875	0.886	0.909	0.951	0.945	0.892	0.893	0.919	0.925	0.879	0.887	0.887	0.882	0.898	0.901	0.906
L07-03	0.855	0.980	1.000	0.999	0.885	0.890	0.903	0.926	0.968	0.964	0.909	0.910	0.936	0.943	0.895	0.904	0.903	0.898	0.915	0.918	0.922
L07-04	0.857	0.981	0.999	1.000	0.887	0.892	0.903	0.927	0.969	0.964	0.910	0.911	0.938	0.944	0.896	0.905	0.904	0.900	0.916	0.919	0.924
L39-01	0.769	0.869	0.885	0.887	1.000	0.796	0.801	0.829	0.865	0.859	0.815	0.817	0.839	0.844	0.799	0.811	0.809	0.805	0.817	0.820	0.830
L39-02	0.768	0.875	0.890	0.892	0.796	1.000	0.806	0.830	0.868	0.861	0.815	0.816	0.840	0.845	0.801	0.811	0.810	0.806	0.818	0.823	0.830
L39-03	0.773	0.886	0.903	0.903	0.801	0.806	1.000	0.838	0.876	0.871	0.822	0.822	0.847	0.853	0.810	0.818	0.817	0.813	0.827	0.831	0.835
L39-04	0.801	0.909	0.926	0.927	0.829	0.830	0.838	1.000	0.902	0.897	0.849	0.851	0.875	0.880	0.834	0.845	0.843	0.839	0.852	0.855	0.864
L39-05	0.835	0.951	0.968	0.969	0.865	0.868	0.876	0.902	1.000	0.936	0.886	0.887	0.913	0.918	0.871	0.882	0.880	0.876	0.889	0.894	0.901
L39-06	0.830	0.945	0.964	0.964	0.859	0.861	0.871	0.897	0.936	1.000	0.881	0.883	0.907	0.914	0.866	0.877	0.875	0.871	0.886	0.888	0.895
L39-07	0.787	0.892	0.909	0.910	0.815	0.815	0.822	0.849	0.886	0.881	1.000	0.836	0.859	0.865	0.819	0.830	0.828	0.824	0.837	0.840	0.849
L39-08	0.790	0.893	0.910	0.911	0.817	0.816	0.822	0.851	0.887	0.883	0.836	1.000	0.861	0.867	0.820	0.833	0.830	0.826	0.840	0.841	0.851
L39-09	0.811	0.919	0.936	0.938	0.839	0.840	0.847	0.875	0.913	0.907	0.859	0.861	1.000	0.890	0.844	0.855	0.853	0.849	0.862	0.865	0.875
L39-10	0.815	0.925	0.943	0.944	0.844	0.845	0.853	0.880	0.918	0.914	0.865	0.867	0.890	1.000	0.849	0.860	0.858	0.854	0.868	0.870	0.879
L39-11	0.772	0.879	0.895	0.896	0.799	0.801	0.810	0.834	0.871	0.866	0.819	0.820	0.844	0.849	1.000	0.815	0.813	0.809	0.823	0.826	0.833
L39-12	0.784	0.887	0.904	0.905	0.811	0.811	0.818	0.845	0.882	0.877	0.830	0.833	0.855	0.860	0.815	1.000	0.825	0.820	0.833	0.836	0.846
L39-13	0.781	0.887	0.903	0.904	0.809	0.810	0.817	0.843	0.880	0.875	0.828	0.830	0.853	0.858	0.813	0.825	1.000	0.819	0.831	0.835	0.843
L39-14	0.777	0.882	0.898	0.900	0.805	0.806	0.813	0.839	0.876	0.871	0.824	0.826	0.849	0.854	0.809	0.820	0.819	1.000	0.827	0.830	0.839
L39-15	0.789	0.898	0.915	0.916	0.817	0.818	0.827	0.852	0.889	0.886	0.837	0.840	0.862	0.868	0.823	0.833	0.831	0.827	1.000	0.843	0.851
L39-16	0.791	0.901	0.918	0.919	0.820	0.823	0.831	0.855	0.894	0.888	0.840	0.841	0.865	0.870	0.826	0.836	0.835	0.830	0.843	1.000	0.854
L39-17	0.802	0.906	0.922	0.924	0.830	0.830	0.835	0.864	0.901	0.895	0.849	0.851	0.875	0.879	0.833	0.846	0.843	0.839	0.851	0.854	1.000

4.5.22. SCALE 6.2.1 CSAS5 and CSAS6 calculations of Phase IV-b

In Phase IV-b calculations of Case 1, as in the Phase IV-a sensitivity calculations, the Monte Carlo code KENO-V.a, in the SCALE 6.2.1 sequence CSAS5, was used. For Case 2, the CSAS6 sequence with KENO-VI was applied. The ENDF/B-VII.1 continuous energy library was used in both methods. The final 2017 Monte Carlo statistics were based on one hundred million active neutron histories, leading to standard deviations of 0.00008 or 0.00009.

4.5.23. Second-order polynomial fit of LCT-007 and LCT-039 k_{eff} results to EALF values

Figure 4.6 shows plots of calculated k_{eff} results sorted after their EALF values. There is one plot (blue) showing all benchmarks and one (yellow) showing a selection of the benchmarks LCT-007-1, -2, -3 and -4 together with LCT-039-1, -6, -7 and -8. Trend-lines together with equations in the same colours are included.

Figure 4.6. k_{eff} results sorted after EALF results for the LCT-007 and -039 benchmarks

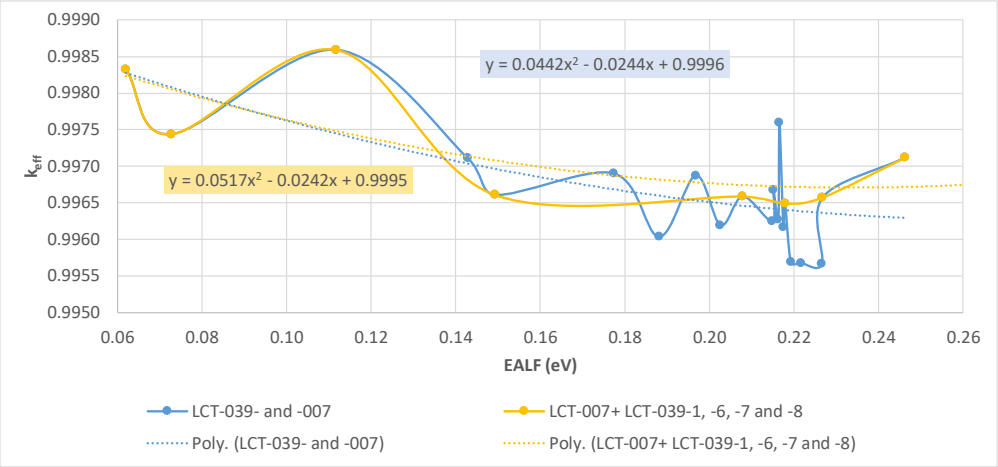

Source: NEA, 2020.

Equations (4.11) and (4.12) will be considered to obtain bias-corrected application values and uncertainties in Phase IV-b. On the yellow curve (eight points), the four highest data points (the three most leftward and the far right) are from the LCT-07 series while the others are from the LCT-039 series.

Extrapolation, without prior knowledge from other benchmarks or from nuclear data covariances, is not an easy task.

k_{eff} (all) = 0.0442 x EALF^2 - 0.0244 x EALF + 0.9996 (4.11)

k_{eff} (selection) = 0.0517 x EALF^2 - 0.0242 x EALF + 0.9995 (4.12)

It is assumed that the bias is determined by equation (4.13) which is based on Equation (4.12) reduced by 1.0000. It is also assumed that there is a constant bias in any extrapolated data above 0.24 eV.

Bias(k_{eff}) = 0.0517 x EALF^2 - 0.0242 x EALF - 0.0005 (4.13)

Table 4.22 shows the 21 calculated results of k_{eff} and EALF values. One Monte Carlo standard deviation is either 0.00008 or 0.00009. The prior benchmark reactivity uncertainties due to specified parameter uncertainties (not to nuclear data uncertainties, as prior sometimes refers to) are included in the last two columns. The next to last column relates to the identical fuel rods and fuel rod positions in each benchmark (Scenario A and Scenario E-II). The last column is based on all clad outer diameters in each benchmark being independent (Scenario E-I and Scenario E-III). The associated (clad outer diameter) sensitivities and reactivity uncertainties are divided by the square root of the number rods.

Table 4.22. k_{eff} and corresponding EALF results for the LCT-007 and -039 benchmarks

Benchmark	k_{eff}	1 (MC) (pcm)	EALF (eV)	Bias (pcm)		1 σ ("prior") (pcm)	
						Scenario	
				Direct	Eq. C.4.13	A, E-II	E-I, E-III
LCT07-1	0.99712	0.00009	0.24621	-288	-332	482	43
LCT07-2	0.99860	0.00008	0.11172	-140	-256	216	64
LCT07-3	0.99744	0.00009	0.07276	-256	-199	109	96
LCT07-4	0.99833	0.00008	0.06201	-167	-180	123	121
LCT39-1	0.99658	0.00008	0.22676	-343	-333	437	45
LCT39-2	0.99760	0.00008	0.21653	-240	-332	427	45
LCT39-3	0.99687	0.00009	0.19673	-313	-326	397	47
LCT39-4	0.99604	0.00009	0.18807	-396	-322	378	48
LCT39-5	0.99711	0.00008	0.14280	-289	-290	289	56
LCT39-6	0.99661	0.00009	0.14926	-339	-296	293	58
LCT39-7	0.99649	0.00009	0.21785	-351	-332	426	49
LCT39-8	0.99659	0.00009	0.20783	-341	-330	410	50
LCT39-9	0.99620	0.00009	0.20260	-380	-328	379	52
LCT39-10	0.99690	0.00008	0.17732	-310	-317	338	54
LCT39-11	0.99567	0.00009	0.22657	-433	-333	442	46
LCT39-12	0.99568	0.00009	0.22163	-432	-332	422	48
LCT39-13	0.99569	0.00008	0.21924	-431	-332	429	47
LCT39-14	0.99617	0.00009	0.21745	-383	-332	413	49
LCT39-15	0.99627	0.00009	0.21612	-373	-332	411	48
LCT39-16	0.99668	0.00009	0.21512	-332	-331	410	49
LCT39-17	0.99625	0.00009	0.21478	-375	-331	405	52

The bias trend with EALF agrees quite well with the prior uncertainty expected from correlated, both within each benchmark and between benchmarks, fuel clad outer diameters. There are also nuclear data and other uncertainties as well as other benchmarks. Such information needs to be evaluated before any further conclusions can be made.

The biases and the standard deviation for the Applications, when accounting for uncertainty correlations, will be based on judgement, using the trend-lines as guides. The correlation coefficients will be applied, to some extent, but they are very close to one or zero.

From other benchmark calculations, the ENDF/B-VII.1 nuclear data should perhaps result in smaller biases than the ones observed here. Such information is neglected here, to limit the study to the specified information.

Further, accounting for measured and evaluated covariance data for the cross-sections could perhaps rule out very large errors that would be hidden by clad outer diameter errors. In principle, it may even be possible to determine the actual average clad outer diameter if the nuclear data and all other uncertainties are known well.

Covariances in nuclear data are here considered as additional measurement data that, just as additional benchmarks from independent critical experiments, could reduce the total uncertainty. No attempt has been made to account for such additional measurement information. Other participants may have done so, and the results would be of interest.

The trends have been considered when estimating the uncertainties (type B) obtained from Phase IV-a. The EALF values of the Applications in Phase IV-b were considered.

Scenario A means that there is essentially only one combined benchmark. The uncertainty is not reduced much by adding more such benchmarks since the dominating uncertainty types are fully correlated between all individual benchmarks.

Concerning the reactivity effects of clad outer diameter and fuel rod position uncertainties, the benchmarks in the Scenario E-II model are considered as being reproduced (uncorrelated) rather than being repeated (Scenario A). The uncertainties in the trend line values are assumed to be related to the number of benchmark data points close to the Application EALF.

The estimated EALF values for Phase IV-b are 0.11127 eV, 0.23309 eV and 0.30323 eV. In the Phase IV-a benchmarks this means few data points for the first value, many data points for the second value and no data points at all for the highest EALF value.

Since it is not known how large the nuclear data biases and uncertainties are, all biases and uncertainties are attributed to nuclear data for validation purposes.

The biases are estimated using Equation (4.13) for the two EALF values within the validation range. For the higher EALF value, the bias curve is assumed to be flat (horizontal) with the same bias as for the 0.23309 EALF value. The uncertainty is assumed to be twice that of the difference between this value and the value estimated for the 0.11127 EALF value. These are all Type B uncertainties, based on judgement.

Results of Phase IV-a that will be applied to Phase IV-b are summarised in Table 4.23.

Table 4.23. Uncertainties based on benchmark selections and whether correlations apply or not

EALF (eV)	Data points	Bias (pcm)	One standard deviation (pcm)			
			Scenario A	Scenario E-II	Scenario E-I	Scenario E-III
0.11127	1	-255	250	150	50	30
0.23309	10	-333	450	100	50	12
0.30323	0	-333	450	400	50	45

Scenario A and the Scenario E-I uncertainties are based on the prior uncertainties. Multiple benchmarks do not add much information.

Scenario E-II, with internally correlated (same as Scenario A) but externally uncorrelated outer clad dimensions (smaller uncertainty), results in other correlated parameters being emphasised. The trend line correlations, in particular for the EALF values around 0.2 eV, results in lower uncertainties than for Scenario A.

Scenario E-I contains correlations for all parameters but only between the benchmarks for the clad outer diameters (different within each benchmark). As in Scenario A, this limits the potential reduction in the overall uncertainty using multiple benchmarks. The uncertainty is very low due to the stochastic spread of the clad outer dimensions within each benchmark.

Scenario E-III contains uncorrelated parameters but both within each benchmark and between the benchmarks for the clad outer diameters. As in Scenario E-II, this results in a reduction in the overall uncertainty using multiple benchmarks. The uncertainty is very low due to the stochastic spread of the clad outer dimensions.

Further the large k_{eff} deviations (biases) observed could not be explained by the Scenario E-I, E-II or E-III parameter uncertainties. There would have to be quite large nuclear data biases to explain such large k_{eff} biases.

4.5.24. Application Case 1: Water-moderated and water-reflected 16×16 fuel assembly

Application Case 1 is a simplified 16×16 PWR fuel assembly fully reflected by water. The purpose could be to estimate the expected result if a k_{eff} measurement could be arranged, without consideration of measurement errors and uncertainties.

The application case was calculated using KENO-V.a with END/F-VII.1 continuous-energy cross-sections.

Sensitivities and associated uncertainties for five parameters were calculated. They are:

- fuel pellet diameter;
- fuel clad inner diameter;
- fuel clad outer diameter;
- guide tube inner diameter;
- guide tuber outer diameter.

The 190 pcm fuel clad outer diameter uncertainty results, by far, in the largest contribution to the 201 pcm k_{eff} uncertainty. The bias uncertainty needs to be combined with this uncertainty.

An EALF value of 0.23856 results in a validation bias of -330 pcm from the trend line Equation (4.13). The uncertainties from Table 4.23 are 450 pcm (Scenario A), 50 (Scenario E-I), 100 pcm (Scenario E-II) and 12 pcm (Scenario E—III). The total uncertainties are thus 493 pcm (Scenario A), 207 pcm (Scenario E-I), 224 pcm (Scenario E-II) and 201 pcm (Scenario E-III).

The results for Phase IV-b Application Case 1 are shown in Table 4.24.

Table 4.24. k_{eff} and EALF results for the Application Case 1 (theoretical)

Scenarios	k_{eff} Nominal	σ (MC)	EALF (eV)	Bias	k_{eff} Bias-corrected	Bias uncertainty (Total)
A	0.96915	0.00009	0.23856	-0.00330	0.97248	0.00493
E-I	=	=	=	=	=	0.00207
E-II	=	=	=	=	=	0.00224
E-III	=	=	=	=	=	0.00201

All biases are identical, but the uncertainties vary significantly. Without information on the accuracy of nuclear data from other validation calculations or from measured and evaluated nuclear data covariances, large errors in the nuclear data could not be excluded from the validation.

The benchmarks are completely independent in the Scenario E-I model and this results in a much smaller uncertainty in the bias. Any large error in the bias-corrected k_{eff} would have been caused by application uncertainties, input and modelling errors but not on nuclear data or calculation methods.

For Scenario E-II and Scenario E-III, similar conclusions as for Scenario E-I can be made.

4.5.25. Application Case 2: LEU-COMP-THERM-079 Configurations

The LEU-COMP-THERM-079 series of experiments involve 4.31 wt.% UO_2 fuel rods in hexagonally pitched arrays with two different fuel-rod pitches of 2.0 and 2.8 cm.

A purpose of Application Case 2 is to apply the benchmark specifications, apply validation biases and uncertainties and finally to compare those results with the evaluated experiment benchmark results.

The geometry input for the two applications was derived from the specifications in the ICSBEP Handbook. The hexagonal geometry justified using KENO-VI rather than KENO-V.a. ENDF/B-VII.1 continuous-energy cross-sections were used.

The results for the two LCT-79 cases 1 and 6 are specified in Table 4.25.

The bias and uncertainties from Phase IV-a are assumed to be applicable. The EALF value is higher for LCT-79 case 1 and no benchmarks are available in that range. The bias increases with the EALF value within the benchmark range of Phase IV-a but is assumed to be flat above that range. The uncertainty is higher, due to the extrapolation of the validation range.

The bias for LCT-79 case 6 is determined from Equation (4.13), which appears to be reasonable also for this EALF value.

Table 4.25. k_{eff} and EALF results for Application Case 2 (LCT-079 cases 1 and 6)

Benchmark	Correlations?	k_{eff} Nominal	σ (MC)	EALF (eV)	Bias	k_{eff} bias-corrected	Uncertainty (Total)
Case 1	Scenario A	0.99922	0.00009	0.30323	-0.00330	1.00252	0.00450
	Scenario E-I	=	=	=	=	=	0.00050
	Scenario E-II	=	=	=	=	=	0.00400
	Scenario E-III	=	=	=	=	=	0.00045
Case 6	Scenario A	0.99911	0.00009	0.11127	-0.00255	1.00166	0.00250
	Scenario E-I	=	=	=	=	=	0.00050
	Scenario E-II	=	=	=	=	=	0.00150
	Scenario E-III	=	=	=	=	=	0.00030

The k_{eff} values specified in the ICSBEP Handbook are 0.9999 and 0.9994 with the uncertainties 0.0016 and 0.0008. Without bias corrections, the calculated results are very good. The bias corrections do not work that well, but the uncertainties of the bias corrections for Scenario A and possibly Scenario E-II are quite large, covering the large deviations from the specified benchmark results.

4.6. Conclusions

Pearson correlation coefficients for correlations between benchmark results (e.g. k_{eff}, reactivity effects) have not been demonstrated to be very useful. However, the efforts to determine such coefficients have been rewarding in that they demonstrate some of the difficulties in finding as well as documenting facts and circumstances that are essential.

A solid and practical procedure for supporting determination and documentation of correlations, both within each benchmark case and between different benchmarks, is recommended. This procedure builds on current practices for evaluation of benchmark experiments and measurements in the ICSBEP and IRPhEP Handbooks. Section 1 of the individual evaluations in the Handbooks involve collecting facts that are potentially important for the measured results, which typically are values and uncertainties of k_{eff}, reactivity parameters, etc. Section 2 involves determination of sensitivities of the measured results to parameters and procedures found to be essential for the results. Section 3 involves simplification (idealisation) of the experiments or other measurements to obtain the evaluated benchmarks, often adding additional uncertainties and sensitivities.

Determination of uncertainty sources (causational) and their sensitivities on the results is thus an established practice. The addition of estimating and documenting correlations (not correlation coefficients) between such sources within a benchmark and between different benchmarks should not be complicated, once a procedure is established.

Pearson correlation coefficients for correlations between parameters (causational sources) that cause uncertainties in the results have been shown to be useful in obtaining results for Phase IV. Very often they are obviously either zero or unity. Some efforts should be made to solve the issue when they are not zero or unity. An example from Phase IV is when only some of the fuel rods in one benchmark are used in another benchmark. Statistical methods can be applied, but they may hide known and useful information. This may even prevent improvements of future experiments. In the Phase IV example, documentation of the identity and location of each fuel rod in each benchmark makes correlation coefficients of only one or zero possible, at the expense of some more work.

Measurements or other observations of correlation coefficients between integral values are useful for recognition of correlations. The causations of the correlations should then be determined, if not already available. Converting available accurate and detailed information from the evaluation of experiments and measurements into vague (“fuzzy”) integral coefficients is not a recommended solution, unless the detailed information is preserved and directly available.

In Phase IV-b, the different results obtained from different correlation assumptions are very informative. Scenario E-II corresponds to the traditional approach of ignoring correlations between benchmarks. The associated uncertainty is reduced by applying many similar benchmarks from Phase IV-a in the validation process of Phase IV-b.

An ongoing IRPhEP evaluation (Mennerdahl, 2019) (accepted by the IRPhEP in October 2018) shows that accounting for correlations between similar benchmarks, with just one parameter being varied, can be used to reduce the uncertainty of a reactivity effect (change in k_{eff}) from several hundred pcm to 50 pcm and lower. Such reactivity effect benchmarks are very important for validation of calculation methods.

Phase IV results and discussions, as well as those of other EGUACSA Phases, are useful for improving ICSBEP and IRPhEP evaluations and their applications in actual validation.

5. Participant E

Participant: Fabian Sommer, Maik Stuke (GRS, Germany)

5.1. Toy model

Used software: Jupyter (IPython) notebook using Python 3 (numpy, scipy, pandas, matplotlib).

Generation of samples: numpy.random.normal, 250 samples.

Case 1: k_{eff}(x,alpha) assuming $x_1$correlated and α values to be nominal

Table 5.1. Case 1 - Resulting k_{eff} mean values and standard deviations

BM 1	1.0171267 ± 0.00537258
BM 2	1.01954905 ± 0.00477564
BM 3	1.01798798 ± 0.00525945
BM 4	1.01150812 ± 0.00509133
BM 5	1.00901019 ± 0.0049875
BM 6	1.01898265 ± 0.00539192
BM 7	1.00625227 ± 0.00537671
BM 8	1.00652457 ± 0.00544388
BM 9	1.00348493 ± 0.00508185

Figure 5.1. Case 1 - Scatter plot of k_{eff} values between benchmark experiments

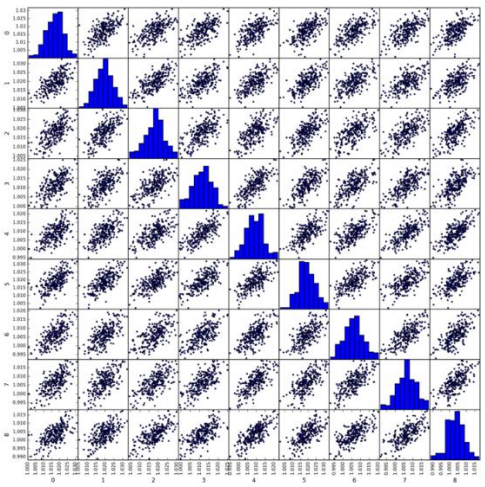

Source: NEA, 2020.
Note: On the diagonal axis the k_{eff} distribution is shown. Note that the numeration of benchmarks runs from 0 to 8, not from 1 to 9.

Figure 5.2. Correlation coefficients assuming Case 1

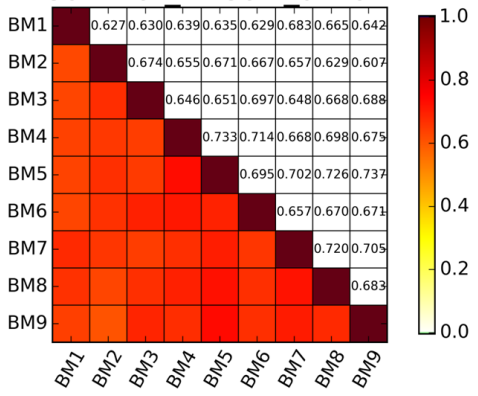

Source: NEA, 2020.

Case2: K_{eff} (x,α) with nominal α and individual (non-correlated) x1

Table 5.2. Case 2 - Resulting k_{eff} mean values and standard deviations

BM 1	1.0171267 ± 0.00537258
BM 2	1.01921443 ± 0.00507729
BM 3	1.01767394 ± 0.00510046
BM 4	1.01143706 ± 0.00475967
BM 5	1.00865622 ± 0.00529865
BM 6	1.01853132 ± 0.00525914
BM 7	1.00560504 ± 0.00525879
BM 8	1.00630481 ± 0.00517455
BM 9	1.00278215 ± 0.00543659

Figure 5.3. Case 2 - Scatter plot of k_{eff} values between benchmark experiments

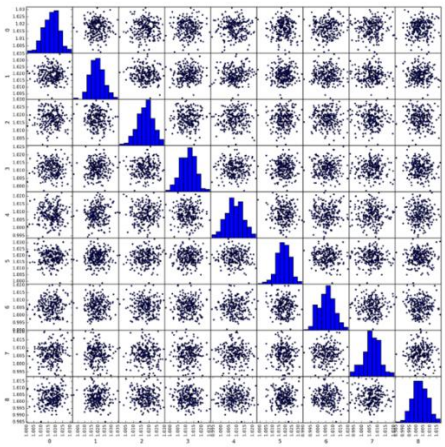

Source: NEA, 2020.
Note: On the diagonal axis the k_{eff} distribution is shown. Note that the numeration of benchmarks runs from 0 to 8, not from 1 to 9.

Figure 5.4. Correlation coefficients assuming Case 2

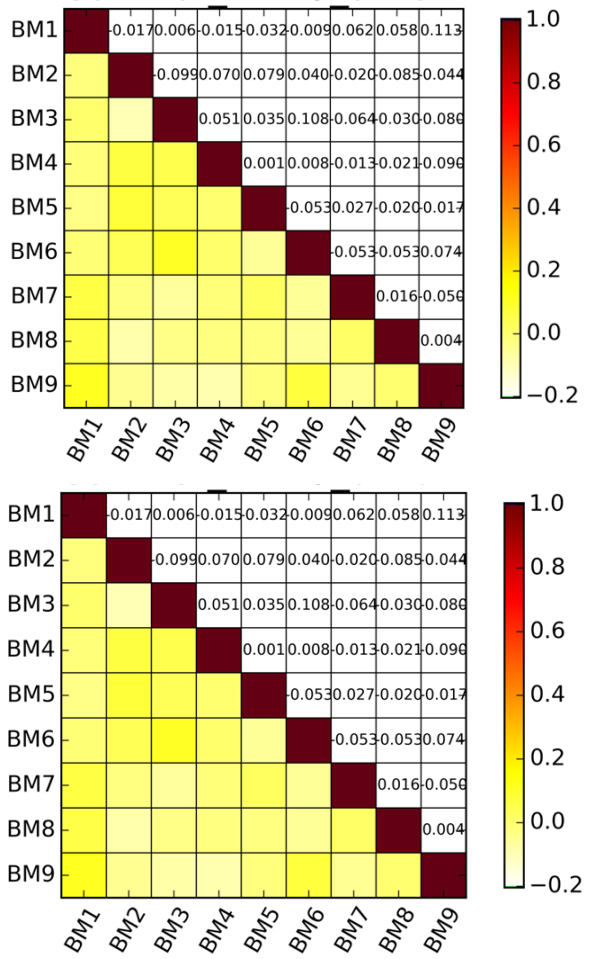

Source: NEA, 2020.

Case 3: k_{eff} (x,α) with sampled (correlated) α and identic (correlated) x1

Table 5.3. Case 3 - Resulting k_{eff} mean values and standard deviations

BM 1	1.0171267 ± 0.00537258
BM 2	1.01921443 ± 0.00507729
BM 3	1.01767394 ± 0.00510046
BM 4	1.01143706 ± 0.00475967
BM 5	1.00865622 ± 0.00529865
BM 6	1.01853132 ± 0.00525914
BM 7	1.00560504 ± 0.00525879
BM 8	1.00630481 ± 0.00517455
BM 9	1.00278215 ± 0.00543659

Figure 5.5. Case 3 - Scatter plot of k_{eff} values between benchmark experiments

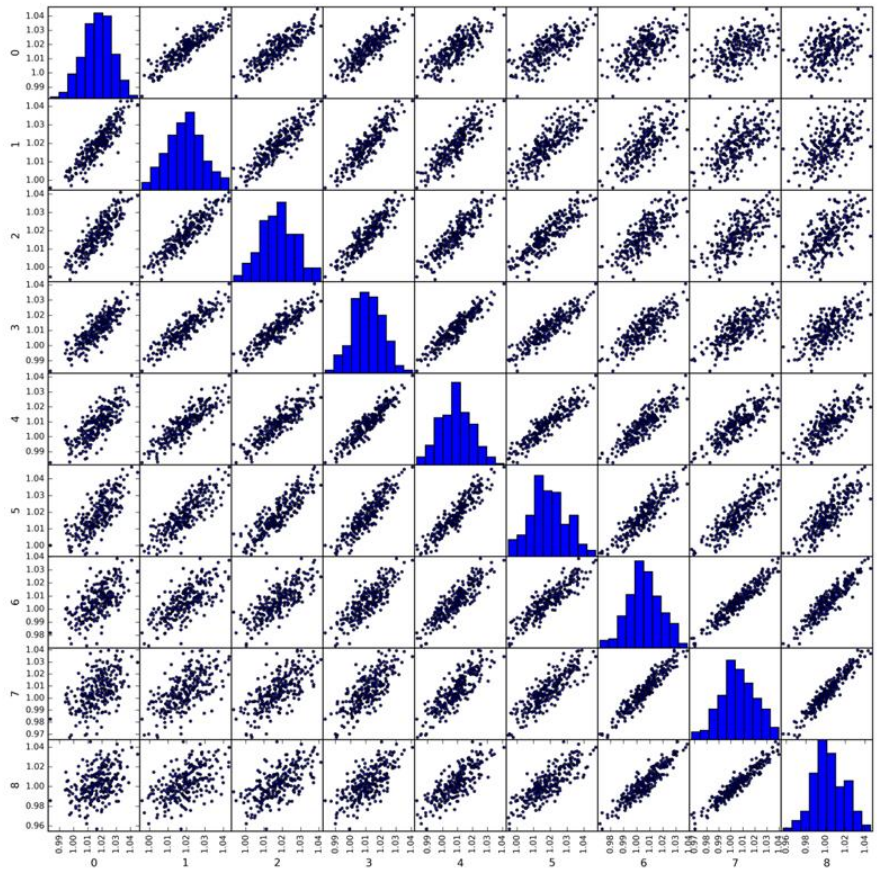

Source: NEA, 2020.

Note: On the diagonal axis the k_{eff} distribution is shown. Note that the numeration of benchmarks runs from 0 to 8, not from 1 to 9.

Figure 5.6. Correlation coefficients assuming Case 3

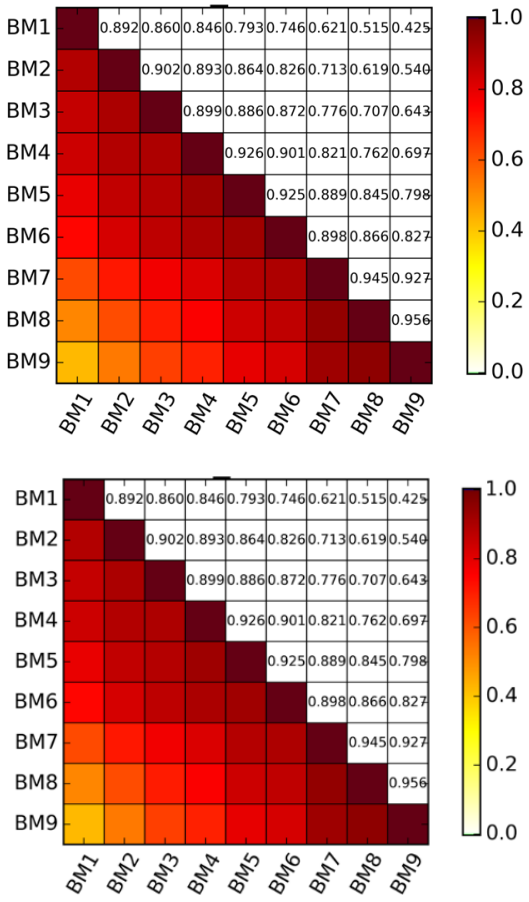

Source: NEA, 2020.

Case 4:k_{eff} (x,α) with sampled (correlated) α and individual (non-correlated) x1

Table 5.4. Case 4 - Resulting k_{eff} mean values and standard deviations

BM 1	1.016964 ± 0.01020565
BM 2	1.01902464 ± 0.00920596
BM 3	1.01746191 ± 0.00928128
BM 4	1.0112099 ± 0.00960843
BM 5	1.0084177 ± 0.01041313
BM 6	1.01826879 ± 0.01028368
BM 7	1.00532399 ± 0.0125605
BM 8	1.00603664 ± 0.0143717
BM 9	1.00251327 ± 0.01618331

Figure 5.7. Case 4 - Scatter plot of k_{eff} values between benchmark experiments

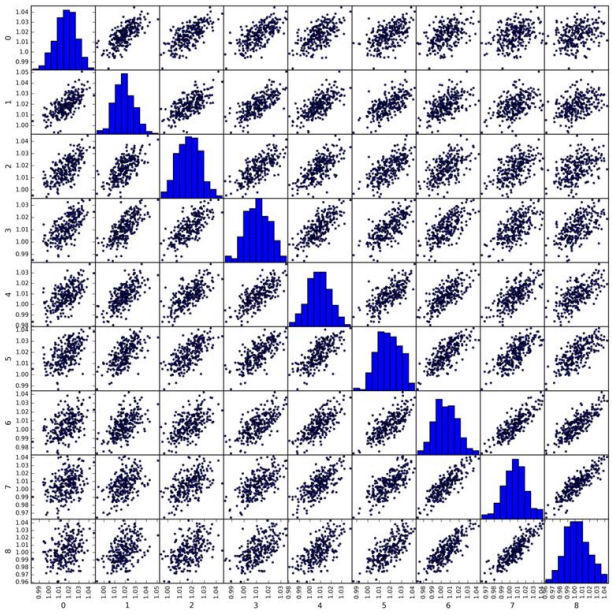

Source: NEA, 2020.
Note: On the diagonal axis the k_{eff} distribution is shown. Note that the numeration of benchmarks runs from 0 to 8, not from 1 to 9.

Figure 5.8. Correlation coefficients assuming Case 4

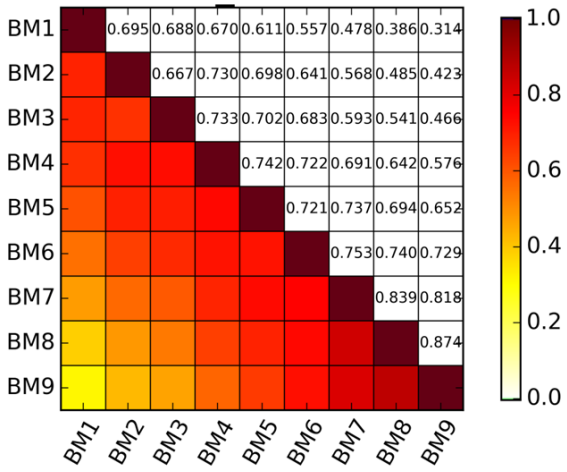

Source: NEA, 2020.

5.1.2. Bias-corrected k_{eff} value

Using Bayesian updating process (described by Hoefer et al. in 2015): Prior k_c of application case: 0.953770640813 ± 0.0001599.

Table 5.5. Posterior distributions

Assumptions	kc
sampled alpha, correlated x1	0.9494730 ± 0.000116
sampled alpha, uncorrelated x1	0.9476004 ± 0.000112
Nominal alpha, correlated x1	0.9450465 ± 0.000080
Nominal alpha, uncorrelated x1	0.9418721 ± 0.000067
Sampled alpha, neglecting covariance	0.9414302 ± 0.000064

Figure 5.9. Distribution functions for prior and posterior distributions assuming sampled alpha values

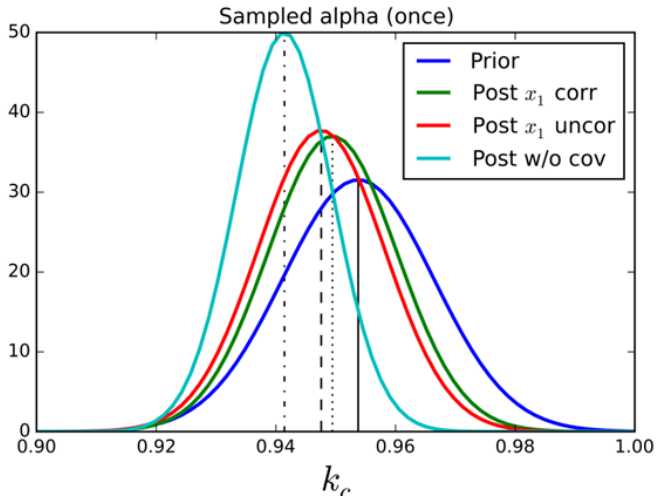

Source: NEA, 2020.

Figure 5.10. Distribution functions for prior and posterior distributions assuming nominal alpha values

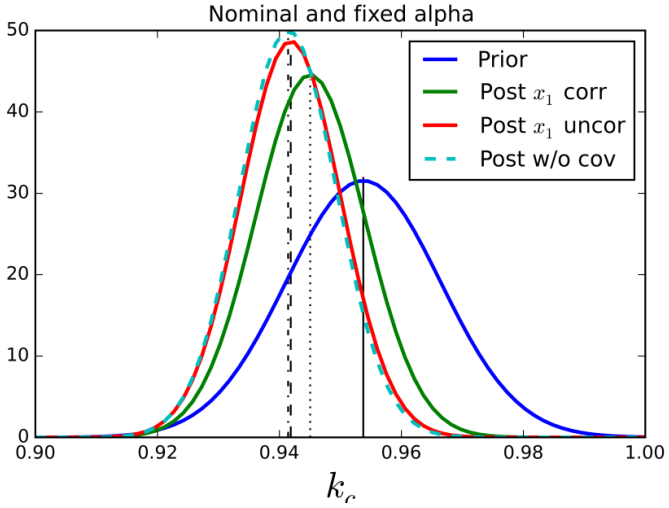

Source: NEA, 2020.

5.2. UACSA BM Phase IV Results

The used methodology is based on the GRS tool SUnCISTT (Behler et al., 2014) using a full Monte Carlo approach (250 samples each experiment).

The criticality calculations were executed with the sequence CSAS5 of SCALE 6.1.2 using the Monte Carlo code KENO-V.a and the continuous energy library based on ENDF/B-VII (10,000 neutrons per generation, 100 skipped generations and a Monte Carlo terminate σ_{MC} of 1×10^{-4} for scenario E and 5×10^{-4} for all others).

The impact of nuclear data uncertainties on k_{eff} was analysed with TSUNAMI of the SCALE 6.1.2 package.

Figure 5.11 shows the k_{eff} values of the individual methods of analysis in comparison. In black the experimental values (k_{eff} = 1.000) are shown with error bars deduced from uncertainty propagation in the handbook. Red shows the results of scenario A and blue of scenario E, both obtained by variation of the system parameters. Green shows the TSUNAMI calculations with the uncertainty of k_{eff} due to nuclear data uncertainties. The SCALE calculations with the used library and the CSAS5 sequence underestimate k_{eff} in general, a known effect for low enriched uranium setups. The larger error bars of the Monte Carlo approach of Scenario A in comparison to the error propagation approach, as done in the Handbook, are not attributed to a conceptional difference between the two methods. They rather arise from the different interpretation of the system parameter uncertainties Scenario E, in which the individual variation of the parameters partly cancel each other out, has significantly lower error bars, except for LCT-07-02, and especially 03 and 04.

Figure 5.11. Experimental k_{eff} for LCT-07 and 39 in comparison to different calculation methods

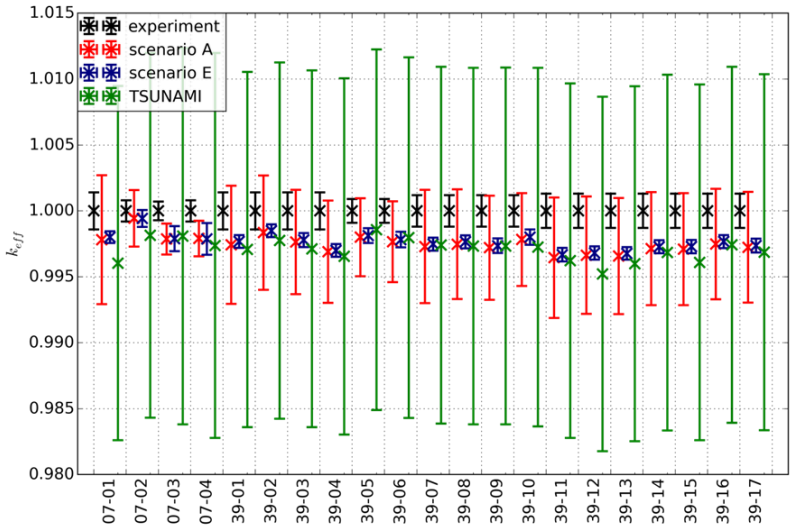

Source: NEA, 2020.

Note: Experimental σ from uncertainty propagation, sampling σ from system parameter uncertainties, TSUNAMI σ from nuclear data uncertainties.

Figure 5.12. Correlation coefficients of k_{eff} due to system parameter uncertainties for a subset of experiments for all five scenarios

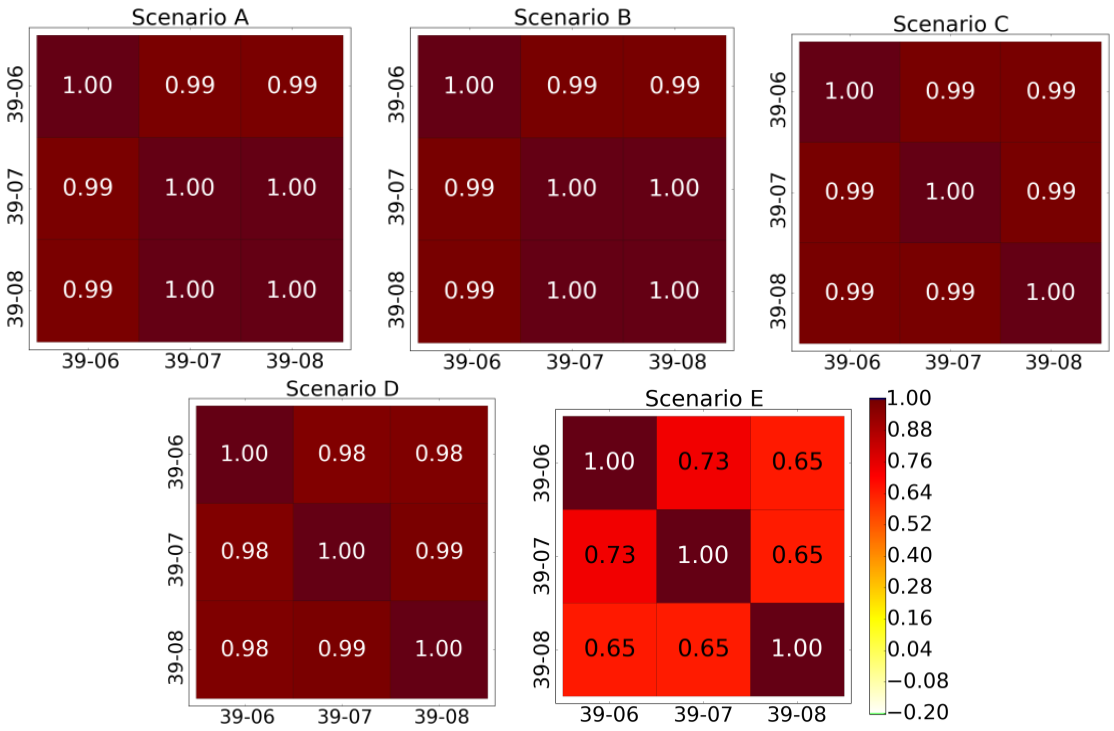

Source: NEA, 2020.

Figure 5.13. Correlation coefficients of k_{eff} for scenarios A (left) and E (right) due to system parameter uncertainties

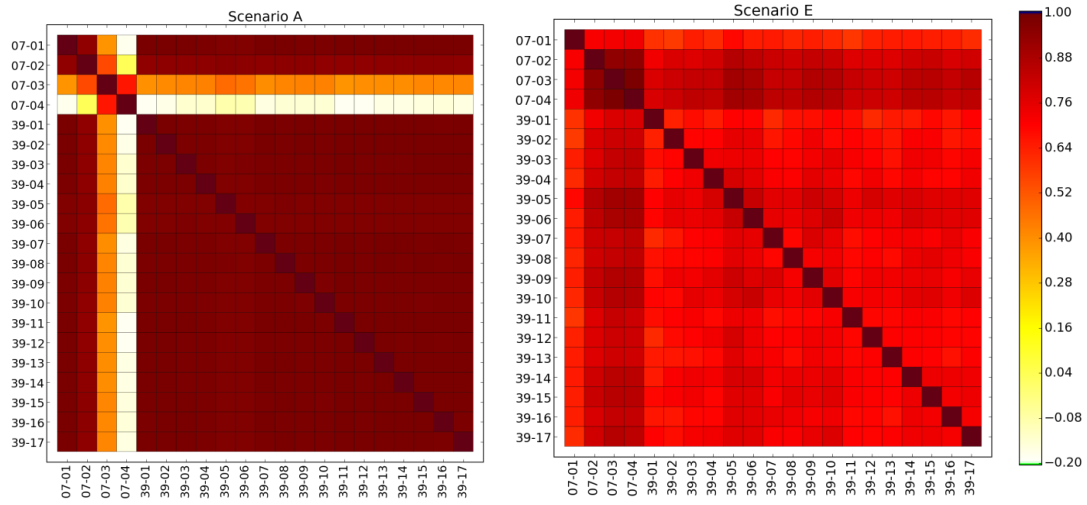

Source: NEA, 2020.

Figure 5.14. Correlation coefficients between experiments and application cases due to nuclear data uncertainties calculated with TSUNAMI

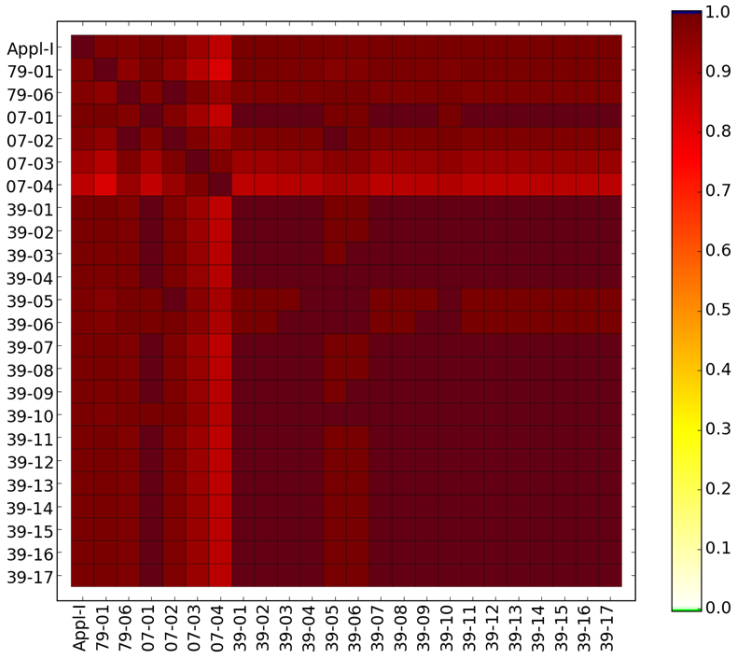

Source: NEA, 2020.

5.2.1. Sensitivity analysis

From the results of the uncertainty analysis using varied parameters, in a Monte Carlo approach the sensitivity of k_{eff} on system parameter uncertainties can be computed. This sensitivity is calculated as the Pearson correlation coefficient between k_{eff} and each varied parameters. Therefore, it specifies to what extent the uncertainty of k_{eff} is related to the uncertainties of the different varied parameters. Note, that this sensitivity calculation does not give any statement about the slope of the dependence.

Figure 5.15. Sensitivity of k_{eff} on varied parameters for scenarios A (left) and E (right) for all experiments

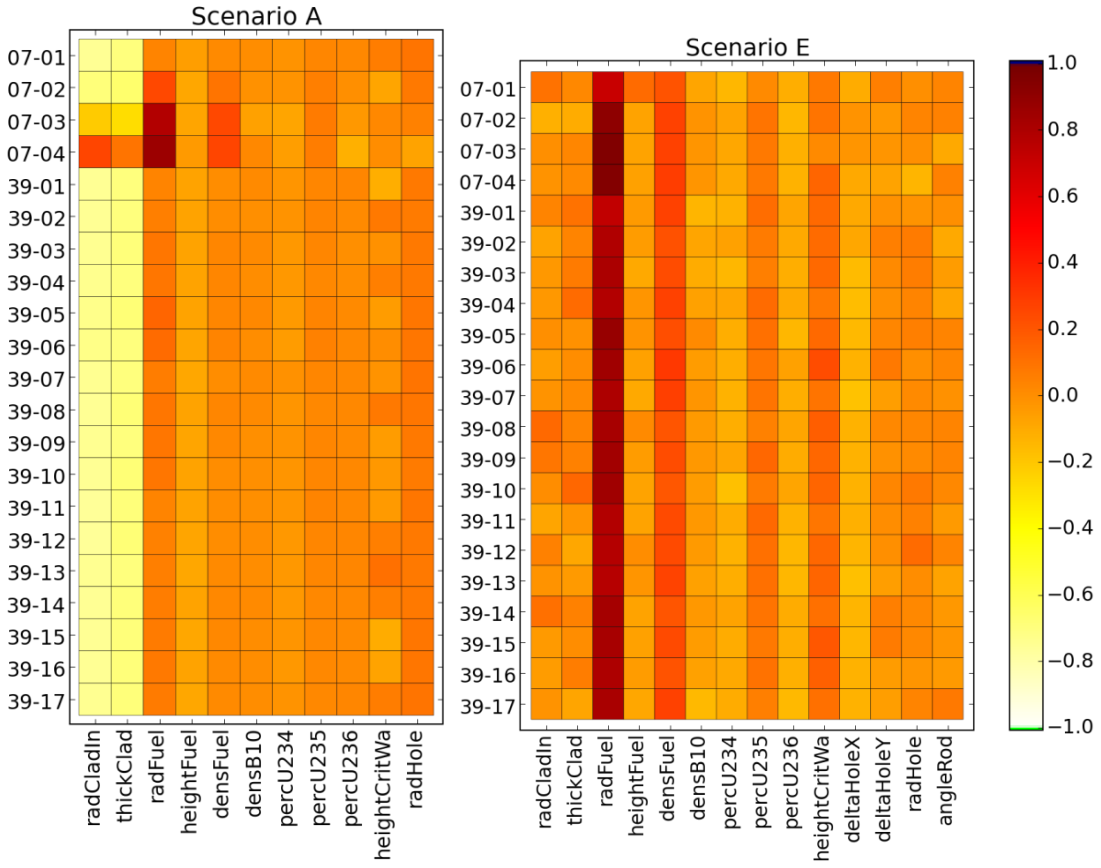

Source: NEA, 2020.
Note: The reduced impact of cladding parameters leads to the effect, that the fuel radius is the leading parameter for scenario E.

5.2.2. Bayesian analysis

Figure 5.16. Prior and posterior distributions for the application cases App.1 (left) and LCT-79-01 (right)

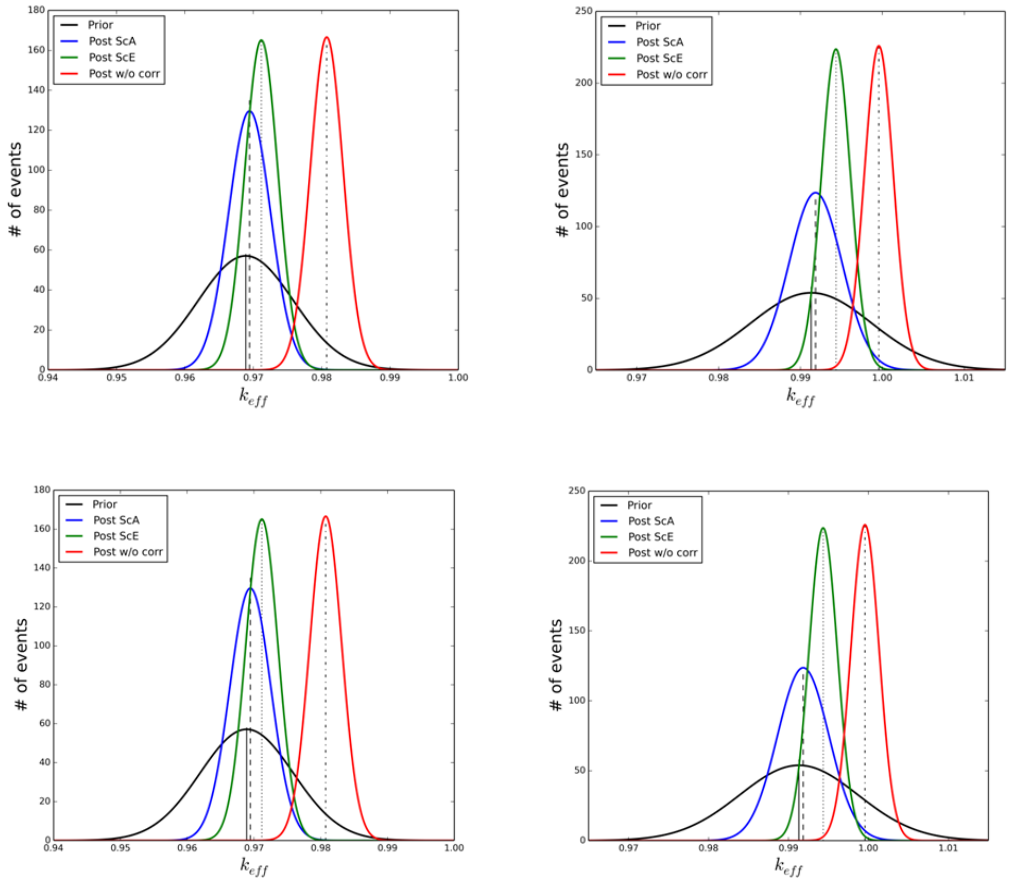

Source: NEA, 2020.
Note: The posterior distributions are shown for scenarios A and E and neglecting systematic uncertainties.

Table 5.6. Prior and posterior distribution characteristics ($k_{eff} \pm 1\sigma$)

	Prior	Post ScA	Post ScE	Post w/o corr
App.1	0.96891 ± 6.9830×10^{-3}	0.96946 ± 3.0770×10^{-3}	0.97118 ± 2.4153×10^{-3}	0.980743 ± 2.3940×10^{-3}
LCT79-01	0.9913 ± 7.4045×10^{-3}	0.99184 ± 3.2262×10^{-3}	0.99434± 1.7835×10^{-3}	0.99957 ± 1.7656×10^{-3}

This work is further described in (Peters, Sommer and Stuke, 2015a; Peters, Sommer and Stuke, 2015b) and (Peters, Sommer and Stuke, 2016). Related previous studies are reported in (Bock, Stuke, 2013; Bock, Behler, 2013).

6. Participant F

Contributor: Nicolas Leclaire (IRSN, France)

Code used for the calculation of uncertainties:

The MORET 5 code (5.C.1 release) is a French Monte Carlo code that solves the transport equation in 3D geometry using cross-sections at the ACE format processed from the French GAIA tool, which is a frame based on NJOY99,NJOY2012 or NJOY2016 versions. It uses probability tables for dealing with the unresolved resonance range and has a sensitivity calculation capability.

It is used either within a multi-group route inside the CRISTAL criticality-safety package, coupled with the deterministic APOLLO2 code, performing P_{ij} cell calculations or in a continuous energy route, as it is the case here.

For the uncertainty calculations, the JEFF-3.1 evaluation of nuclear data was used.

Mathematical approach and scaling factors:

Uncertainty calculations pertaining to the geometry were performed doing two independent Monte Carlo MORET 5 calculations for a variation of the parameter greater than the uncertainty. The values of the parameter variations, allowing access to the scaling factors, are reported in the Excel file. It was checked that the variation corresponded to the linearity domain of the perturbation.

The Monte Carlo standard deviation of calculations was set equal to 0.00020.

Uncertainty calculations pertaining to the chemistry were performed using the correlated sampling method implemented in the MORET 5. code. The weight of neutrons in the simulation is slightly modified in order to account for the perturbation of macroscopic cross-section. The perturbation is performed in one run. The advantage of such method is that the uncertainty of the propagated uncertainty is very low (< 1 pcm).

For the configurations with water holes unequally spread over the lattice, two spatial zones were considered for the uncertainty calculation. A first uncertainty calculation was performed where the parameter was varied only in the internal zone with water holes and then another calculation was performed where the parameter was varied only in the external zone without holes. The overall uncertainty was determined taking the square root of the sum of squares of the two propagated uncertainties.

Two scenarios were considered:

Scenario A:

All uncertainties are treated as being systematic.

Scenario E:

Uncertainties treated as being 100% systematic:

- fuel impurity;
- ^{235}U enrichment;
- pellet diameter;
- critical height of water.

Pitch: 90% random and 10 % systematic.

Clad thickness: 100% random.

Density of fuel: 90% systematic and 10% random.

In the correlation matrix, only 32% of the random part of the uncertainty pertaining to chemistry (density) is accounted for. Only 5% of the random part of the uncertainty of pitch and clad thickness is accounted for in the calculation of correlation factors of the matrix.

Uncertainties neglected:

The list of uncertainties that have been investigated is reported in Table 6.1.

Table 6.1. Sources of uncertainties investigated in this work

Parameter	Action
Fuel rod cladding inner diameter, cm	Neglected because accounted for in the thickness
Fuel rod cladding thickness, cm	OK
Fuel pellet diameter, cm	OK
Height of fissile column, cm	Neglected
Fuel rod pitch, cm	OK
Fuel density, g/cm3	OK
Fuel impurity (atomic density of 10B), atom/barn•cm	OK
^{234}U content in U, At.-%	Neglected
^{235}U content in U, At.-%	OK
^{236}U content in U, At.-%	Neglected
^{238}U content in U, At.-%	OK
Critical water height, cm	OK

7. Participant G

Contributor: W. Marshall (ORNL, United States)

7.1. CSAS/KENO

The CSAS5 sequence within SCALE provides automated cross-section processing and three-dimensional (3D) neutron transport via the Monte Carlo technique. The multi-group (MG) processing is provided by XSProc, incorporating the functions provided in earlier SCALE releases by BONAMI, CENTRM, PMC, and WORKER. The working library generated by XSProc is then passed to KENO-V.a for the calculation of the effective neutron multiplication factor, k_{eff}.

KENO-V.a is a 3D Monte Carlo transport program used within SCALE primarily to calculate k_{eff} values. The geometry capabilities are somewhat restricted, but these limitations allow for significantly faster execution times compared to generalised geometry alternatives. KENO-V.a supports all the geometric descriptions needed in this work, including primarily cylinders and rectangular parallelepipeds (called *cuboids* in KENO).

Most of the calculations performed in this effort use the 252-group neutron cross-section library based on ENDF/B-VII.1. As mentioned above, the MG cross-section processing is provided by XSProc. The unit cells used for this processing are either the SQUAREPITCH LATTICECELL or the infinite, homogeneous medium (INFHOMMEDIUM) cell. The fuel rod unit cells are processed as LATTICECELLs, and other mixtures are processed as infinite homogeneous medium cells. Some calculations were performed with KENO in continuous energy mode to confirm that the MG results are accurate, but those results are not included as part of the benchmark submittal.

7.2. Sampler

The Sampler sequence is the most important computer code used in this research. Sampler is referred to as a "super-sequence" within SCALE because it wraps around other sequences, such as CSAS, and perturbs inputs via Monte Carlo sampling. It should be noted that none of the nuclear data sampling capabilities are used. The composition and dimension sampling used here is activated with the *perturb_geometry* option.

7.3. Scenario A

The critical experiment correlations were generated with 150 realisations per experiment. The Monte Carlo uncertainty of the individual KENO calculations for these calculations ranged between approximately 0.00050 Δk and 0.00080 Δk. Each individual calculation was finished in under 15 minutes, leading to a total run time on the order of 550 CPU-hours.

7.4. Scenario E

The critical experiment correlations were generated with 300 realisations per experiment. The Monte Carlo uncertainty of the individual KENO calculations for these calculations was controlled to be 0.00010 Δk. Each individual calculation was finished in approximately 4 hours, leading to a total run time on the order of 24,000 CPU-hours.

8. Participant H

Contributor: M. Chernykh, S. Tittelbach, J. C. Neuber (WTI GmbH, Germany)

WTI has contributed to the following tasks of the UACSA Phase IV Benchmark:

- Phase IV-a, Exercise 2: Analytic Toy Model;
- Phase IV-a, Exercise 1: Generation of the Integral Experiment Covariance Data for Experiments with Water-reflected UO_2 Fuel Rod Arrays;
- Phase IV-b, Application Case 1: Study on Importance of Accounting for the Integral Experiment Correlations in the Criticality Safety Validation for Water-Moderated and Water-reflected 16x16 Fuel Assembly.

8.1. Methods

8.1.1. Calculation code

The criticality calculations are performed with the CSAS25 sequence of the SCALE 6.1.2 program system. The neutron multiplication factors were calculated by the three-dimensional Monte-Carlo (MC) program KENO-V.a using 238-group neutron cross-sections (V7-238) based on the ENDF/B-VII.0 evaluation. The number of neutron generations with 1000 neutrons per generation as well as the number of first neutron generations to be skipped is chosen in such a way, that the standard deviation of the calculated neutron multiplication factors is below 50 pcm.

The analysis of the analytic toy model is performed using Microsoft Excel spreadsheet application.

8.1.2. Sensitivity coefficients

Sensitivity coefficients S are determined as a slope of a linear interpolation of the calculated neutron multiplication factors k by varying the investigated model parameter x, i. e. $S = \frac{\partial k}{\partial x}$. An exemplary analysis with the sensitivity coefficient S = -0.6064 is shown in Figure 8.1. The determination of each sensitivity coefficient is based on 30 random samples within the specified range of the investigated parameter.

Figure 8.1. Example for determination of sensitivity coefficients

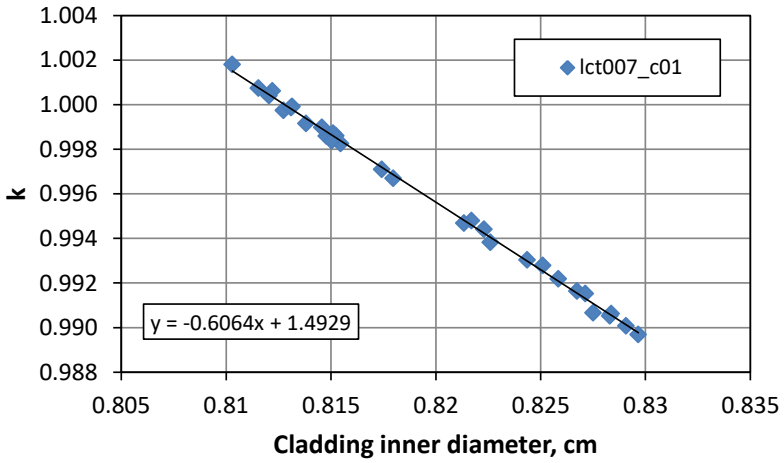

Source: NEA, 2020.

8.1.3. Correlation coefficients

Correlation coefficients between benchmark experiments are determined all together in one go using Monte-Carlo techniques. To make this possible the basic geometry and material parameters of all the experimental configurations $i = 1, \ldots, N_E$ are pooled in one and only one random vector $x = (x_1, x_2, \ldots)^T$. By appropriate choice of probability density functions for the investigated model parameters this representation allows the modelling of the stochastic dependence between some model parameters from different experimental configurations.

Let n_D denote the number of MC samples $x_n^{MC} = \left(x_{1n}^{MC}, x_{2n}^{MC}, \ldots, x_{\beta n}^{MC}\right)^T$ drawn from the probability density function of each sampled model parameter. Each sample x_n^{MC} generates N_E specific random configurations reflecting the configurational variations due to the uncertainties in the model parameters of the N_E experimental configurations. The performed analysis is based on $n_D = 1000$ MC samples. Let

$$k_n^{MC} = \left((k_1)_n, \ldots, \left(k_{N_E}\right)_n\right)^T$$

denote the set of k_{eff} values obtained for the N_E random configurations with the n^{th} MC sample x_n^{MC}. From the ensemble $\{k_n^{MC};\ n = 1, \ldots, n_D\}$ of the resulting k_{eff} value sets k_n^{MC} the sample mean value:

$$\hat{k}^{MC} = \frac{1}{n_D} \sum_{n=1}^{n_D} k_n^{MC}$$

and then the sample covariance matrix:

$$S^{MC} = \frac{1}{n_D - 1} \sum_{n=1}^{n_D} \left(k_n^{MC} - \hat{k}^{MC}\right) \left(k_n^{MC} - \hat{k}^{MC}\right)^T$$

are determined. The correlation coefficients K_{ij} represent the normalised elements of the covariance matrix S^{MC} and are determined as follows:

$$K_{ij} = \frac{S_{ij}^{MC}}{\sqrt{S_{ii}^{MC} S_{jj}^{MC}}}.$$

8.1.4. Validation of criticality calculations

The detailed description of the applied methodology is given in Supplement 1 to German standard DIN 25478.

The bias-corrected neutron multiplication factor of the analysed application case (e.g. FA configuration) with calculated $k_{eff}(A)$ is determined as follows:

$$k_S = k_{eff}(A) + \Delta k_B.$$

Δk_B represents the bias of $k_{eff}(A)$ and is obtained from the evaluation of appropriately selected critical experimental configurations as follows:

$$\Delta k_B = \frac{1}{N_E}\sum_{i=1}^{N_E}(\Delta k_B)_i = \frac{1}{N_E}\sum_{i=1}^{N_E}\left(k_i^E - k_i^C\right)$$

where N_E is the number of evaluated critical configurations, k_i^E denotes the experimentally determined k_{eff} value of the i^{th} experimental configuration, and k_i^C is the k_{eff} value calculated for this configuration.

The variance of the bias-corrected neutron multiplication factor becomes, therefore,

$$V[k_S] = V\left[k_{eff}(A)\right] + \frac{1}{N_E^2}\sum_{i,j=1}^{N_E} cov\left(k_i^C, k_j^C\right) - \frac{2}{N_E}\sum_{i=1}^{N_E} cov\left(k_{eff}(A), k_i^C\right).$$

$V\left[k_{eff}(A)\right]$ denotes the variance of the calculated mean value of $k_{eff}(A)$. The terms $cov\left(k_{eff}(A), k_i^C\right)$ represent the covariances between $k_{eff}(A)$ and the calculational results k_i^C. These covariances are due to the uncertainties in the applied nuclear data and can be estimated by means of the TSUNAMI code of the SCALE program system.

The variances $V\left[k_i^C\right] \equiv cov\left(k_i^C, k_i^C\right)$ of the calculational results and the covariances $cov\left(k_i^C, k_j^C\right)$ between these results are due not only to the uncertainties in the nuclear data, but also to the uncertainties in the dimensions, chemical compositions and positioning of the materials employed in the experimental configurations. Using first-order perturbation theory each term can be split as follows:

$$cov\left(k_i^C, k_j^C\right) \approx C_{ij}^{ND} + C_{ij}^{M}\ , i \wedge j = 1, \ldots, N_E\ .$$

C_{ij}^{ND} denotes the covariance arising from the uncertainties in the nuclear data and can be estimated by means of the TSUNAMI code. C_{ij}^{M} is the covariance term resulting from the uncertainties in the geometry and material data of the experimental configurations i and j, respectively. The elements S_{ij}^{MC} of the matrix S^{MC} described above are determined using the MC techniques and serve as the estimates of the terms C_{ij}^{M}.

The 95 %/95 % confidence limit $k_{95/95}$ is determined as:

$$k_{95/95} = k_S + \lambda_{95/95}\,\sigma$$

with the standard deviation $\sigma = \sqrt{V[k_s]}$.

The Parameter $\lambda_{95/95} \equiv \lambda(N, 0.05, 0.05)$ with:

$$\lambda(N, \alpha, \gamma) = \frac{2(N-1)}{2(N-1) - \Phi_{1-\alpha}^2} \cdot \left[\Phi_{1-\gamma} + \frac{\Phi_{1-\alpha}}{\sqrt{2(N-1)}} \cdot \sqrt{[2(N-1) - \Phi_{1-\alpha}^2] \cdot \frac{1}{N} + \Phi_{1-\gamma}^2}\right]$$

where N is the number of MC samples and Φ_q the q[th] quantile of the standard distribution. For $\alpha = 0.05$ and $\gamma = 0.05$ the 0.95[th] quantile equals to $\Phi_{0.95} = 1.64485$.

8.1.5. Specific features of the analysis

The determination of the covariance and correlation matrices for Scenarios A through E of the Phase IV-a, Exercise 1 was performed under the assumption of complete stochastic dependence of fuel rod positions within each benchmark configuration (e.g. the same correlations for Scenarios A through C). Results of the analysis are summarised in Table 8.8. through Table 8.12. Additionally, the Scenarios A and E were analysed according to the benchmark specifications under the assumption of stochastic independence of fuel rod positions using continuous neutron cross-sections (CE_V7_ENDF) based on the ENDF/B-VII.0 evaluation (see Table 8.13 and Table 8.14).

For the sake of simplicity the parameter $\lambda_{95/95}$ is set to 1.927 throughout the analysis irrespective of the performed number of MC samples.

8.2. Results of the analysis

8.2.1. Analytic toy model

Task 1a: Assuming no stochastic dependence for x_1

Table 8.1. Covariances (top) and correlations (bottom) due to system parameters (Task 1a)

covariance	Toy 1	Toy 2	Toy 3	Toy 4	Toy 5	Toy 6	Toy 7	Toy 8	Toy 9
Toy 1	2.59E-05	2.28E-07	8.05E-07	9.39E-07	4.63E-07	-4.34E-07	2.45E-07	-1.58E-08	9.08E-07
Toy 2	2.28E-07	2.69E-05	2.54E-08	-6.31E-07	-1.20E-06	-1.16E-07	1.33E-07	-9.59E-07	1.05E-06
Toy 3	8.05E-07	2.54E-08	2.62E-05	8.67E-07	-3.20E-07	-1.97E-07	-8.08E-07	-1.40E-06	5.48E-07
Toy 4	9.39E-07	-6.31E-07	8.67E-07	2.72E-05	2.43E-07	4.09E-07	-2.01E-07	-1.17E-06	-4.28E-07
Toy 5	4.63E-07	-1.20E-06	-3.20E-07	2.43E-07	2.77E-05	1.01E-07	-1.16E-06	1.32E-06	-1.04E-06
Toy 6	-4.34E-07	-1.16E-07	-1.97E-07	4.09E-07	1.01E-07	2.53E-05	-1.26E-06	2.77E-07	-3.24E-07
Toy 7	2.45E-07	1.33E-07	-8.08E-07	-2.01E-07	-1.16E-06	-1.26E-06	2.80E-05	7.07E-07	2.05E-07
Toy 8	-1.58E-08	-9.59E-07	-1.40E-06	-1.17E-06	1.32E-06	2.77E-07	7.07E-07	2.80E-05	-8.51E-07
Toy 9	9.08E-07	1.05E-06	5.48E-07	-4.28E-07	-1.04E-06	-3.24E-07	2.05E-07	-8.51E-07	3.03E-05

correlation	Toy 1	Toy 2	Toy 3	Toy 4	Toy 5	Toy 6	Toy 7	Toy 8	Toy 9
Toy 1	1.00	0.01	0.03	0.04	0.02	-0.02	0.01	0.00	0.03
Toy 2	0.01	1.00	0.00	-0.02	-0.04	0.00	0.00	-0.03	0.04
Toy 3	0.03	0.00	1.00	0.03	-0.01	-0.01	-0.03	-0.05	0.02
Toy 4	0.04	-0.02	0.03	1.00	0.01	0.02	-0.01	-0.04	-0.01
Toy 5	0.02	-0.04	-0.01	0.01	1.00	0.00	-0.04	0.05	-0.04
Toy 6	-0.02	0.00	-0.01	0.02	0.00	1.00	-0.05	0.01	-0.01
Toy 7	0.01	0.00	-0.03	-0.01	-0.04	-0.05	1.00	0.03	0.01
Toy 8	0.00	-0.03	-0.05	-0.04	0.05	0.01	0.03	1.00	-0.03
Toy 9	0.03	0.04	0.02	-0.01	-0.04	-0.01	0.01	-0.03	1.00

Task 1b: Assuming stochastic dependence for x_1

Table 8.2. Covariances (top) and correlations (bottom) due to system parameters (Task 1b)

covariance	Toy 1	Toy 2	Toy 3	Toy 4	Toy 5	Toy 6	Toy 7	Toy 8	Toy 9
Toy 1	2.59E-05	1.72E-05	1.68E-05	1.90E-05	1.84E-05	1.80E-05	1.93E-05	1.83E-05	1.82E-05
Toy 2	1.72E-05	2.55E-05	1.68E-05	1.82E-05	1.89E-05	1.73E-05	1.93E-05	1.82E-05	1.79E-05
Toy 3	1.68E-05	1.68E-05	2.58E-05	1.87E-05	1.85E-05	1.82E-05	1.90E-05	1.82E-05	1.83E-05
Toy 4	1.90E-05	1.82E-05	1.87E-05	2.98E-05	2.07E-05	1.96E-05	2.05E-05	1.93E-05	1.94E-05
Toy 5	1.84E-05	1.89E-05	1.85E-05	2.07E-05	2.88E-05	1.95E-05	2.05E-05	2.02E-05	1.94E-05
Toy 6	1.80E-05	1.73E-05	1.82E-05	1.96E-05	1.95E-05	2.73E-05	1.96E-05	1.92E-05	1.84E-05
Toy 7	1.93E-05	1.93E-05	1.90E-05	2.05E-05	2.05E-05	1.96E-05	2.95E-05	2.03E-05	2.08E-05
Toy 8	1.83E-05	1.82E-05	1.82E-05	1.93E-05	2.02E-05	1.92E-05	2.03E-05	2.79E-05	1.95E-05
Toy 9	1.82E-05	1.79E-05	1.83E-05	1.94E-05	1.94E-05	1.84E-05	2.08E-05	1.95E-05	2.78E-05

correlation	Toy 1	Toy 2	Toy 3	Toy 4	Toy 5	Toy 6	Toy 7	Toy 8	Toy 9
Toy 1	1.00	0.67	0.65	0.68	0.67	0.68	0.70	0.68	0.68
Toy 2	0.67	1.00	0.65	0.66	0.69	0.65	0.70	0.68	0.67
Toy 3	0.65	0.65	1.00	0.67	0.68	0.69	0.69	0.68	0.68
Toy 4	0.68	0.66	0.67	1.00	0.70	0.69	0.69	0.67	0.67
Toy 5	0.67	0.69	0.68	0.70	1.00	0.69	0.70	0.71	0.68
Toy 6	0.68	0.65	0.69	0.69	0.69	1.00	0.69	0.69	0.67
Toy 7	0.70	0.70	0.69	0.69	0.70	0.69	1.00	0.71	0.73
Toy 8	0.68	0.68	0.68	0.67	0.71	0.69	0.71	1.00	0.70
Toy 9	0.68	0.67	0.68	0.67	0.68	0.67	0.73	0.70	1.00

Task 2

Table 8.3. Covariances (top) und correlations (bottom) due to nuclear data (Task 2)

covariance	Appl.	Toy 1	Toy 2	Toy 3	Toy 4	Toy 5	Toy 6	Toy 7	Toy 8	Toy 9
Appl.	9.31E-05	5.69E-05	6.41E-05	7.10E-05	7.76E-05	8.41E-05	9.18E-05	1.11E-04	1.25E-04	1.38E-04
Toy 1	5.69E-05	7.03E-05	6.88E-05	6.70E-05	6.49E-05	6.32E-05	6.21E-05	5.66E-05	5.33E-05	5.00E-05
Toy 2	6.41E-05	6.88E-05	6.88E-05	6.85E-05	6.80E-05	6.77E-05	6.82E-05	6.71E-05	6.69E-05	6.64E-05
Toy 3	7.10E-05	6.70E-05	6.85E-05	6.98E-05	7.08E-05	7.20E-05	7.40E-05	7.73E-05	8.00E-05	8.24E-05
Toy 4	7.76E-05	6.49E-05	6.80E-05	7.08E-05	7.33E-05	7.59E-05	7.95E-05	8.71E-05	9.28E-05	9.80E-05
Toy 5	8.41E-05	6.32E-05	6.77E-05	7.20E-05	7.59E-05	7.99E-05	8.50E-05	9.66E-05	1.05E-04	1.13E-04
Toy 6	9.18E-05	6.21E-05	6.82E-05	7.40E-05	7.95E-05	8.50E-05	9.16E-05	1.08E-04	1.19E-04	1.30E-04
Toy 7	1.11E-04	5.66E-05	6.71E-05	7.73E-05	8.71E-05	9.66E-05	1.08E-04	1.36E-04	1.56E-04	1.75E-04
Toy 8	1.25E-04	5.33E-05	6.69E-05	8.00E-05	9.28E-05	1.05E-04	1.19E-04	1.56E-04	1.82E-04	2.07E-04
Toy 9	1.38E-04	5.00E-05	6.64E-05	8.24E-05	9.80E-05	1.13E-04	1.30E-04	1.75E-04	2.07E-04	2.36E-04

correlation	Appl.	Toy 1	Toy 2	Toy 3	Toy 4	Toy 5	Toy 6	Toy 7	Toy 8	Toy 9
Appl.	1.00	0.70	0.80	0.88	0.94	0.98	0.99	0.99	0.96	0.93
Toy 1	0.70	1.00	0.99	0.96	0.90	0.84	0.77	0.58	0.47	0.39
Toy 2	0.80	0.99	1.00	0.99	0.96	0.91	0.86	0.69	0.60	0.52
Toy 3	0.88	0.96	0.99	1.00	0.99	0.96	0.93	0.79	0.71	0.64
Toy 4	0.94	0.90	0.96	0.99	1.00	0.99	0.97	0.87	0.80	0.74
Toy 5	0.98	0.84	0.91	0.96	0.99	1.00	0.99	0.93	0.87	0.82
Toy 6	0.99	0.77	0.86	0.93	0.97	0.99	1.00	0.96	0.92	0.88
Toy 7	0.99	0.58	0.69	0.79	0.87	0.93	0.96	1.00	0.99	0.98
Toy 8	0.96	0.47	0.60	0.71	0.80	0.87	0.92	0.99	1.00	1.00
Toy 9	0.93	0.39	0.52	0.64	0.74	0.82	0.88	0.98	1.00	1.00

Table 8.4. Summary of results for Task 2

	Task 2a	Task 2b
N_B	9	9
$V[k_C]$	9.31E-05	9.31E-05
$\frac{1}{N_B^2}\sum_{i,j=1}^{N_B} \mathrm{cov}\left((k_B)_i,(k_B)_j\right)_{Geom}$	2.96E-06	1.98E-05
$\frac{1}{N_B^2}\sum_{i,j=1}^{N_B} \mathrm{cov}\left((k_B)_i,(k_B)_j\right)_{ND}$	9.01E-05	9.01E-05
$-\frac{2}{N_B}\sum_{i=1}^{N_B} \mathrm{cov}(k_C,(k_B)_i)$	-1.82E-04	-1.82E-04
$V[k_S]$	4.14E-06	2.10E-05
σ	0.00203	0.00459
k_C	0.95363	0.95363
Δk_B	-0.01203	-0.01206
$k_S = k_C + \Delta k_B$	0.94160	0.94156
$k_{95\%/95\%}$	0.94541	0.95016

Participant H's results for Tasks 2a and 2b presented in Figure.3.5 and summarised in Table 3.3 of the main report (NEA, 2022) erroneously correspond to the non-bias-corrected multiplication factor k_C and the bias Δk_B itself. The obtained results should be interpreted as follows:

Table 8.5. Results for Task 2a and Task 2b

Evaluation	Task 2a		Task 2b	
	k_{eff}	1-σ uncertainty	k_{eff}	1-σ uncertainty
H	0.94160	0.00203	0.94156	0.00459

8.2.2. Phase IV-a, Exercise 1

Table 8.6. Sensitivity coefficients to individual parameter variations for each experimental configuration

ID	Cladding inner diameter	Cladding thickness	Pellet diameter	Height of fissile column	Fuel density	^{10}B atomic density	^{234}U content	^{235}U content	^{236}U content	^{238}U content	Critical height
lct007_c01	-0.606	-1.149	0.195	0.000	0.009	-6214.0	0.011	0.043	0.026	0.001	0.000
lct007_c02	-0.253	-0.487	0.383	0.000	0.016	-1208.9	-0.072	0.021	0.007	-0.029	0.001
lct007_c03	-0.046	-0.103	0.558	0.000	0.020	496.1	-0.047	0.072	-0.059	-0.015	0.001
lct007_c04	0.052	0.037	0.672	0.000	0.022	-3858.0	-0.093	0.084	0.053	-0.018	0.001
lct039_c01	-0.550	-1.035	0.221	0.000	0.012	-2922.5	-0.050	0.015	-0.022	-0.091	0.001
lct039_c02	-0.539	-0.993	0.206	0.000	0.010	-3692.3	-0.040	0.024	-0.013	-0.050	0.001
lct039_c03	-0.501	-0.897	0.257	0.000	0.011	-3322.8	-0.010	0.025	0.010	0.027	0.001
lct039_c04	-0.477	-0.895	0.259	0.000	0.010	-1304.1	-0.003	0.039	-0.063	0.013	0.000
lct039_c05	-0.355	-0.637	0.309	0.000	0.010	-6595.6	-0.075	0.038	0.023	0.001	0.001
lct039_c06	-0.369	-0.687	0.313	0.000	0.010	-872.7	-0.075	0.032	-0.007	-0.063	0.002
lct039_c07	-0.536	-0.978	0.260	0.000	0.010	-4397.9	0.014	0.016	-0.062	-0.068	0.001
lct039_c08	-0.515	-0.957	0.268	0.000	0.011	-5435.3	-0.139	0.026	-0.002	-0.024	0.001
lct039_c09	-0.495	-0.889	0.283	0.000	0.011	-3960.7	-0.099	0.036	-0.023	-0.044	0.001
lct039_c10	-0.439	-0.783	0.317	0.000	0.009	-11119.9	-0.002	0.037	-0.026	0.014	0.001
lct039_c11	-0.556	-1.064	0.202	0.000	0.011	-2902.4	0.011	0.014	-0.070	-0.048	0.001
lct039_c12	-0.548	-1.012	0.238	0.000	0.008	-4660.7	-0.075	0.013	-0.002	0.010	0.001
lct039_c13	-0.541	-1.011	0.227	0.000	0.009	-1213.9	-0.136	0.045	-0.082	-0.043	0.001
lct039_c14	-0.526	-0.989	0.219	0.000	0.011	-4116.8	-0.196	0.029	-0.090	0.034	0.001
lct039_c15	-0.526	-0.961	0.247	0.000	0.009	-4325.0	-0.019	0.036	-0.020	-0.079	0.001
lct039_c16	-0.527	-0.963	0.265	0.000	0.011	-297.3	-0.007	0.047	0.083	-0.011	0.001
lct039_c17	-0.523	-0.953	0.249	0.000	0.011	-2550.7	-0.100	0.042	0.016	-0.033	0.000

Table 8.7. Impact of parameter uncertainties on total uncertainty of each experimental configuration

ID	Cladding inner diameter	Cladding thickness	Pellet diameter	Height of fissile column	Fuel density	^{10}B atomic density	^{234}U content	^{235}U content	^{236}U content	^{238}U content	Critical height
lct007_c01	0.72	0.69	0.07	0.02	0.03	0.01	0.00	0.02	0.00	0.00	0.00
lct007_c02	0.67	0.65	0.30	0.01	0.10	0.00	0.02	0.02	0.00	0.13	0.05
lct007_c03	0.24	0.28	0.88	0.01	0.25	0.00	0.02	0.13	0.03	0.14	0.03
lct007_c04	0.24	0.09	0.91	0.03	0.23	0.02	0.04	0.13	0.02	0.14	0.05
lct039_c01	0.71	0.67	0.08	0.00	0.04	0.01	0.01	0.01	0.00	0.20	0.01
lct039_c02	0.73	0.67	0.08	0.01	0.03	0.01	0.00	0.01	0.00	0.12	0.02
lct039_c03	0.74	0.66	0.11	0.01	0.04	0.01	0.00	0.01	0.00	0.07	0.02
lct039_c04	0.72	0.68	0.12	0.01	0.04	0.00	0.00	0.02	0.01	0.04	0.01
lct039_c05	0.73	0.65	0.19	0.00	0.05	0.02	0.01	0.03	0.00	0.00	0.02
lct039_c06	0.70	0.65	0.18	0.00	0.05	0.00	0.01	0.02	0.00	0.21	0.03
lct039_c07	0.72	0.66	0.10	0.01	0.03	0.01	0.00	0.01	0.01	0.16	0.02
lct039_c08	0.73	0.67	0.11	0.00	0.04	0.01	0.02	0.01	0.00	0.06	0.02
lct039_c09	0.73	0.66	0.12	0.01	0.04	0.01	0.01	0.02	0.00	0.11	0.02
lct039_c10	0.74	0.66	0.16	0.00	0.04	0.03	0.00	0.02	0.00	0.04	0.03
lct039_c11	0.72	0.68	0.08	0.01	0.03	0.01	0.00	0.01	0.01	0.11	0.01
lct039_c12	0.73	0.67	0.09	0.00	0.02	0.01	0.01	0.01	0.00	0.02	0.01
lct039_c13	0.72	0.68	0.09	0.00	0.03	0.00	0.02	0.02	0.01	0.10	0.02
lct039_c14	0.72	0.68	0.09	0.01	0.04	0.01	0.02	0.01	0.01	0.08	0.02
lct039_c15	0.72	0.66	0.10	0.01	0.03	0.01	0.00	0.02	0.00	0.19	0.02
lct039_c16	0.73	0.67	0.11	0.00	0.03	0.00	0.00	0.02	0.01	0.03	0.02
lct039_c17	0.73	0.67	0.10	0.02	0.04	0.00	0.01	0.02	0.00	0.08	0.01

Table 8.8. Correlation coefficients (x1000) for Scenario A (stochastic dependence of fuel rod positions)

Sc. A, 238 Group	LCT-07-01	LCT-07-02	LCT-07-03	LCT-07-04	LCT-39-01	LCT-39-02	LCT-39-03	LCT-39-04	LCT-39-05	LCT-39-06	LCT-39-07	LCT-39-08	LCT-39-09	LCT-39-10	LCT-39-11	LCT-39-12	LCT-39-13	LCT-39-14	LCT-39-15	LCT-39-16	LCT-39-17
LCT-07-01	1000	941	420	-128	989	988	986	974	974	975	987	987	985	981	989	988	987	988	988	986	986
LCT-07-02	941	1000	584	91	944	944	946	938	951	952	946	948	948	951	944	943	944	946	946	947	945
LCT-07-03	420	584	1000	691	434	440	449	455	499	498	441	448	458	480	434	438	443	445	445	452	448
LCT-07-04	-128	91	691	1000	-111	-103	-90	-78	-28	-27	-103	-91	-79	-55	-108	-105	-100	-95	-98	-87	-96
LCT-39-01	989	944	434	-111	1000	988	985	976	975	978	987	988	986	982	988	988	987	987	987	986	987
LCT-39-02	988	944	440	-103	988	1000	986	975	975	976	987	987	986	981	988	986	987	987	988	986	987
LCT-39-03	986	946	449	-90	985	986	1000	973	975	976	985	984	984	981	986	985	984	985	986	985	984
LCT-39-04	974	938	455	-78	976	975	973	1000	967	969	975	976	974	972	977	974	975	975	976	974	976
LCT-39-05	974	951	499	-28	975	975	975	967	1000	972	975	976	975	974	976	975	975	975	977	976	976
LCT-39-06	975	952	498	-27	978	976	976	969	972	1000	977	978	978	976	978	977	976	978	978	978	977
LCT-39-07	987	946	441	-103	987	987	985	975	975	977	1000	987	985	981	987	987	986	987	987	986	986
LCT-39-08	987	948	448	-91	988	987	984	976	976	978	987	1000	985	982	988	986	987	987	987	986	986
LCT-39-09	985	948	458	-79	986	986	984	974	975	978	985	985	1000	981	986	984	985	985	986	984	985
LCT-39-10	981	951	480	-55	982	981	981	972	974	976	981	982	981	1000	983	981	982	982	982	981	981
LCT-39-11	989	944	434	-108	988	988	986	977	976	978	987	988	986	983	1000	988	987	988	988	987	987
LCT-39-12	988	943	438	-105	988	986	985	974	975	977	987	986	984	981	988	1000	986	986	987	986	987
LCT-39-13	987	944	443	-100	987	987	984	975	975	976	986	987	985	982	987	986	1000	986	987	986	986
LCT-39-14	988	946	445	-95	987	987	985	975	975	978	987	987	985	982	988	986	986	1000	988	985	986
LCT-39-15	988	946	445	-98	987	988	986	976	977	978	987	987	986	982	988	987	987	988	1000	987	986
LCT-39-16	986	947	452	-87	986	986	985	974	976	978	986	986	984	981	987	986	986	985	987	1000	985
LCT-39-17	986	945	448	-96	987	987	984	976	976	977	986	986	985	981	987	987	986	986	986	985	1000

Table 8.9. Correlation coefficients (x1000) for Scenario B (stochastic dependence of fuel rod positions)

Sc. B, 238 Group	LCT-07-01	LCT-07-02	LCT-07-03	LCT-07-04	LCT-39-01	LCT-39-02	LCT-39-03	LCT-39-04	LCT-39-05	LCT-39-06	LCT-39-07	LCT-39-08	LCT-39-09	LCT-39-10	LCT-39-11	LCT-39-12	LCT-39-13	LCT-39-14	LCT-39-15	LCT-39-16	LCT-39-17
LCT-07-01	1000	945	438	-99	989	989	987	976	973	975	988	987	987	980	989	989	989	989	988	988	987
LCT-07-02	945	1000	584	106	947	947	948	942	955	956	948	950	952	953	948	947	947	951	950	952	951
LCT-07-03	438	584	1000	683	450	449	464	472	526	513	455	464	472	494	445	447	449	461	459	463	458
LCT-07-04	-99	106	683	1000	-86	-82	-65	-52	14	1	-78	-65	-58	-24	-88	-85	-83	-75	-71	-66	-67
LCT-39-01	989	947	450	-86	1000	987	986	974	973	975	987	986	986	981	988	987	987	987	988	986	986
LCT-39-02	989	947	449	-82	987	1000	986	974	975	976	988	987	985	980	987	987	987	987	987	986	986
LCT-39-03	987	948	464	-65	986	986	1000	974	974	976	985	985	984	980	985	986	986	986	986	986	985
LCT-39-04	976	942	472	-52	974	974	974	1000	964	966	975	974	975	971	975	976	974	976	975	976	975
LCT-39-05	973	955	526	14	973	975	974	964	1000	972	973	975	975	973	973	974	974	975	974	974	975
LCT-39-06	975	956	513	1	975	976	976	966	972	1000	975	976	977	975	976	976	976	977	976	977	977
LCT-39-07	988	948	455	-78	987	988	985	975	973	975	1000	986	986	980	987	987	986	987	986	986	986
LCT-39-08	987	950	464	-65	986	987	985	974	975	976	986	1000	985	980	986	986	986	986	985	986	985
LCT-39-09	987	952	472	-58	986	985	984	975	975	977	986	985	1000	981	986	986	986	986	986	987	984
LCT-39-10	980	953	494	-24	981	980	980	971	973	975	980	980	981	1000	980	981	980	981	981	981	981
LCT-39-11	989	948	445	-88	988	987	985	975	973	976	987	986	986	980	1000	988	987	987	987	987	986
LCT-39-12	989	947	447	-85	987	987	986	976	974	976	987	986	986	981	988	1000	987	987	986	987	987
LCT-39-13	989	947	449	-83	987	987	986	974	974	976	986	986	986	980	987	987	1000	987	987	987	986
LCT-39-14	989	951	461	-75	987	987	986	976	975	977	987	986	986	981	987	987	987	1000	987	987	985
LCT-39-15	988	950	459	-71	988	987	986	975	974	976	986	985	986	981	987	986	987	987	1000	986	986
LCT-39-16	988	952	463	-66	986	986	986	976	974	977	986	986	987	981	987	987	987	987	986	1000	986
LCT-39-17	987	951	458	-67	986	986	985	975	975	977	986	985	984	981	986	987	986	985	986	986	1000

Table 8.10. Correlation coefficients (x1000) for Scenario C (stochastic dependence of fuel rod positions)

Sc. C, 238 Group	LCT-07-01	LCT-07-02	LCT-07-03	LCT-07-04	LCT-39-01	LCT-39-02	LCT-39-03	LCT-39-04	LCT-39-05	LCT-39-06	LCT-39-07	LCT-39-08	LCT-39-09	LCT-39-10	LCT-39-11	LCT-39-12	LCT-39-13	LCT-39-14	LCT-39-15	LCT-39-16	LCT-39-17
LCT-07-01	1000	941	440	-116	988	988	986	976	976	976	987	987	986	982	989	989	988	987	988	987	988
LCT-07-02	941	1000	593	92	945	945	948	938	953	952	947	947	948	952	944	945	944	946	944	946	947
LCT-07-03	440	593	1000	660	455	452	473	472	525	520	459	461	474	501	448	456	451	466	464	470	472
LCT-07-04	-116	92	660	1000	-101	-97	-74	-70	-10	-16	-89	-89	-73	-41	-106	-96	-100	-87	-85	-82	-78
LCT-39-01	988	945	455	-101	1000	988	986	976	976	976	987	987	985	982	988	988	987	987	986	987	987
LCT-39-02	988	945	452	-97	988	1000	985	974	975	975	986	986	985	981	987	987	986	986	986	985	986
LCT-39-03	986	948	473	-74	986	985	1000	973	978	978	985	985	984	982	986	986	986	985	985	986	986
LCT-39-04	976	938	472	-70	976	974	973	1000	966	968	973	976	974	972	977	975	975	975	974	975	975
LCT-39-05	976	953	525	-10	976	975	978	966	1000	973	976	976	977	976	976	976	975	977	978	979	978
LCT-39-06	976	952	520	-16	976	975	978	968	973	1000	976	976	977	977	977	977	975	976	977	977	978
LCT-39-07	987	947	459	-89	987	986	985	973	976	976	1000	986	985	982	987	986	986	987	985	986	987
LCT-39-08	987	947	461	-89	987	986	985	976	976	976	986	1000	985	982	987	987	986	986	985	985	987
LCT-39-09	986	948	474	-73	985	985	984	974	977	977	985	985	1000	982	985	986	984	985	985	985	986
LCT-39-10	982	952	501	-41	982	981	982	972	976	977	982	982	982	1000	982	983	982	982	982	983	984
LCT-39-11	989	944	448	-106	988	987	986	977	976	977	987	987	985	982	1000	988	987	988	986	988	988
LCT-39-12	989	945	456	-96	988	987	986	975	976	977	986	987	986	983	988	1000	986	987	987	987	987
LCT-39-13	988	944	451	-100	987	986	986	975	975	975	986	986	984	982	987	986	1000	985	987	987	987
LCT-39-14	987	946	466	-87	987	986	985	975	977	976	987	986	985	982	988	987	985	1000	986	986	986
LCT-39-15	988	944	464	-85	986	986	985	974	978	977	985	985	985	982	986	987	987	986	1000	986	987
LCT-39-16	987	946	470	-82	987	985	986	975	979	977	986	985	985	983	988	987	987	986	986	1000	987
LCT-39-17	988	947	472	-78	987	986	986	975	978	978	987	987	986	984	988	987	987	986	987	987	1000

Table 8.11. Correlation coefficients (x1000) for Scenario D (stochastic dependence of fuel rod positions)

Sc. D, 238 Group	LCT-07-01	LCT-07-02	LCT-07-03	LCT-07-04	LCT-39-01	LCT-39-02	LCT-39-03	LCT-39-04	LCT-39-05	LCT-39-06	LCT-39-07	LCT-39-08	LCT-39-09	LCT-39-10	LCT-39-11	LCT-39-12	LCT-39-13	LCT-39-14	LCT-39-15	LCT-39-16	LCT-39-17
LCT-07-01	1000	474	245	42	466	456	461	474	424	483	463	461	449	451	469	462	450	447	479	474	470
LCT-07-02	474	1000	413	223	486	470	501	473	465	448	439	469	451	417	442	461	469	448	483	468	457
LCT-07-03	245	413	1000	720	275	250	280	304	353	315	248	276	292	289	295	269	263	288	284	259	250
LCT-07-04	42	223	720	1000	48	13	55	72	147	102	19	47	17	72	56	15	25	31	33	20	19
LCT-39-01	466	486	275	48	1000	500	464	486	442	475	474	483	469	450	452	528	444	473	471	447	494
LCT-39-02	456	470	250	13	500	1000	465	490	421	494	452	478	469	447	469	488	449	446	478	488	478
LCT-39-03	461	501	280	55	464	465	1000	456	460	459	469	480	452	441	474	468	441	446	489	502	490
LCT-39-04	474	473	304	72	486	490	456	1000	465	458	480	434	467	463	443	462	458	430	433	469	453
LCT-39-05	424	465	353	147	442	421	460	465	1000	464	467	420	443	455	428	440	458	444	432	505	462
LCT-39-06	483	448	315	102	475	494	459	458	464	1000	432	449	439	432	429	484	479	444	461	434	426
LCT-39-07	463	439	248	19	474	452	469	480	467	432	1000	492	445	458	455	470	416	469	472	492	476
LCT-39-08	461	469	276	47	483	478	480	434	420	449	492	1000	446	424	477	423	438	473	464	464	445
LCT-39-09	449	451	292	17	469	469	452	467	443	439	445	446	1000	442	437	448	449	421	466	461	494
LCT-39-10	451	417	289	72	450	447	441	463	455	432	458	424	442	1000	454	410	442	429	449	458	413
LCT-39-11	469	442	295	56	452	469	474	443	428	429	455	477	437	454	1000	455	445	452	479	463	450
LCT-39-12	462	461	269	15	528	488	468	462	440	484	470	423	448	410	455	1000	478	437	474	462	462
LCT-39-13	450	469	263	25	444	449	441	458	458	479	416	438	449	442	445	478	1000	444	450	459	450
LCT-39-14	447	448	288	31	473	446	446	430	444	444	469	473	421	429	452	437	444	1000	461	477	473
LCT-39-15	479	483	284	33	471	478	489	433	432	461	472	464	466	449	479	474	450	461	1000	480	463
LCT-39-16	474	468	259	20	447	488	502	469	505	434	492	464	461	458	463	462	459	477	480	1000	501
LCT-39-17	470	457	250	19	494	478	490	453	462	426	476	445	494	413	450	462	450	473	463	501	1000

Table 8.12. Correlation coefficients (x1000) for Scenario E (stochastic dependence of fuel rod positions)

Sc. D, 238 Group	LCT-07-01	LCT-07-02	LCT-07-03	LCT-07-04	LCT-39-01	LCT-39-02	LCT-39-03	LCT-39-04	LCT-39-05	LCT-39-06	LCT-39-07	LCT-39-08	LCT-39-09	LCT-39-10	LCT-39-11	LCT-39-12	LCT-39-13	LCT-39-14	LCT-39-15	LCT-39-16	LCT-39-17
LCT-07-01	1000	474	245	42	466	456	461	474	424	483	463	461	449	451	469	462	450	447	479	474	470
LCT-07-02	474	1000	413	223	486	470	501	473	465	448	439	469	451	417	442	461	469	448	483	468	457
LCT-07-03	245	413	1000	720	275	250	280	304	353	315	248	276	292	289	295	269	263	288	284	259	250
LCT-07-04	42	223	720	1000	48	13	55	72	147	102	19	47	17	72	56	15	25	31	33	20	19
LCT-39-01	466	486	275	48	1000	500	464	486	442	475	474	483	469	450	452	528	444	473	471	447	494
LCT-39-02	456	470	250	13	500	1000	465	490	421	494	452	478	469	447	469	488	449	446	478	488	478
LCT-39-03	461	501	280	55	464	465	1000	456	460	459	469	480	452	441	474	468	441	446	489	502	490
LCT-39-04	474	473	304	72	486	490	456	1000	465	458	480	434	467	463	443	462	458	430	433	469	453
LCT-39-05	424	465	353	147	442	421	460	465	1000	464	467	420	443	455	428	440	458	444	432	505	462
LCT-39-06	483	448	315	102	475	494	459	458	464	1000	432	449	439	432	429	484	479	444	461	434	426
LCT-39-07	463	439	248	19	474	452	469	480	467	432	1000	492	445	458	455	470	416	469	472	492	476
LCT-39-08	461	469	276	47	483	478	480	434	420	449	492	1000	446	424	477	423	438	473	464	464	445
LCT-39-09	449	451	292	17	469	469	452	467	443	439	445	446	1000	442	437	448	449	421	466	461	494
LCT-39-10	451	417	289	72	450	447	441	463	455	432	458	424	442	1000	454	410	442	429	449	458	413
LCT-39-11	469	442	295	56	452	469	474	443	428	429	455	477	437	454	1000	455	445	452	479	463	450
LCT-39-12	462	461	269	15	528	488	468	462	440	484	470	423	448	410	455	1000	478	437	474	462	462
LCT-39-13	450	469	263	25	444	449	441	458	458	479	416	438	449	442	445	478	1000	444	450	459	450
LCT-39-14	447	448	288	31	473	446	446	430	444	444	469	473	421	429	452	437	444	1000	461	477	473
LCT-39-15	479	483	284	33	471	478	489	433	432	461	472	464	466	449	479	474	450	461	1000	480	463
LCT-39-16	474	468	259	20	447	488	502	469	505	434	492	464	461	458	463	462	459	477	480	1000	501
LCT-39-17	470	457	250	19	494	478	490	453	462	426	476	445	494	413	450	462	450	473	463	501	1000

Table 8.13. Correlation coefficients (x1000) for Scenario A (stochastic independence of fuel rod positions)

Sc. A, CE	LCT-07-01	LCT-07-02	LCT-07-03	LCT-07-04	LCT-39-01	LCT-39-02	LCT-39-03	LCT-39-04	LCT-39-05	LCT-39-06	LCT-39-07	LCT-39-08	LCT-39-09	LCT-39-10	LCT-39-11	LCT-39-12	LCT-39-13	LCT-39-14	LCT-39-15	LCT-39-16	LCT-39-17
LCT-07-01	1000	942	448	-100	990	988	986	977	975	976	988	988	985	981	989	988	988	987	987	987	988
LCT-07-02	942	1000	598	116	944	944	947	940	953	956	949	949	948	952	945	946	947	945	948	949	950
LCT-07-03	448	598	1000	664	453	457	471	472	525	530	465	469	478	504	458	458	465	464	468	477	475
LCT-07-04	-100	116	664	1000	-90	-82	-68	-63	-1	4	-71	-68	-60	-30	-87	-85	-75	-82	-68	-64	-65
LCT-39-01	990	944	453	-90	1000	988	986	976	976	977	987	987	986	982	988	988	987	987	987	987	988
LCT-39-02	988	944	457	-82	988	1000	985	975	975	976	987	986	985	981	987	988	987	987	987	986	987
LCT-39-03	986	947	471	-68	986	985	1000	974	975	977	986	985	983	980	986	987	986	986	986	985	986
LCT-39-04	977	940	472	-63	976	975	974	1000	966	966	976	976	975	970	976	976	976	975	973	975	975
LCT-39-05	975	953	525	-1	976	975	975	966	1000	972	976	976	976	975	976	976	977	976	976	976	977
LCT-39-06	976	956	530	4	977	976	977	966	972	1000	978	977	977	976	977	976	978	977	977	979	977
LCT-39-07	988	949	465	-71	987	987	986	976	976	978	1000	986	985	981	987	987	987	986	986	986	987
LCT-39-08	988	949	469	-68	987	986	985	976	976	977	986	1000	985	982	986	987	986	986	986	986	986
LCT-39-09	985	948	478	-60	986	985	983	975	976	977	985	985	1000	981	984	985	986	985	984	985	985
LCT-39-10	981	952	504	-30	982	981	980	970	975	976	981	982	981	1000	981	981	981	982	980	982	982
LCT-39-11	989	945	458	-87	988	987	986	976	976	977	987	986	984	981	1000	987	987	987	986	987	987
LCT-39-12	988	946	458	-85	988	988	987	976	976	976	987	987	985	981	987	1000	987	987	987	986	987
LCT-39-13	988	947	465	-75	987	987	986	976	977	978	987	986	986	981	987	987	1000	986	986	986	987
LCT-39-14	987	945	464	-82	987	987	986	975	976	977	986	986	985	982	987	987	986	1000	986	986	986
LCT-39-15	987	948	468	-68	987	987	986	973	976	977	986	986	984	980	986	987	986	986	1000	986	986
LCT-39-16	987	949	477	-64	987	986	985	975	976	979	986	986	985	982	987	986	986	986	986	1000	987
LCT-39-17	988	950	475	-65	988	987	986	975	977	977	987	986	985	982	987	987	987	986	986	987	1000

Table 8.14. Correlation coefficients (x1000) for Scenario E (stochastic independence of fuel rod positions)

Sc. E, CE	LCT-07-01	LCT-07-02	LCT-07-03	LCT-07-04	LCT-39-01	LCT-39-02	LCT-39-03	LCT-39-04	LCT-39-05	LCT-39-06	LCT-39-07	LCT-39-08	LCT-39-09	LCT-39-10	LCT-39-11	LCT-39-12	LCT-39-13	LCT-39-14	LCT-39-15	LCT-39-16	LCT-39-17
LCT-07-01	1000	653	627	630	639	666	660	661	643	647	666	658	678	675	658	667	657	667	658	696	697
LCT-07-02	653	1000	841	849	695	693	724	724	790	767	712	723	733	768	677	704	707	713	719	714	728
LCT-07-03	627	841	1000	931	664	698	740	699	801	795	718	718	740	773	657	696	719	706	711	712	741
LCT-07-04	630	849	931	1000	665	685	743	711	794	800	720	722	747	777	658	695	721	706	712	714	733
LCT-39-01	639	695	664	665	1000	672	669	648	680	679	708	670	682	687	661	681	698	674	668	695	690
LCT-39-02	666	693	698	685	672	1000	687	691	705	701	695	711	733	711	665	704	698	697	672	719	703
LCT-39-03	660	724	740	743	669	687	1000	697	723	728	694	708	707	728	667	692	680	682	671	686	711
LCT-39-04	661	724	699	711	648	691	697	1000	704	721	674	679	713	707	665	679	667	682	665	679	674
LCT-39-05	643	790	801	794	680	705	723	704	1000	767	716	730	732	749	670	718	715	697	703	724	717
LCT-39-06	647	767	795	800	679	701	728	721	767	1000	718	703	733	731	669	700	702	700	701	731	721
LCT-39-07	666	712	718	720	708	695	694	674	716	718	1000	716	711	719	682	694	706	701	708	726	749
LCT-39-08	658	723	718	722	670	711	708	679	730	703	716	1000	721	717	665	709	703	709	673	719	700
LCT-39-09	678	733	740	747	682	733	707	713	732	733	711	721	1000	739	657	713	697	698	701	727	737
LCT-39-10	675	768	773	777	687	711	728	707	749	731	719	717	739	1000	681	711	719	702	705	728	739
LCT-39-11	658	677	657	658	661	665	667	665	670	669	682	665	657	681	1000	709	677	676	661	693	682
LCT-39-12	667	704	696	695	681	704	692	679	718	700	694	709	713	711	709	1000	728	710	680	720	713
LCT-39-13	657	707	719	721	698	698	680	667	715	702	706	703	697	719	677	728	1000	733	700	735	734
LCT-39-14	667	713	706	706	674	697	682	682	697	700	701	709	698	702	676	710	733	1000	697	729	711
LCT-39-15	658	719	711	712	668	672	671	665	703	701	708	673	701	705	661	680	700	697	1000	706	715
LCT-39-16	696	714	712	714	695	719	686	679	724	731	726	719	727	728	693	720	735	729	706	1000	730
LCT-39-17	697	728	741	733	690	703	711	674	717	721	749	700	737	739	682	713	734	711	715	730	1000

8.2.3. Phase IV-b, Application Case 1

Table 8.15. Summary of results for Application Case 1

	Task e (Sc. A)	Task d (Sc. E)	Task d (Sc. E)
Library	**ENDF/B-VII.0**	**ENDF/B-VII.0**	**ENDF/B-VII.0**
Energy groups	**238**	**238**	**CE**
Fuel rod positions	**dependent**	**dependent**	**independent**
k_C	0.97350	0.97350	0.97383
Δk_B	0.00386	0.00381	0.00332
$k_S = k_C + \Delta k_B$	0.97737	0.97732	0.97715
$V(k_S)_{geom}$	1.32E-05	9.48E-07	3.09E-07
σ	0.00364	0.00097	0.00056
$\lambda_{95/95}$	1.927	1.927	1.927
$k_{95/95} = k_S + \lambda_{95/95}\,\sigma$	0.98437	0.97919	0.97822

References

Behler, M., M. Bock, F. Rowold and M. Stuke (2014), "SUnCISTT – A general tool for uncertainty and sensitivity analysis"; *Proceedings of PSAM12 - Probabilistic Safety Assessment and Management,* 22-27 June 2014, Honolulu, Hawaii, United States, July 2014.

Bock M. and M. Behler (2013), "Impact of correlated benchmark experiments on the computational bias in criticality safety assessment", *Proceedings ANS Nuclear Criticality Safety Division Topical Meeting (NCSD 2013*), Wilmington, North Carolina, United States, 2013.

Bock M. and M. Stuke (2013), "Determination of correlations among benchmark experiments by Monte Carlo sampling techniques"; *Proceedings of NCSD 2013 "Criticality Safety in the Modern Era: Raising the Bar"*, Wilmington,NC United States, July 2013.

Buss, O., A. Hoefer and J.C. Neuber (2011), "NUDUNA – nuclear data uncertainty analysis", *Proceedings International Conference on Nuclear Criticality (ICNC 2011)*, Edinburgh, Scotland, 2011.

Hoefer, A., O. Buss, M. Hennebach, M. Schmid and D. Porsch (2015), "MOCABA: A general Monte Carlo -Bayes procedure for improved predictions of integral functions of nuclear data", *Ann. Nucl. Energy*, Vol. 77, pp. 514-521, 2015.

Mennerdahl, D. (2019), "KRITZ-1-ML measurements on regular H_2O/U(1.35)O2 MARVIKEN fuel rod lattices at temperatures up to 250°C, KRITZ-LWR-RESR-004", *International Handbook of Evaluated Reactor Physics Benchmark Experiments*, , OECD Publishing, Paris, 2019, https://doi.org/10.1787/a112bf8e-en.

NEA (2023), *Role of Integral Experiment Covariance Data for Criticality Safety Validation, EG UACSA Benchmark Phase IV*, NEA/NSC/R(2021)1, OECD Publishing, Paris.

NEA (2015), *International Handbook of Evaluated Criticality Safety Benchmark Experiments*, NEA/NSC/DOC(95)03, OECD Publishing, Paris, https://doi.org/10.1787/110ba6fc-en.

ORNL (2009), *SCALE: A Modular Code System for Performing Standardized Computer Analyses for Licensing Evaluations* ORNL/TM-2005/39, Version 6.0, Vols. I–III, January 2009.

Peters, E., F. Sommer and M. Stuke (2015a), "Impact of correlated data in validation procedures"; *Proceedings of International Collaboration of Nuclear Criticality Safety, ICNC 2015,* Charlotte, 13-17 September 2015, North Carolina, United States.

Peters, E., F. Sommer and M. Stuke (2015b), "Sensitivities and correlations of critical experiments due to uncertainties of system parameters and nuclear data", *Proceedings of International Collaboration of Nuclear Criticality Safety, ICNC 2015,* 13-17 September 2015, Charlotte, North Carolina, United States.

Peters, E., F. Sommer and M. Stuke (2016), "Modeling of critical experiments and its impact on integral covariance matrices and correlation coefficients", arXiv:1602.04038 [physics.data-an], *Annals of Nuclear Energy,* 92:355-362, pp.355-362; https://doi.org/10.1016/j.anucene.2016.02.011, February 2016.

Poullot, G. and D. Hanlon (2015a), "Water-reflected 4.738-wt% enriched Uranium dioxide fuel-rod arrays, LEU-COMP-THERM-007", *International Handbook of Evaluated Criticality Safety Benchmark Experiments*, OECD Publishing, https://doi.org/10.1787/110ba6fc-en.

Poullot, G. and D. Hanlon (2015b), "Incomplete arrays of water-reflected 4.738-wt.%-enriched Uranium dioxide fuel-rod arrays, LEU-COMP-THERM-039", in *International Handbook of Evaluated Criticality Safety Benchmark Experiments*, OECD Publishing, https://doi.org/10.1787/110ba6fc-en.